博士論文

Magnetic Structures of Itinerant Electron Systems on the Extended Spatially Completely Anisotropic Triangular Lattice

（拡張空間異方的三角格子上の磁気構造の磁気構造）

広島大学大学院先端物質科学研究科

河野　佑紀

2022年3月

目次

1. 主論文
Magnetic Structures of Itinerant Electron Systems on the Extended Spatially Completely Anisotropic Triangular Lattice
(拡張空間異方的三角格子上の遍歴電子系の磁気構造)
河野　佑紀

2. 公表論文
(1) On Scaling Relations of Organic Antiferromagnets with Magnetic Anions
Hiroshi Shimahara and Yuki Kono
Journal of the Physical Society of Japan, **86**, 043704-1 - 043704-5 (2017).

(2) Magnetic Structures of Electron Systems on the Extended Spatially Completely Anisotropic Triangular Lattice near Quantum Critical Points
Yuki Kono and Hiroshi Shimahara
Journal of the Physical Society of Japan, **90**, 024708-1 - 124711-8 (2021).

主論文

Acknowledgments

I would like to thank Professor Hiroshi Shimahara for his careful guidance and many advices. I am indebted to Professor Yutaka Nishio for useful discussions, information, and experimental data. I am indebted to Professors Sinya Uji, Yugo Oshima, Takaaki Minamidate, Shuhei Fukuoka, and Takuya Kobayashi for useful discussions.

Contents

1 Introduction and Purpose **6**
- 1.1 Extended Spatially Completely Anisotropic Triangular Lattice 6
- 1.2 Organic Compound λ-$(BETS)_2FeCl_4$ 11
- 1.3 Purpose of the Thesis 13

2 Scaling Relations in Mixed Crystal Systems **16**
- 2.1 Scaling Relations in Organic Compound 16
- 2.2 Model Hamiltonian 18
  - 2.2.1 Analysis Based on the Random Phase Approximation . 20
  - 2.2.2 Analysis Based on the Mean Field Theory 21

3 Magnetic Structures of Electron Systems on the ESCATL **24**
- 3.1 Energy Dispersion 24
- 3.2 Parameter Sets and Fermi Surface 26
- 3.3 Mean Field Theory 28
- 3.4 Magnetic Structure of λ-Fe 33
- 3.5 Phase Diagram and Effect of Imbalance of Spatial Anisotropy 36
- 3.6 Summary and Discussion 36

4 Summary of Thesis and Conclusion **45**

A Trapezoidal Formula **47**

B Linear Response Theory **52**

C Derivation of Eq. (3.50) **56**

D Derivation of Eq. (2.15) **65**

E Derivation of Eq. (2.19) **68**

F Derivation of Eqs. (2.28) and (2.29) 74

Chapter 1

Introduction and Purpose

1.1 Extended Spatially Completely Anisotropic Triangular Lattice

Electron systems on triangular lattices have been extensively researched because they exhibit interesting phenomena, such as quantum spin liquids, magnetic plateaus, and spiral magnetic structures [1–3]. They originate from the geometrical frustration of the spin alignment. The frustration is maximum when the magnitudes of antiferromagnetic exchange interactions on the bonds are all equal, and the spatial anisotropy of the antiferromagnetic exchange interactions reduces the geometrical frustration. However, the effect of spatial anisotropy can be significant when real compounds are examined. Some compounds contain spatially anisotropic triangular lattices that consist of two types of triangles of the bonds. These lattices are called extended spatially completely anisotropic triangular lattice (ESCATL). The localized spin model on the ESCATL has six kinds of exchange interactions with the coupling constants J_l and J'_l as shown in Fig. 1.1, whereas the itinerant electron model on the ESCATL has six kinds of transfer integrals t_l and t'_l as shown in Fig. 1.2, where l=1, 2, and 3.

When we consider special cases, the ESCATL is reduced to some frustrated lattices. For example, when $J_l = J'_l$ for all l and $J_2 = J_3$, it reduces to the spatially anisotropic triangular lattice (SATL) [2,4–9]. The SATL has been studied as the lattice that is composed of π-electron systems in β-$Me_{4-n}Et_nX[Pd(dmit)_2]_2$ (X = P, Cs, N, Sb, and As) and κ-(BEDT-TTF)$_2$Cu(CN)$_3$, where dimt and BEDT-TTF stand for 1,3-dithiol-2-thione-4,5-dithiolate and bis(ethylenedithio)tetrathiafulvalene. Hereafter, we abbreviate β-$Me_{4-n}Et_nX[Pd(dmit)_2]_2$ and κ-(BEDT-TTF)$_2$Cu(CN)$_3$ as X-n and κ-ET, respectively. In κ-ET, it has been suggested from the experimen-

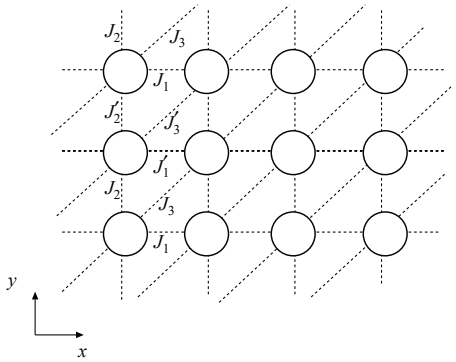

Figure 1.1: Extended spatially completely anisotropic triangular lattice and definition of exchange coupling constants.

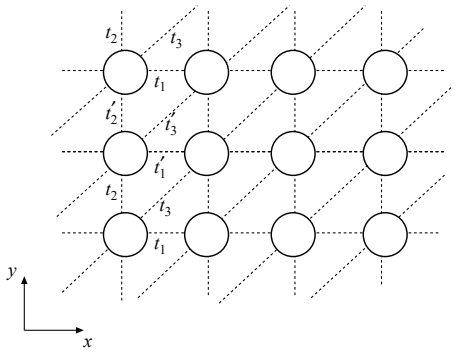

Figure 1.2: Definitions of the transfer integrals on the ESCATL.

tal results of susceptibility and nuclear magnetic resonance (NMR) that the ground state is quantum spin liquid [10]. The SATL has also been studied in the spin system of Cs_2CuBr_4 and Cs_2CuCl_4. In the compound Cs_2CuBr_4, a magnetization plateau was observed in the magnetization process [11, 12].

When $J_l = J'_l$ for all l, it is reduced to the spatially completely anisotropic triangular lattice (SCATL) [4]. Hauke examined it for X-n (X= P, Cs, N, Sb and As) and showed that the ground states of As-2 and Sb-0 are the Néel-(π, π) states shown in Fig. 1.3(a) [4].

When $J'_3 = 0$, the ESCATL reduces to the trellis lattice [13]. The trellis lattice is contained the compounds $SrCu_2O_3$, NaV_2O_5, and $Ag_xV_2O_5$ [14–16]. When $J'_3 = J_1 = J'_1 = 0$, the ESCATL reduces to the honeycomb lattice [17]. The honeycomb lattice is contained the compounds $InCu_{2/3}V_{1/3}O_3$ and $Na_3T_2SbO_6$ (T = Cu, Ni, and Co) [18]. Compared to these lattices, the ESCATL has the unique feature of the imbalance of the spatial anisotropies in two types of triangles.

In this thesis, we introduce the itinerant electron model on the ESCATL to examine the compound λ-$(BETS)_2XCl_4$ (X=Fe, Ga, Fe_xGa_{1-x}), where BETS stands for bis(ethylenedithio)tetraselenafulvalene. Hereinafter, we abbreviate λ-$(BETS)_2XCl_4$ as λ-X. We extend the knowledge of the ESCATL antiferromagnets and examine the magnetic structure of the λ-X system. The ESCATL in π-electron system corresponds to each BETS molecule as shown in Fig. 1.2. The λ-Fe system exhibits an antiferromagnetic long-range order (AF LRO) [19, 20]. In the λ-Fe system, as the temperature decreases, the magnetization m of the itinerant π-electrons saturate first, and the 3d-spins follow a constant exchange field created by the π electrons [21, 22]. We consider a realistic situation in which the spiral state is suppressed [4]. We assume the Néel and up-up-down-down (uudd) phases defined in Fig. 1.3 and 1.4 as collinear spin structures [28]. In this thesis, we examine the magnetic structure of ESCATL antiferromagnets in the ground state within a mean-field approximation. In particular, we reveal the effect of the imbalance of the spatial anisotropies in two types of triangles. We define the parameter $r_{\rm imb}$ that represents the imbalance of spatial anisotropies as

$$r_{\rm imb} \equiv \frac{t_3/t_2 - t'_3/t'_2}{t_3/t_2} \tag{1.1}$$

because $t_1 = t'_1$ is satisfied in the λ-Fe system [23].

The organic compound λ-$(BEDT\text{-}STF)_2XCl_4$ (X=Fe,Ga) [24, 25], where BEDT-STF stands for bis(ethylenedithio)diselenadithiafulvalene, is a material in which Se atoms of BETS molecules are replaced with S atoms. This replacement is effectively a negative pressure applied to the λ-X system. In

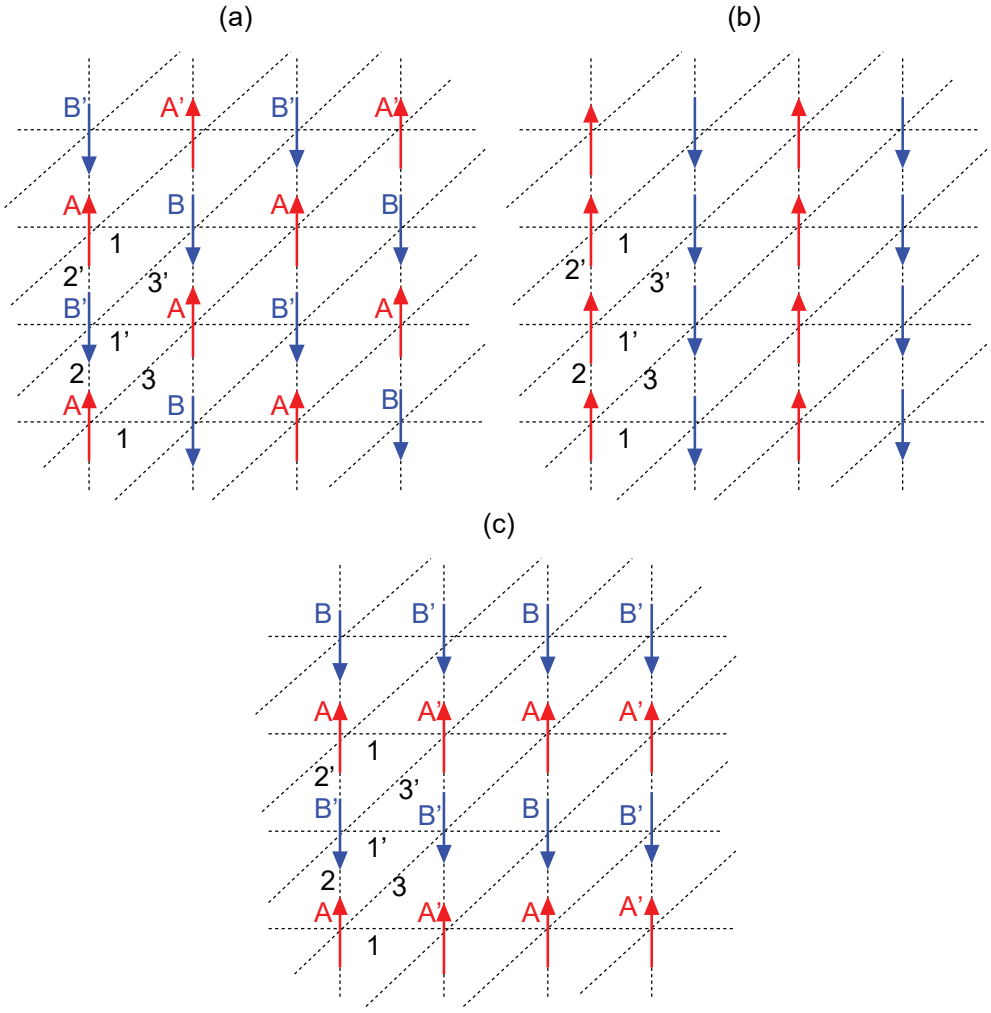

Figure 1.3: Magnetic structures which is examined. (a) Néel-(π, π) state, (b) Néel-$(\pi, 0)$ state, (c) Néel-$(0, \pi)$ state.

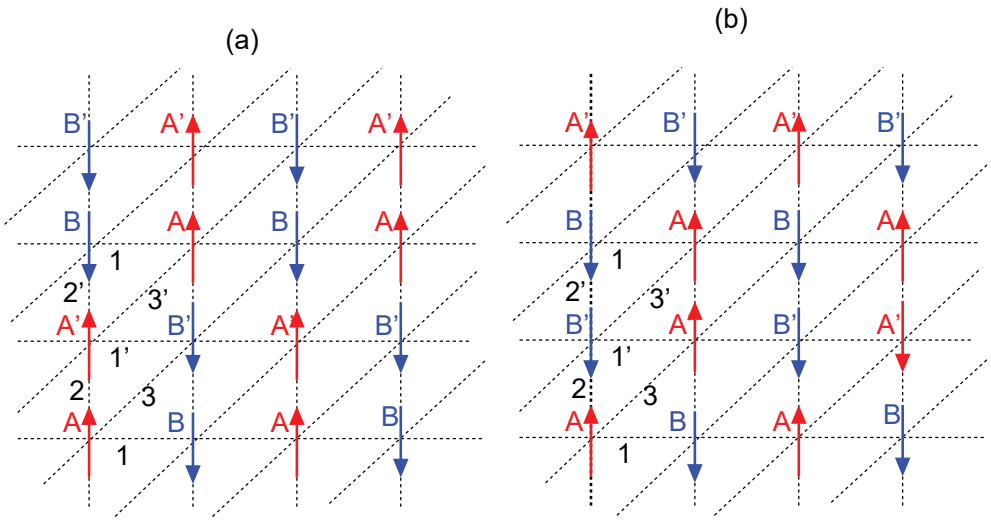

Figure 1.4: Magnetic structures which are examined. (a) uudd-2 state and (b) uudd-2′ state.

the λ-(BEDT-STF)$_2$FeCl$_4$ system, the metal-insulator transition accompanied by the paramagnetic-antiferromagnetic transition has been observed at $T_{\rm N} = 16$ K [26, 27]. In organic compound λ-D_2A, where D and A represent a doner and an anion, respectively, the dimerized doners form the ESCATL. We examine wide ranges of parameters so that we can consider compounds that have not yet been discovered.

For the localized spin model on the ESCATL, the classical phase diagram includes five different collinear antiferromagnetic phases and spiral phase [28]. It was shown that the imblance of the spatial anisotropies, which are parameterized by J_3/J_2 and J_3'/J_2', stabilizes the uudd phase shown in Fig. 1.4(a) and (b).

A uudd phase has been studied in several materials [29–34]. It has been suggested that in the solid ^{3}He the ground state is the uudd state [29]. Roger examined the magnetism of ^{3}He by a two-parameter model based on three-spin exchange and planar four-spin exchange [30]. In the insulating perovskite HoMnO$_3$, which is a frustrated spin system having ferromagnetic nearest-neighbor and antefferomagnetic next-nearest-neighbor interactions within a MnO$_2$, the uudd phase has been experimentally suggested [31, 32]. Kaplan proposed a possible mechanism for this state by the frustrated classical Heisenberg model in one dimension with nearest-neighbor biquadratic exchange [33]. Zou et al. found the uudd structure in the spinel conpound GeCu$_2$O$_4$ by the effective classical spin Hamiltonian containing

nearest-neighbor biquadratic exchange interaction [34].

1.2 Organic Compound λ-$(BETS)_2FeCl_4$

In the compound λ-$(BETS)_2FeCl_4$, the BETS layers and $FeCl_4$ anion layers are stacked alternately, and the BETS layers and $FeCl_4$ anion layers have π electrons and 3d spins, respectively. The λ-Fe system is highly conductive in the direction parallel to the ac plane, whereas it has low conductivity in the b-axis direction because the electron transfer is blocked by the anion layer. The crystal system is triclinic and the space group in paramagnetic phase is $P\bar{1}$ [35]. The cell parameters are $a = 16.164$ Å, $b = 18.538$ Å, and $c = 6.593$ Å, $\alpha = 98.40°$, $\beta = 96.67°$, and $\gamma = 112.52°$.

The λ-Fe system has interesting properties that originate from two kinds of magnetic degrees of freedom: conduction π-electrons and localized 3d spins [36]. In this system, the metal−insulator phase transition accompanied by the paramagnetic−antiferromagnetic transition has been observed at $T_N \simeq 8.3$ K [19, 20]. Akiba et al. fitted the specific heat data with the curve for the six-level Schottky-type specific heat and found that as the temperature decreases, the magnetization of the π electrons saturates first, and the 3d spins follow a constant exchange field created by the π electrons [21, 22]. However, in the pure two-dimensional π-electron system, which is realized in the λ-Ga system [37–39], the AF LRO has not been observed. One of the reason for the behavior is low-dimensionality of the system [40]. This implies that 3d spins are indispensable for the stabilization of the AF LRO of π-electrons in the λ-Fe system. Shimahara and Ito revealed that the AF LRO of π-electrons in the λ-Fe system is stablized by the magnetic anisotropy and/or three-dimensionality introduced by the 3d spins [41].

The total entropy of the λ-Fe system is obtained from the experimental result of the specific heat [21]. The total entropy at high temperature above T_N is equal to $R \ln 6$, which is consumed as the temperature decreases.

In the λ-Fe system, the easy magnetization axis is tilted about 30° from the c-axis to the b*-axis [22, 42, 43]. When a magnetic field is parallel to the easy magnetization axis, a spin-flop transition is observed approximately at 1.2 T [42–44].

There are various theoretical studies on the λ-Fe system [45–47]. In the spin-wave theory, the value of T_N and the behavior of the sublattice magnetizations of small spin and large spin as functions of the temperature T are derived [45]. The results agree with the observations in the λ-Fe. From the free energy function model, the sharp peak of specific heat around T_N is

a phenomenon unique to coupled magnetic systems in which $T_{\rm N} \ll J_1$ [46]. This condition is not satisfied in conventional antiferromagnets. The above results give a physical explanation for the intriguing behaviors observed in the λ-Fe system. Shimahara expanded the scaling theory of critical phenomena to a coupled magnetic system consisting of two subsystems and derived an extended relation for critical exponents [47]. He applied this theory to the λ-Fe system and derived the critical exponents, which are $\alpha = 3/4$, $\beta = 1/8$, $\gamma = 1$, $\delta = 9$, $\psi = 1/5$ and $\nu = 5/8$. The value of α is close to the experimental result $\alpha = 0.77$.

In the classical Heisenberg model, the magnetic structure of the λ-Fe system has been examined at $T = 0$ [28]. The spiral state has the lowest energy for the candidate parameter values for the λ-Fe system [23]. However, the spiral state could be suppressed by quantum fluctuations and anisotropy introduced by 3d spins, which are not included in the classical Heisenberg model because the experimental results suggest that the ground state of the λ-Fe system is a collinear with two sublattices [19, 21, 22, 39, 42, 43, 48–50]. If the spiral state is suppressed, the Néel-(π, π) state has the lowest energy. The uudd-2 state has the second-lowest energy, which is slightly greater than that of the Néel-(π, π) state [28]. Because the candidate parameter values are obtained in a simplified model [23], they contain errors. Hence, the magnetic structure of the λ-Fe system in the ground state is likely the Néel-(π, π) or uudd-2 state.

The localized spin model is an effective model for the λ-Fe system in the insulating phase. However, it does not take into account the itinerant features of the π-electrons. The λ-Fe system is in the vicinity of the quantum critical point ($U \simeq U_c$) [51], and such a situation cannot be reproduced in the localized spin model, where U and $U_{\rm c}$ are the on-site Coulomb energy and the critical value of U between the antiferromagnetic and paramagnetic phases, respectively. Therefore, we examine the Hubbard model [52] on the ESCATL and apply it to the π-electron system in the λ-Fe system. The a- and c-axes of the λ-Fe system correspond to the 1- and 1′- bonds and 2- and 2′- bonds in Fig. 1.5, respectively.

There are several studies of the magnetic structure of the λ-Fe system in the itinerant electron model [20, 44, 53, 54]. Hotta and Fukuyama examined the effect of the 3d-spins on the π electron system considering the magnetic structure inside the dimer and obtained a unified phase diagram within the mean-field approximation [53]. Brossard et al. examined the magnetic structure of the 3d-spin system [20], where they assumed the antiferromagnetic transition induced by an Ruderman-Kittel-Kasuya-Yosida (RKKY) interaction [55–57], which is the interaction between 3d-spins mediated π-electrons. These studies assume a physical picture in which 3d-spins sustain the AF

LRO. However, this physical picture is inconsistent with the experimental result of magnetic specific heat mentioned above [21]. In this thesis, we assumes that π-electrons sustain the AF LRO, the physical picture of which is appropriated by the recent experimental results [21]. Hence, we ignore the effect of the 3d-spins system in the $FeCl_4$ anions. In the λ-X system, the BETS molecules form dimers, which are regarded as lattice sites in this thesis.

The Fermi surfaces of the λ-Fe system were obtained by an extended Hückel tight-binding band structure calculations [20]. The Brillouin zone is folded in half because $(t_2, t_3) \neq (t_2', t_3')$. A closed Fermi surface exists, which is consistent with the experimental results of the Shubnikov-de Haas and angular-dependent magnetoresistance oscillations [58]. The Fermi surface has the nesting vector $\boldsymbol{Q} \simeq (\pi/c, 0)$. The modulation vector (π/c,0) in the half-Brillouin zone cannot resolve the modulation vectors (π/c,0) and (π/c,π/a) in the original Brillouin zone, which correspond to the Néel-(π,π) and Néel-(π,0) states defined as Fig. 1.5(a)-(b). The modulation vector (0,0) in the half-Brillouin zone cannot resolve the modulation vectors (0,0) and (0,π/a) in the original Brillouin zone, which correspond to the ferromagnetic and Néel-(0,π) states defined in Fig. 1.5(c). The uudd phases have the modulation vector (π/c,$\pi/2a$).

1.3 Purpose of the Thesis

In this thesis, we examine the itinerant electron systems on the ESCATL. The ESCATL have the unique feature of the imbalance of the spatial anisotropies in two types of triangles. We examine the magnetic structure in the ground state and reveal the effect of the imbalance of the spatial anisotropies. We examine the Néel and uudd phases defined in Fig. 1.3 and 1.4 as collinear spin structures.

Next, we apply the theory to the λ-Fe system. As mentioned in the previous section, the magnetic structure of the λ-Fe system has been examined by the localized spin model on ESCATL in previous study [28]. However, this model does not take into account the fact that the Coulomb energy U of the λ-Fe system is near the quantum critical point ($U \simeq U_c$) [51]. Hence, we consider the itinerant model on the ESCATL and examine the magnetic structure in the ground state within the mean-field approximation.

In Chapter 2, we review the paper on the scaling relations of the mixed crystal λ-Fe_xGa_{1-x}. In Chapter 3, we examine the magnetic structure of the electron system on the ESCATL. We adopt the Hubbard model as the model of the π-electron system. We calculate the total energies in the mean-field

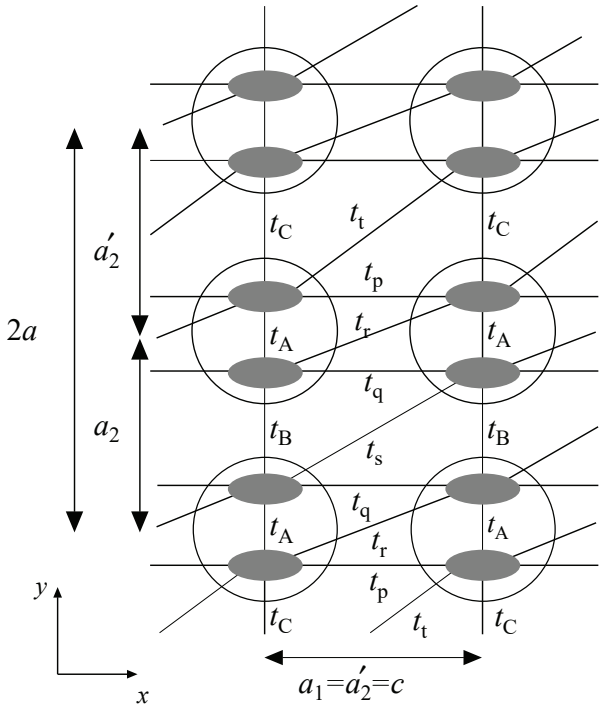

Figure 1.5: Schematic diagram of the BETS layers in λ-X and the ESCATL. The small ellipses and large circles in the figure represent BETS molecules and dimerized BETSmolecules, respectively. The transfer integrals $t_{\rm A}$, $t_{\rm B}$, $t_{\rm C}$, $t_{\rm s}$, $t_{\rm t}$, $t_{\rm p}$, $t_{\rm q}$, and $t_{\rm r}$ are defined from Mori and Kobayashi [53]. The transfer integrals in this thesis are expressed as $t_1 = (-t_{\rm p} - t_{\rm q} + t_{\rm r})/2$, $t_2 = t_{\rm B}/2$, $t'_2 = t_{\rm C}/2$, $t_3 = t_{\rm s}/2$, and $t'_3 = t_{\rm t}/2$. We refer to the lattice constants of the bonds with the transfer integrals t_1, t'_1, t_2, and t'_2 as a_1, a'_1, a_2, and a'_2, respectively, and define $c = a_1 = a'_1$ and $a = (a_2 + a'_2)/2$. The lattice constant in the crystal a-axis of the compound corresponds to $2a$ in the present model.

approximation and examine the stable magnetic structure. We reveal the effect of the imbalance of the spatial anisotropies of two type of triangles. In Chapter 4 is the conclusion.

Chapter 2

Scaling Relations in Mixed Crystal Systems

In this chapter, we review the paper on the scaling relations of the λ-Fe_xGa_{1-x} system [51]. From experiments on specific heat of the λ-Fe_xGa_{1-x} system, it has been suggested that magnetization m of π electrons and the antiferromagnetic transition temperature $T_{\rm N}$ are proportional to x for $0.6 \leq x \leq 1$. We examine the scaling relation of $T_{\rm N}$ by the introduction of the interaction between π-electrons mediated 3d spins. Next, we examine the scaling relation of m in the low temperature region below $T_{\rm N}$.

2.1 Scaling Relations in Organic Compound

The λ-Fe_xGa_{1-x} system exihibits an interesting x-T phase diagram [59–62]. The itinerant π-electrons in the BETS layers and localized spins in the $FeCl_4$ anion layers are responsible for this phase diagram. For $0.35 < x < 1$, the antiferromagnetic insulating phase occurs. For $0 < x < 0.35$, superconductivity occurs. Near $x = 0.35$, the superconducting phase and the antiferromagnetic insulating phase competes.

In the λ-Fe_xGa_{1-x} system, the specific heat $C(x,T)$ and transition temperature $T_{\rm N}$ satisfy the scaling relations

$$C(xT, x) = xC(T, 1) \tag{2.1}$$

and

$$T_N(x) = xT(1) \tag{2.2}$$

for $0.6 \leq x \leq 1$, respectively [59]. The specific heat data of the λ-Fe_xGa_{1-x}

system is in good agreement with the curves for the six-level Schottky-type specific heat below the crossover temperature $T_0(x)$ [$< T_{\rm N}$] [21]. This means that as the temperature decreases from $T_0(x)$, the conduction π electrons saturate first, 3d spins passively follow a constant exchange field $h(x)$ created by the π electrons. Because $h(x)$ is proportional to the sublattice magnetization m of π electrons,

$$m(T, x) = m(0, x) = \text{constant} \tag{2.3}$$

below T_0. For example, at $x = 1$, as T increases from $T = 0$ to $T_0 \simeq 6.0$ K, the sublatice magnetization M of 3d spins decreases, while the value of m is almost constant [50]. Because the magnitude of the specific heat $C(x, T)$ is proportional to that of the effective field $h(x)$, we obtain

$$m(T, x) = xm(T, 1) \tag{2.4}$$

below T_0.

The scaling relation of the antiferromagnetic transition temperature $T_{\rm N}$ has been examined within a mean-field approximation by Terao and Ohashi [54]. They assumed an antiferromagnetic transition induced by an RKKY interaction, which is the interaction between 3d spins mediated by π electrons. However, in this previous study, some problems remain. The mean-field approximation is not appropriate for the estimation of $T_{\rm N}$ because this approximation ignores the spin fluctuations. In addition, the antiferromagnetic transition induced by an RKKY interaction contradicts the physical picture that is obtained from the experimental result of the specific heat [21].

In this thesis, we examine the scaling relation (2.1)-(2.4), which is taken into account the experimental results of the specific heat [21]. The scaling relation (2.1)-(2.4) has been suggested from experimental results of specific heat in $x = 0.6, 0.7, 1.0$. However, in $x = 0.4$, the experimental results deviate from the scaling relation because superconductivity occurs. We examine the scaling relations in the range where superconductivity is suppressed.

We consider an itinerant electron model as a model for the λ-$\mathrm{Fe}_x\mathrm{Ga}_{1-x}$ system. In this model, we can examine the shrinkage of m, which cannot be reproduced in the localized spin model. Hence, we examine the scaling relation in an extended Kondo lattice model [20, 44, 53, 54], which is the model that is taken into account the itinerant nature of π electrons in the λ-$\mathrm{Fe}_x\mathrm{Ga}_{1-x}$ system.

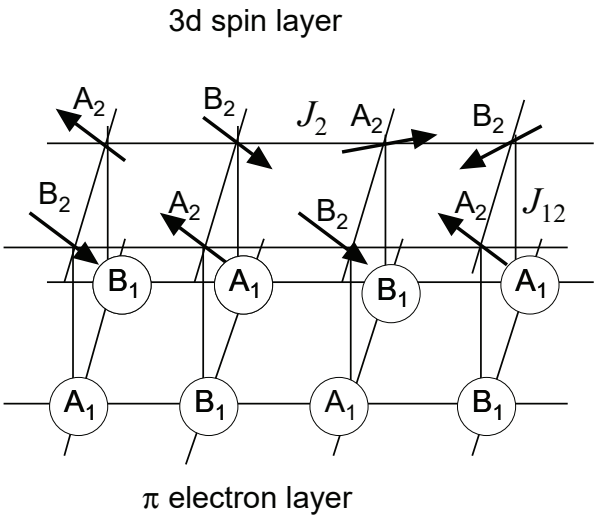

Figure 2.1: Model Hamiltonian

2.2 Model Hamiltonian

The Hamiltonian of an extended Kondo lattice model for the λ-Fe_xGa_{1-x} system is defined as

$$H = H_1 + H_2 + H_{12} \tag{2.5}$$

with

$$H_1 = \sum_{i,j} t_{ij} c^\dagger_{i\sigma} c_{j\sigma}, \tag{2.6}$$

$$H_2 = \sum_{(i',j')} \sum_{\mu=x,y,z} \theta_{i'} \theta_{j'} J_2^\mu S_{i'}^\mu S_{j'}^\mu, \tag{2.7}$$

$$H_{12} = \frac{1}{2} \sum_{(i,i')} \sum_{\mu=x,y,z} \theta_{i'} J_{12}^\mu S_{i'}^\mu \hat{\sigma}_i^\mu, \tag{2.8}$$

where $S_{i'}^\mu$ and $c_{i\sigma}$ are the spin operator with length $S = 5/2$ on the anion site i' and the annihilation operator of the π electron on the BETS site i with σ,

respectively. Here,

$$n_{i\sigma} = c^{\dagger}_{i\sigma} c_{i\sigma}, \tag{2.9}$$

$$\hat{\sigma}^{\mu}_{i} = \sum_{\sigma_1\sigma_2} c^{\dagger}_{i\sigma_1} \sigma^{\mu}_{\sigma_1\sigma_2} c_{i\sigma_2}, \tag{2.10}$$

where σ^{μ}_{i} is the Pauli matrix, and θ'_i is defined as $\theta_{i'} = 0$ or 1 when i' is on an $FeCl_4$ or $GaCl_4$ anion, respectively. We refer to the lattices in the BETS and $FeCl_4$ layers as L_1 and L_2, respectively. We refer to the number of nearest neighbor sites in L_2 and that between L_1 and L_2 as z_2 and z_{12}, respectively. We take $z_{12} = 1$. The structure of the system is depicted in Fig. 2.1. The electron number density of π electrons n is equal to 1 (half-filling). Because the λ-Fe_xGa_{1-x} system has magnetic anisotropy, $J^x_{12} = J^y_{12} \leq J^z_{12} \equiv J_{12}$ and $J^x_2 = J^y_2 \leq J^z_2 \equiv J_2$. We ignore J_2 because $J_2 \ll U, J_{12}$ [49].

The particle number operator $n_{i\sigma}$ is written as

$$n_{i\sigma} = \frac{\hat{n}_i}{2} + \sigma_i \hat{m}_i, \tag{2.11}$$

where $\hat{m}_i \equiv \hat{\sigma}^z_i$. Therefore,

$$\begin{aligned} U n_{i\uparrow} n_{i\downarrow} =& U(\frac{\hat{n}_i}{2} + \hat{m}_i)(\frac{\hat{n}_i}{2} - \hat{m}_i) \\ =& \frac{U}{4}\hat{n}^2_i - U\hat{m}^2_i. \end{aligned} \tag{2.12}$$

In previous studies, the antiferromagnetic transition induced by an RKKY interaction between localized spins mediated by conduction π-electrons [55–57] have been assumed. However, in the λ-Fe_xGa_{1-x} system, π-electrons sustain the AF LRO and the role of 3d spins is passive [21, 22]. For this reason, we consider the 'reverse' RKKY interaction between conduction π-electrons mediated by localized spins. Regarding the θ_i distribution as random, we replace θ_i with x. Introducing the susceptibility $\chi_2(T)$ of the 3d spin system, Eq. (2.8) becomes

$$H_{12} = \frac{U}{4}\hat{n}^2_i - U\hat{m}^2_i - \sum_i \frac{1}{2} x J^2_{12} \chi_2(T) \hat{m}^2_i. \tag{2.13}$$

We define $\tilde{U}$ as

$$\tilde{U} = U + \frac{1}{2} x J^2_{12} \chi_2(T). \tag{2.14}$$

The susceptibility of the free 3d spins is

$$\chi_2(T) = \frac{S(S+1)}{k_{\rm B}T}. \tag{2.15}$$

When we substitute Eq. (2.15) into Eq. (2.14), we obtain

$$\tilde{U} = U + \frac{1}{2} x J_{12}^2 \frac{S(S+1)}{k_B T}. \tag{2.16}$$

Let $U_{\rm c}$ be the lower limit where the AF LRO vanishes in a pure π-electron system. When $\tilde{U} = U_{\rm c}$, $T = T_{\rm N}$. Therefore,

$$T_N = x \frac{S(S+1)}{6} \frac{J_{12}^2}{U_c - U}. \tag{2.17}$$

When $U_{\rm c}$ depends weakly on T, the transition temperature satisfies Eq. (2.17), and we obtain

$$T_N \propto x. \tag{2.18}$$

For $x = 1$, when we substitute $J_{12} \simeq 9.3$ K and $T_{\rm N} \simeq 8.3$ K [49] for Eq. (2.18), we obtain $U_{\rm c} - U \simeq 15.2$ K. Because $U_{\rm c}$ is an order of magnitude of 1 eV $= 1 \times 10^4$ K, we obtain $U_{\rm c} - U \ll U$. This means that the system is near the quantum critical point.

2.2.1 Analysis Based on the Random Phase Approximation

In this subsection, we illustrate the theory using the random phase approximation (RPA) although the above argmenent does not depend on this approximation. We assume that a commensurate nesting vector $\boldsymbol{Q}$ such as $(\pi/c,\pi/a)$ and $(\pi/c,0)$.

The spin susceptibility $\chi^s(T)$ is written as

$$\chi^s(T) = \frac{\chi_{10}(T)}{1 - U\chi_{10}(T)}. \tag{2.19}$$

$\chi_{10}(T)$ is the susceptibility of free electrons and written as

$$\chi_{10}(T) = \frac{1}{N} \sum_{\boldsymbol{k}} \frac{f(\xi_{\boldsymbol{k}}) - f(\xi_{\boldsymbol{k}+\boldsymbol{Q}})}{\xi_{\boldsymbol{k}+\boldsymbol{Q}} - \xi_{\boldsymbol{k}}} \tag{2.20}$$

$$= \frac{1}{N}\sum_{\boldsymbol{k}} \frac{\tanh(\frac{\bar{\xi}_{\boldsymbol{k}}-\bar{\delta}_{\boldsymbol{k}}}{2k_BT}) + \tanh(\frac{\bar{\xi}_{\boldsymbol{k}}+\bar{\delta}_{\boldsymbol{k}}}{2k_BT})}{4\bar{\xi}_{\boldsymbol{k}}}, \tag{2.21}$$

where

$$\bar{\xi}_{\boldsymbol{k}} = \frac{1}{2}(\xi_{\boldsymbol{k}} - \xi_{\boldsymbol{k}+\boldsymbol{Q}}), \tag{2.22}$$

$$\bar{\delta}_{\boldsymbol{k}} = \frac{1}{2}(\xi_{\boldsymbol{k}} + \xi_{\boldsymbol{k}+\boldsymbol{Q}}), \tag{2.23}$$

N denotes the number of the sites, and $\sum_{\boldsymbol{k}}$ is taken over a Brillouin zone. When $\chi^s(T)$ diverges, the system undergoes antiferromagnetic transition. The Coulomb energy $U_{\rm c}$ at the quantum critical point satisfies $1 = U_{\rm c}\chi_0(T)$. Hence, U_c is

$$U_{\rm c} = 1/\chi_0(T). \tag{2.24}$$

When $\delta_{\boldsymbol{k}} \neq 0$, the system is far from the perfect nesting. In this case, $\chi_0(T)$ is independent of T, Whereas when nesting of the Fermi surface is perfect, $\chi_0(T)$ is proportional to $\ln T$. When the area of the imperfect Fermi surface is large, $T_{\rm N}$ satisfies $T_{\rm N} \propto x$.

2.2.2 Analysis Based on the Mean Field Theory

In this subsection, we adopt the mean-field approximation, which is qualitatively applicable at low temperatures to examine the scaling relations for m below the crossover temperature T_0.

The sublattice magnetization m of π electrons is defined as

$$m \equiv (-1)^i \frac{1}{2}\sum_{\sigma_1\sigma_2} \langle c^\dagger_{i\sigma_1}\sigma^z_{\sigma_1\sigma_2}c_{i\sigma_2}\rangle, \tag{2.25}$$

where i is the site index in L_1. We assign i as even numbers in sublattices A_1 and odd numbers in sublattices B_1. The sublattice magnetization M of the 3d spins is defined as

$$M \equiv (-1)^{i+1}\langle S^z_{i'}\rangle \tag{2.26}$$

where i is the site index in L_2.

For the distribution of $FeCl_4$ anions, we define

$$\langle \theta_i S_i^z \rangle = (-1)^{i+1} xM \tag{2.27}$$

within the mean-field approximation.

The self-consistent equation for the sublattice magnetization M is

$$M = SB_S(\beta \alpha_2 S), \tag{2.28}$$

where $\alpha_2 = J_{12} m$. The self-consistent equation for the sublattice magnetization m is

$$m = \chi_0(\alpha_1, T)\alpha_1, \tag{2.29}$$

where $\alpha_1 = \frac{1}{2} J_{12} M + Um$,

$$\chi_{10}(\alpha_1, T) = \frac{1}{N} {\sum_{\boldsymbol{k}}}' \frac{\tanh(\frac{E_{\boldsymbol{k}} - \delta_{\boldsymbol{k}}}{2k_B T}) + \tanh(\frac{E_{\boldsymbol{k}} + \delta_{\boldsymbol{k}}}{2k_B T})}{2E_{\boldsymbol{k}}}, \tag{2.30}$$

$E_{\boldsymbol{k}} = \sqrt{\xi_{\boldsymbol{k}}^2 + {\alpha_1}^2}$, and $\sum_{\boldsymbol{k}}'$ is taken over the half-Brillouin zone in the antiferromagnetic phases. From Eq. (2.29), we obtain

$$m = x \frac{1}{2} \frac{J_{12} M \chi_{10}}{1 - U\chi_{10}}. \tag{2.31}$$

We divide the momentum space into two types of parts $R_{\rm p}$ and $R_{\rm i}$, where the nesting of Fermi surfaces are perfect and imperfect, respectively.

$$\chi_{10} = \chi_{10}^{\rm P} + \chi_{10}^{\rm i} \tag{2.32}$$

where $\chi_{10}^{\rm P}$ and $\chi_{10}^{\rm i}$ are the contributions from the summation of $\boldsymbol{k} \in R_{\rm p}$ and $\boldsymbol{k} \in R_{\rm i}$, respectively. From Eq. (2.29), when $m =$ constant, M and $\chi_{10}(T)$ are independent of T because T dependence of these do not cancel each other out. In this case, we replace M and $\chi_{10}^{\rm i}$ with these in the limit $T \to 0$. Taking $T \to 0$, we obtain $M \simeq S$ and $f(E_{\boldsymbol{k}}) = \theta(E_{\boldsymbol{k}})$, where $\theta(E_{\boldsymbol{k}})$ is Heaviside step function. Then, we obtain

$$m(T) = x \frac{1}{2} \frac{J_{12} S \chi_{10}}{1 - U\chi_{10}}. \tag{2.33}$$

We examine the x dependence of χ_{10}. In $\boldsymbol{k} \in R_{\rm p}$, $\theta(E_{\boldsymbol{k}} - |\delta_{\boldsymbol{k}}|) = 1$ and

$\theta(E_{\boldsymbol{k}} + |\delta_{\boldsymbol{k}}|) = 1$. In $\boldsymbol{k} \in R_{\rm i}$, $\theta(E_{\boldsymbol{k}} + |\delta_{\boldsymbol{k}}|) = 0$. Hence, we obtain

$$\chi_{10} = \frac{1}{N}{\sum_{\boldsymbol{k}\in R_{\rm p}}}' \frac{1}{E_{\boldsymbol{k}}} + \frac{1}{N}{\sum_{\boldsymbol{k}\in R_{\rm i}}}' \frac{\theta(E_{\boldsymbol{k}} - |\delta_{\boldsymbol{k}}|)}{E_{\boldsymbol{k}}}. \tag{2.34}$$

The term on the right is written as

$$\frac{1}{N}{\sum_{\boldsymbol{k}\in R_p}}' \frac{1}{E_{\boldsymbol{k}}} \simeq \bar{\rho}_{\rm F} \log \frac{\rm W}{\tilde{\alpha}_{1\rm X}}, \tag{2.35}$$

where $\rho_{\rm F}$ is the average density of states in $\boldsymbol{k} \in R_{\rm p}$, W is the band width, and

$$\tilde{\alpha}_1 = U\bar{m} + \frac{1}{2}J_{12}S. \tag{2.36}$$

Here, $m = x\bar{m}$.

The second term of Eq. (2.34) is the order of the average of $\ln(W/|\delta_{\boldsymbol{k}}|)$. Therefore, $\chi^{\rm i}_{10}$ is expressed as

$$\chi^{i}_{10} = \sum_{k=0}^{\infty} a_k (\frac{\tilde{\alpha}_1}{2W}x)^k, \tag{2.37}$$

where a_k are constants and does not depend on x. When χ_{10} is independent of T, $\bar{\rho}_{\rm p}$ is small, because $\chi^{p}_{10} \propto \bar{\rho}_{\rm p} \ln T$. When we ignore the first term of Eq. (2.34) depending on $\bar{\rho}_{\rm p}$, we obtain

$$m \propto x, \tag{2.38}$$

where $O(\tilde{\alpha}_1 x/2W)$ is ignored. This condition is satisfied when the nesting of the Fermi surface is far from perfect, i.e. the logarithmic singularity is weak. Then, Eq. (2.38) is consistent with Eq. (2.4).

Chapter 3

Magnetic Structures of Electron Systems on the ESCATL

In this chapter, we examine magnetic structures of an itinerant electron model on the ESCATL within the mean-field approximation. In particular, we examine the effect of the imbalance of spatial anisotropies of two types of triangles. We consider three types of Néel states and two types of uudd states. We apply the theory to the λ-Fe system.

3.1 Energy Dispersion

In this section, we derive the electron energy dispersion relation for the ESCATL. The Hamiltonian is written as

$$H_t = \sum_{i,j} \sum_{\sigma} t_{ij} c_{i\sigma}^{\dagger} c_{j\sigma}, \tag{3.1}$$

where $c_{i\sigma}$ is the annihilation operator of the π electron on site i with spin σ.

We assume a unit cell as shown in Fig. 3.1 because $(t_2, t_3) \neq (t_2', t_3')$. The length of the lattice constant in the a-direction is same as the original lattice and that in the c-direction is twice as large as that in the original lattice. The labels $p = 1, 2$ denote two sites in the unit cell. We define

$$c_{\boldsymbol{k}p\sigma} = \sqrt{\frac{2}{N}} \sum_{(i,p)} e^{-i\boldsymbol{k}\cdot\boldsymbol{R}_{ip}} c_{ip\sigma}, \tag{3.2}$$

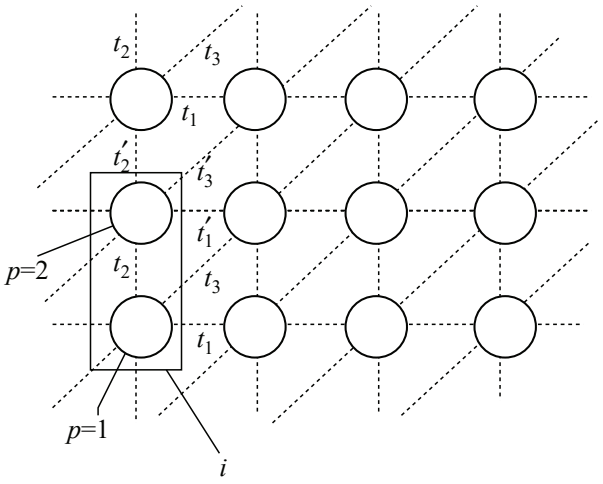

Figure 3.1: Definitions of the unit cell on the ESCATL.

where N denotes the number of the sites. Therefore,

$$c_{ip\sigma} = \sqrt{\frac{2}{N}} \sum_{\boldsymbol{k}} e^{i\boldsymbol{k}\cdot\boldsymbol{R}_{ip}} c_{\boldsymbol{k}p\sigma}, \tag{3.3}$$

where $\sum_{\boldsymbol{k}}$ is taken over the Brillouin zone.

It follows from Eq. (3.3), the Hamiltonian is written as

$$H = \sum_{\boldsymbol{k}} (c^{\dagger}_{\boldsymbol{k}1\sigma} c^{\dagger}_{\boldsymbol{k}2\sigma}) \hat{\mathcal{E}}_{\boldsymbol{k}\sigma} \begin{pmatrix} c_{\boldsymbol{k}1\sigma} \\ c_{\boldsymbol{k}2\sigma} \end{pmatrix}. \tag{3.4}$$

Here, the matrix $\hat{\mathcal{E}}_{\boldsymbol{k}\sigma}$ is

$$\hat{\mathcal{E}}_{\boldsymbol{k}\sigma} = \begin{pmatrix} \tilde{\xi}^{11}_{\boldsymbol{k}\sigma} & \tilde{\xi}^{12}_{\boldsymbol{k}\sigma} \\ \tilde{\xi}^{21}_{\boldsymbol{k}\sigma} & \tilde{\xi}^{22}_{\boldsymbol{k}\sigma} \end{pmatrix}, \tag{3.5}$$

where

$$\tilde{\xi}^{11}_{\boldsymbol{k}\sigma} = \tilde{\xi}^{22}_{\boldsymbol{k}\sigma} = 2t_1 \cos k_x, \tag{3.6}$$

$$\begin{aligned} \tilde{\xi}^{12}_{\boldsymbol{k}\sigma} =& (t_2 + t_2') \cos k_y + (t_3 + t_3') \cos(k_x + k_y) \\ &+ i[(t_2 - t_2') \sin k_x + (t_3 - t_3') \sin(k_x + k_y)], \end{aligned} \tag{3.7}$$

$$\begin{aligned}\tilde{\xi}^{21}_{\boldsymbol{k}\sigma} =&(t_2+t_2')\cos k_y + (t_3+t_3')\cos(k_x+k_y) \\ &- i[(t_2+t_2')\sin k_x + (t_2-t_2')\sin(k_x+k_y)].\end{aligned} \tag{3.8}$$

We diagonalize the Hamiltonian using the unitary matrix

$$\begin{pmatrix} c_{\boldsymbol{k}1\sigma} \\ c_{\boldsymbol{k}2\sigma} \end{pmatrix} = U_{\boldsymbol{k}\sigma} \begin{pmatrix} \alpha_{\boldsymbol{k}\sigma} \\ \beta_{\boldsymbol{k}\sigma} \end{pmatrix}. \tag{3.9}$$

Tha Hamiltonian is written as

$$H = \sum_{\boldsymbol{k}} (\epsilon^{+}_{\boldsymbol{k}\sigma} \alpha^{\dagger}_{\boldsymbol{k}\sigma} \alpha_{\boldsymbol{k}\sigma} + \epsilon^{-}_{\boldsymbol{k}\sigma} \beta^{\dagger}_{\boldsymbol{k}\sigma} \beta_{\boldsymbol{k}\sigma}), \tag{3.10}$$

where

$$\epsilon^{\pm}_{\boldsymbol{k}\sigma} = 2t_1 \cos k_x \pm \eta_{\boldsymbol{k}} \tag{3.11}$$

with

$$\begin{aligned}\eta_{\boldsymbol{k}} = \{&[(t_2+t_2')\cos k_y + (t_3+t_3')\cos(k_x+k_y)]^2 \\ &+ [(t_2-t_2')\sin k_y + (t_3-t_3')\sin(k_x+k_y)]^2\}^{\frac{1}{2}}.\end{aligned} \tag{3.12}$$

The lattice constants $a_1 = a_1'$ and $(a_2+a_2')/2$ are absorbed into the definitions of the momentum components k_x and k_y.

3.2 Parameter Sets and Fermi Surface

We adopt parameter sets shown in table 3.1 obtained by Kobayashi and Mori [53]. In parameter sets P'_{K} and P'_{M}, t_3 is variable, and the other transfer integrals remain unchanged from P_{K} and P_{M}, respectively. We define the parameter

$$r_{\mathrm{imb}} \equiv \frac{t_3/t_2 - t_3'/t_2'}{t_3/t_2}, \tag{3.13}$$

which represents the imbalance of spatial anisotropies of two type of triangles. We vary r_{imb} by varying t_3.

Figure 3.2 shows the Fermi surfaces for parameter sets P_{K} and P_{M} [54]. Fermi surfaces are folded in half because $(t_2, t_3) \neq (t_2', t_3')$. A closed Fermi surface exists, which is consistent with the experimental results of the Shubnikov-de Haas and angular-dependent magnetoresistance oscillations [61]. The Fermi surfaces have the nesting vector $\boldsymbol{Q} \simeq (\pi/c, 0)$.

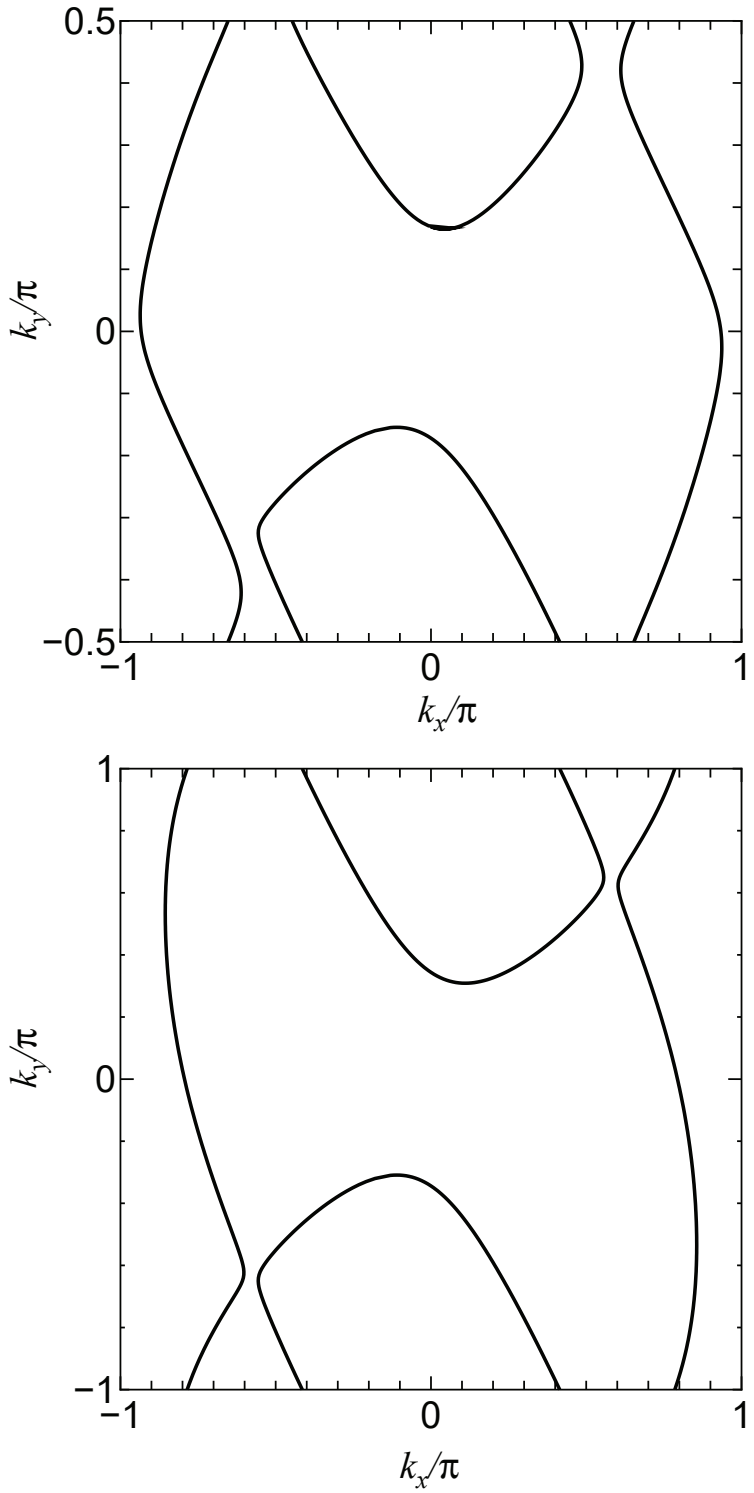

Figure 3.2: Fermi surfaces of the λ-Fe system when parameter sets $\mathrm{P_K}$ and $\mathrm{P_M}$ are assumed.

Table 3.1: Parameter sets $\mathrm{P_K}$ and $\mathrm{P_M}$ are based on values of transfer integrals t_B, t_C, t_p, t_q, t_r, t_s, and t_t obtained by Hükkel method [53]. The transfer integrals in the table are expressed as $t_1 = (-t_\mathrm{p} - t_\mathrm{q} + t_\mathrm{r})/2$, $t_2 = t_\mathrm{B}/2$, $t'_2 = t_\mathrm{C}/2$, $t_3 = t_\mathrm{s}/2$ and $t'_3 = t_\mathrm{t}/2$. Parameter sets $\mathrm{P'_K}$ and $\mathrm{P'_M}$ correspond to $\mathrm{P_K}$ and $\mathrm{P_M}$ which t_3 is variable and the other transfer integrals remain unchanged. The values of the transfer integrals are in unit 10^{-2} eV.

Transfer integrals	$\mathrm{P_K}$	$\mathrm{P'_K}$	$\mathrm{P_M}$	$\mathrm{P'_M}$
t_1	4.6325	4.6325	6.295	6.295
t_2	5.7555	5.7555	5.29	5.29
t_3	2.535	Variable	5.965	Variable
t'_2	4.145	4.145	6.205	6.205
t'_3	0.1955	0.1955	0.965	0.965

3.3 Mean Field Theory

The Hubbard Hamiltonian is

$$H = H_t + H_U, \tag{3.14}$$

where

$$H_t = \sum_{i,j}\sum_{\sigma} t_{ij} c^\dagger_{i\sigma} c_{j\sigma} - \mu \sum_i (\sum_\sigma c^\dagger_{i\sigma} c_{i\sigma} - n), \tag{3.15}$$

$$H_U = U \sum_i \hat{n}_{i\uparrow}\hat{n}_{i\downarrow}. \tag{3.16}$$

Here, $c_{i\sigma}$ is the annihilation operator of the electron on site i with spin σ, n is the number of electrons per site, and $\hat{n}_{i\sigma} = c^\dagger_{i\sigma} c_{i\sigma}$. t_{ij}, μ, and U represent the transfer integral between the sites i and j, the chemical potential, and the on-site Coulomb energy between electrons, respectivity.

We assume the Néel-(π,π), Néel-$(0,\pi)$, Néel-$(\pi,0)$, uudd-2, and uudd-2′ states as the collinear states with two sublattices. Figures 1.3(a)-(c) and 1.4(a)-(b) show the Néel and uudd states, respectively. We define four kinds of sublattices A, A′, B, and B′ as shown in Fig. 1.3(a)-(c) and 1.4(a)-(b) because $(t_2, t_3) \neq (t'_2, t'_3)$. However, the resulting states are eventually two sublattice states because of the spatial inversion symmetry. We define $c^{(X)}_{i\sigma}$

for $i \in X$=A, A$'$, B, and B$'$. We define the sublattice magnetizations m_X as

$$m_X \equiv \langle s_i^X \rangle = \frac{1}{2} \sum_{\sigma_1 \sigma_2} \langle c_{i\sigma_1}^{(X)\dagger} \sigma_{\sigma_1 \sigma_2}^z c_{i\sigma_2}^{(X)} \rangle \tag{3.17}$$

for $i \in X$ and

$$m_{\rm A} = m_{\rm A'} = -m_{\rm B} = -m_{\rm B'} \equiv m, \tag{3.18}$$

where $\langle \cdots \rangle$ is the statistical average.

The Hamiltonian in the mean-field approximation is written as

$$H_U = U \sum_X \sum_{i \in X} \{ \langle \hat{n}_{i\uparrow} \rangle \hat{n}_{i\downarrow} + \hat{n}_{i\uparrow} \langle \hat{n}_{i\downarrow} \rangle - \langle \hat{n}_{i\uparrow} \rangle \langle \hat{n}_{i\downarrow} \rangle \}. \tag{3.19}$$

The number of electrons per site n is expressed as

$$n = \langle \hat{n}_{i\uparrow} \rangle + \langle \hat{n}_{i\downarrow} \rangle \tag{3.20}$$

and

$$\langle n_{i\sigma} \rangle = \frac{n}{2} + s_\sigma s_X m \tag{3.21}$$

for $i \in X$, where $s_{\rm A} = s_{\rm A'} = 1$, $s_{\rm B} = s_{\rm B'} = -1$, $s_\uparrow = 1$ and $s_\downarrow = -1$.

We define

$$c_{\boldsymbol{k}\sigma}^{(X)} = \sqrt{\frac{4}{N}} \sum_{i \in X} e^{-i\boldsymbol{k}\cdot\boldsymbol{R}_i} c_{i\sigma}^{(X)}, \tag{3.22}$$

where the summation $\sum_{\boldsymbol{k}}^{'}$ is taken over the first Brillouin zone in antiferromagnetic phases.

It follows from Eq. (3.22), the Hamiltonian is rewritten as

$$H = \sum_{\boldsymbol{k}\sigma}^{'} (c_{\boldsymbol{k}\sigma}^{({\rm A})\dagger}, c_{\boldsymbol{k}\sigma}^{({\rm A'})\dagger}, c_{\boldsymbol{k}\sigma}^{({\rm B})\dagger}, c_{\boldsymbol{k}\sigma}^{({\rm B'})\dagger}) \hat{\mathcal{E}}_{\boldsymbol{k}\sigma} \begin{pmatrix} c_{\boldsymbol{k}\sigma}^{({\rm A})} \\ c_{\boldsymbol{k}\sigma}^{({\rm A'})} \\ c_{\boldsymbol{k}\sigma}^{({\rm B})} \\ c_{\boldsymbol{k}\sigma}^{({\rm B'})} \end{pmatrix}. \tag{3.23}$$

The components of the matrix $\hat{\tilde{\mathcal{E}}}_{\boldsymbol{k}\sigma}$ are

$$\hat{\tilde{\mathcal{E}}}_{\boldsymbol{k}\sigma} = \begin{pmatrix} \tilde{\xi}^{(\mathrm{AA})}_{\boldsymbol{k}\sigma} & \tilde{\xi}^{(\mathrm{AA'})}_{\boldsymbol{k}\sigma} & \tilde{\xi}^{(\mathrm{AB})}_{\boldsymbol{k}\sigma} & \tilde{\xi}^{(\mathrm{AB'})}_{\boldsymbol{k}\sigma} \\ \tilde{\xi}^{(\mathrm{A'A})}_{\boldsymbol{k}\sigma} & \tilde{\xi}^{(\mathrm{A'A'})}_{\boldsymbol{k}\sigma} & \tilde{\xi}^{(\mathrm{A'B})}_{\boldsymbol{k}\sigma} & \tilde{\xi}^{(\mathrm{A'B'})}_{\boldsymbol{k}\sigma} \\ \tilde{\xi}^{(\mathrm{BA})}_{\boldsymbol{k}\sigma} & \tilde{\xi}^{(\mathrm{BA'})}_{\boldsymbol{k}\sigma} & \tilde{\xi}^{(\mathrm{BB})}_{\boldsymbol{k}\sigma} & \tilde{\xi}^{(\mathrm{BB'})}_{\boldsymbol{k}\sigma} \\ \tilde{\xi}^{(\mathrm{B'A})}_{\boldsymbol{k}\sigma} & \tilde{\xi}^{(\mathrm{B'A'})}_{\boldsymbol{k}\sigma} & \tilde{\xi}^{(\mathrm{B'B})}_{\boldsymbol{k}\sigma} & \tilde{\xi}^{(\mathrm{B'B'})}_{\boldsymbol{k}\sigma} \end{pmatrix}. \tag{3.24}$$

The diagonal components of the matrix $\hat{\tilde{\mathcal{E}}}_{\boldsymbol{k}\sigma}$ are written as

$$\tilde{\xi}^{(XX)}_{\boldsymbol{k}\sigma} = -s_X s_\sigma U m - \mu. \tag{3.25}$$

Because the matrix $\hat{\tilde{\mathcal{E}}}_{\boldsymbol{k}\sigma}$ is a unitary matrix, the off-diagonal components satisfy

$$\tilde{\xi}^{XY}_{\boldsymbol{k}} = (\tilde{\xi}^{YX}_{\boldsymbol{k}})^*. \tag{3.26}$$

For the Néel-(π, π) state,

$$\tilde{\xi}^{(\mathrm{AB})}_{\boldsymbol{k}\sigma} = \tilde{\xi}^{(\mathrm{A'B'})}_{\boldsymbol{k}\sigma} = 2t_1 \cos(k_x), \tag{3.27}$$

$$\tilde{\xi}^{(\mathrm{AB'})}_{\boldsymbol{k}\sigma} = \tilde{\xi}^{(\mathrm{A'B})}_{\boldsymbol{k}\sigma} = t_2 e^{-ik_y} + t'_2 e^{ik_y}, \tag{3.28}$$

$$\tilde{\xi}^{(\mathrm{AA'})}_{\boldsymbol{k}\sigma} = \tilde{\xi}^{(\mathrm{BB'})}_{\boldsymbol{k}\sigma} = t_3 e^{-i(k_x+k_y)} + t'_3 e^{i(k_x+k_y)}. \tag{3.29}$$

For the Néel-$(\pi, 0)$ state,

$$\tilde{\xi}^{(\mathrm{AB})}_{\boldsymbol{k}\sigma} = \tilde{\xi}^{(\mathrm{A'B'})}_{\boldsymbol{k}\sigma} = 2t_1 \cos k_x, \tag{3.30}$$

$$\tilde{\xi}^{(\mathrm{AA'})}_{\boldsymbol{k}\sigma} = \tilde{\xi}^{(\mathrm{BB'})}_{\boldsymbol{k}\sigma} = t_2 e^{-ik_y} + t'_2 e^{ik_y}, \tag{3.31}$$

$$\tilde{\xi}^{(\mathrm{AB'})}_{\boldsymbol{k}\sigma} = \tilde{\xi}^{(\mathrm{BA'})}_{\boldsymbol{k}\sigma} = t_3 e^{-i(k_x+k_y)} + t'_3 e^{i(k_x+k_y)}. \tag{3.32}$$

For the Néel-$(0, \pi)$ state,

$$\tilde{\xi}^{(\mathrm{AA'})}_{\boldsymbol{k}\sigma} = \tilde{\xi}^{(\mathrm{BB'})}_{\boldsymbol{k}\sigma} = 2t_1 \cos k_x, \tag{3.33}$$

$$\tilde{\xi}^{(\mathrm{AB'})}_{\boldsymbol{k}\sigma} = \tilde{\xi}^{(\mathrm{A'B'})}_{\boldsymbol{k}\sigma} = t_2 e^{-ik_y} + t'_2 e^{ik_y}, \tag{3.34}$$

$$\tilde{\xi}^{(\mathrm{AB}')}_{\boldsymbol{k}\sigma} = \tilde{\xi}^{(\mathrm{BA}')}_{\boldsymbol{k}\sigma} = t_3 e^{-i(k_x+k_y)} + t_3' e^{i(k_x+k_y)}. \tag{3.35}$$

For the uudd-2 state,

$$\tilde{\xi}^{(\mathrm{AB})}_{\boldsymbol{k}\sigma} = \tilde{\xi}^{(\mathrm{A}'\mathrm{B}')}_{\boldsymbol{k}\sigma} = 2t_1 \cos k_x, \tag{3.36}$$

$$\tilde{\xi}^{(\mathrm{AA}')}_{\boldsymbol{k}\sigma} = \tilde{\xi}^{(\mathrm{BB}')}_{\boldsymbol{k}\sigma} = t_2 e^{-ik_y} + t_3 e^{i(k_x+k_y)}, \tag{3.37}$$

$$\tilde{\xi}^{(\mathrm{A}'\mathrm{B})}_{\boldsymbol{k}\sigma} = \tilde{\xi}^{(\mathrm{B}'\mathrm{A})}_{\boldsymbol{k}\sigma} = t_2' e^{ik_y} + t_3' e^{-i(k_x+k_y)}. \tag{3.38}$$

For the uudd-2′ state,

$$\tilde{\xi}^{(\mathrm{AB})}_{\boldsymbol{k}\sigma} = \tilde{\xi}^{(\mathrm{A}'\mathrm{B}')}_{\boldsymbol{k}\sigma} = 2t_1 \cos k_x, \tag{3.39}$$

$$\tilde{\xi}^{(\mathrm{A}'\mathrm{B})}_{\boldsymbol{k}\sigma} = \tilde{\xi}^{(\mathrm{B}'\mathrm{A})}_{\boldsymbol{k}\sigma} = t_2 e^{-ik_y} + t_3' e^{i(k_x+k_y)}, \tag{3.40}$$

$$\tilde{\xi}^{(\mathrm{BB}')}_{\boldsymbol{k}\sigma} = \tilde{\xi}^{(\mathrm{AA}')}_{\boldsymbol{k}\sigma} = t_2' e^{-ik_y} + t_3 e^{i(k_x+k_y)}. \tag{3.41}$$

We diagonalize Eq. (3.23) by the unitary transformation

$$\begin{pmatrix} c^{(A)}_{\boldsymbol{k}\sigma} \\ c^{(A')}_{\boldsymbol{k}\sigma} \\ c^{(B)}_{\boldsymbol{k}\sigma} \\ c^{(B')}_{\boldsymbol{k}\sigma} \end{pmatrix} = U_{\boldsymbol{k}\sigma} \begin{pmatrix} \gamma^{(1)}_{\boldsymbol{k}\sigma} \\ \gamma^{(2)}_{\boldsymbol{k}\sigma} \\ \gamma^{(3)}_{\boldsymbol{k}\sigma} \\ \gamma^{(4)}_{\boldsymbol{k}\sigma} \end{pmatrix}. \tag{3.42}$$

The Hamiltonian (3.14) is rewritten as

$$\begin{aligned} H =& {\sum_{\boldsymbol{k},\sigma}}' (\gamma^{(1)\dagger}_{\boldsymbol{k}\sigma}, \gamma^{(2)\dagger}_{\boldsymbol{k}\sigma}, \gamma^{(3)\dagger}_{\boldsymbol{k}\sigma}, \gamma^{(4)\dagger}_{\boldsymbol{k}\sigma}) U^{\dagger}_{\boldsymbol{k}\sigma} \hat{\mathcal{E}}_{\boldsymbol{k}\sigma} U_{\boldsymbol{k}\sigma} \begin{pmatrix} \gamma^{(1)}_{\boldsymbol{k}\sigma} \\ \gamma^{(2)}_{\boldsymbol{k}\sigma} \\ \gamma^{(3)}_{\boldsymbol{k}\sigma} \\ \gamma^{(4)}_{\boldsymbol{k}\sigma} \end{pmatrix} \\ & + NU(\frac{n^2}{4} - m^2) + Nm\mu \\ =& \sum_{\nu} {\sum_{\boldsymbol{k},\sigma}}' E^{(\nu)}_{\boldsymbol{k}\sigma} \gamma^{(\nu)\dagger}_{\boldsymbol{k}\sigma} \gamma^{(\nu)}_{\boldsymbol{k}\sigma} + NU(\frac{n^2}{4} - m^2) + Nm\mu, \end{aligned} \tag{3.43}$$

where

$$E^{(\nu)}_{\boldsymbol{k}\sigma} = \sum_{X_1,X_2} [u^{(X_1\nu)}_{\boldsymbol{k}\sigma}]^* \tilde{\xi}^{(X_1X_2)}_{\boldsymbol{k}\sigma} u^{(X_2\nu)}_{\boldsymbol{k}\sigma}, \tag{3.44}$$

$$\gamma^{(\nu)}_{\boldsymbol{k}\sigma} = \sum_{X} [u^{(X\nu)}_{\boldsymbol{k}\sigma}]^* c^{(X)}_{\boldsymbol{k}\sigma}, \tag{3.45}$$

and

$$c^{(X)}_{\boldsymbol{k}\sigma} = \sum_{\nu} u^{(X\nu)}_{\boldsymbol{k}\sigma} \gamma^{(\nu)}_{\boldsymbol{k}\sigma}. \tag{3.46}$$

$E^{(\nu)}_{\boldsymbol{k}\sigma}$ are eigenvalues of the matrix $\hat{\mathcal{E}}_{\boldsymbol{k}\sigma}$, where ν=1, 2, 3, and 4. $u^{(X\nu)}_{\boldsymbol{k}\sigma}$ are the matrix elements of the unitary matrix $U_{\boldsymbol{k}\sigma}$. We numerically calculate the eigenvalues $E^{(\nu)}_{\boldsymbol{k}\sigma}$ and components $u^{(X\nu)}_{\boldsymbol{k}\sigma}$ of the unitary matrix $U_{\boldsymbol{k}\sigma}$ for matrix $\hat{\mathcal{E}}_{\boldsymbol{k}\sigma}$.

The self-consistent equation for m_X is obtained as

$$\begin{aligned} m_X =& \frac{1}{2} s_X \sum_{\sigma_1\sigma_2} \langle c^{(X)\dagger}_{i\sigma_1} \sigma^z_{\sigma_1\sigma_2} c^{(X)}_{i\sigma_2} \rangle \\ =& \frac{1}{2} s_X \sum_{\sigma} s_\sigma \frac{4}{N} {\sum_{\boldsymbol{k}}}' [u^{(X\nu)}_{\boldsymbol{k}\sigma}]^* f(E^{\nu}_{\boldsymbol{k}\sigma}) u^{(X\nu)}_{\boldsymbol{k}\sigma}, \end{aligned} \tag{3.47}$$

where $\langle \gamma^{(\nu)\dagger}_{\boldsymbol{k}\sigma} \gamma^{(\nu)}_{\boldsymbol{k}\sigma} \rangle = f(E^{(\nu)}_{\boldsymbol{k}\sigma})$. We solve Eq. (3.47) under the condition of half filling

$$n = \frac{2}{N} \sum_{\nu} {\sum_{\boldsymbol{k},\sigma}}' f(E^{(\nu)}_{\boldsymbol{k}\sigma}) = 1. \tag{3.48}$$

The total energy E at $T = 0$ is obtained as

$$\frac{E}{N} = \frac{\langle H \rangle}{N} = \frac{1}{N} {\sum_{\nu}} {\sum_{\boldsymbol{k},\sigma}}' E^{(\nu)}_{\boldsymbol{k}\sigma} f(E^{(\nu)}_{\boldsymbol{k}\sigma}) - U(\frac{n^2}{4} - m^2) + \mu n. \tag{3.49}$$

We define the energy ΔE as $\Delta E = (E - E_{\rm PM})/N$, where E and $E_{\rm PM}$ are the energies of the antiferromagnetic and paramegnetic states, respectively.

The spin susceptibility $\chi(\boldsymbol{q})$ is

$$\chi(\boldsymbol{q}) = \frac{1}{N}\sum_{\boldsymbol{k}}\left(\left\{\frac{f(E^{(0)}_{\boldsymbol{k}1}) - f(E^{(0)}_{\boldsymbol{k}+\boldsymbol{q}1})}{4(E^{(0)}_{\boldsymbol{k}+\boldsymbol{q}1} - E^{(0)}_{\boldsymbol{k}1})} + \frac{f(E^{(0)}_{\boldsymbol{k}2}) - f(E^{(0)}_{\boldsymbol{k}+\boldsymbol{q}2})}{4(E^{(0)}_{\boldsymbol{k}2} - E^{(0)}_{\boldsymbol{k}+\boldsymbol{q}2})}\right\}A_{\boldsymbol{k}} + \left\{\frac{f(E^{(0)}_{\boldsymbol{k}1}) - f(E^{(0)}_{\boldsymbol{k}+\boldsymbol{q}2})}{4(E^{(0)}_{\boldsymbol{k}+\boldsymbol{q}2} - E^{(0)}_{\boldsymbol{k}1})} + \frac{f(E^{(0)}_{\boldsymbol{k}2}) - f(E^{(0)}_{\boldsymbol{k}+\boldsymbol{q}1})}{4(E^{(0)}_{\boldsymbol{k}2} - E^{(0)}_{\boldsymbol{k}+\boldsymbol{q}1})}\right\}B_{\boldsymbol{k}}\right) \tag{3.50}$$

above $T_{\rm N}$, where $E^{(0)}_{\boldsymbol{k}1} = \epsilon_{\boldsymbol{k}1} + \sqrt{(\epsilon^{+}_{\boldsymbol{k}23})^2 + (\epsilon^{-}_{\boldsymbol{k}23})^2}$, $E^{(0)}_{\boldsymbol{k}2} = \epsilon_{\boldsymbol{k}1} - \sqrt{(\epsilon^{+}_{\boldsymbol{k}23})^2 + (\epsilon^{-}_{\boldsymbol{k}23})^2}$,

$$A_{\boldsymbol{k}} = 1 + \frac{\epsilon^{+}_{\boldsymbol{k}23}\epsilon^{+}_{\boldsymbol{k}+\boldsymbol{q}23} + \epsilon^{-}_{\boldsymbol{k}23}\epsilon^{-}_{\boldsymbol{k}+\boldsymbol{q}23}}{\sqrt{[(\epsilon^{+}_{\boldsymbol{k}+\boldsymbol{q}23})^2 + (\epsilon^{-}_{\boldsymbol{k}+\boldsymbol{q}23})^2][(\epsilon^{+}_{\boldsymbol{k}23})^2 + (\epsilon^{-}_{\boldsymbol{k}23})^2]}}, \tag{3.51}$$

$$B_{\boldsymbol{k}} = 1 - \frac{\epsilon^{+}_{\boldsymbol{k}23}\epsilon^{+}_{\boldsymbol{k}+\boldsymbol{q}23} + \epsilon^{-}_{\boldsymbol{k}23}\epsilon^{-}_{\boldsymbol{k}+\boldsymbol{q}23}}{\sqrt{[(\epsilon^{+}_{\boldsymbol{k}+\boldsymbol{q}23})^2 + (\epsilon^{-}_{\boldsymbol{k}+\boldsymbol{q}23})^2][(\epsilon^{-}_{\boldsymbol{k}23})^2 + (\epsilon^{+}_{\boldsymbol{k}23})^2]}}, \tag{3.52}$$

$\epsilon_{\boldsymbol{k}1} = 2t_1\cos k_x, \epsilon^{+}_{\boldsymbol{k}23} = (t_2 + t_3)\cos(k_y) + (t'_2 + t'_3)\cos(k_x + k_y)$, and $\epsilon^{-}_{\boldsymbol{k}23} = (t_2 - t_3)\sin(k_y) + (t'_2 - t'_3)\sin(k_x + k_y)$.

3.4 Magnetic Structure of λ-Fe

In this section, we present the results with N=1024 $\times$ 1024. We examine the stable magnetic structure near the quantum critical point ($U \simeq U_{\rm c}$).

Figures 3.3 and 3.4 show the sublattice magnetization m and the energy ΔE as functions of U for parameter sets $\rm P_K$ and $\rm P_M$, respectively. For parameter set $\rm P_K$, the Néel-(π,π) state has the lowest energy, whereas for parameter set $\rm P_M$, the uudd-2 state has the lowest energy. For parameter set $\rm P_M$, the energy for the Néel-(π,π) is slightly larger enegy than that of the uudd-2 state. The magnetic structure of the λ-Fe system in the ground state is most likely the Néel-(π,π) or uudd-2 state because the values of the transfer integrals in parameter sets $\rm P_K$ and $\rm P_K$ contain errors. The phase transition for $\rm P_K$ is of the second-order, whereas that for $\rm P_M$ is of the first-order, where the value of m jumps from paramagnetic to uudd-2 phases.

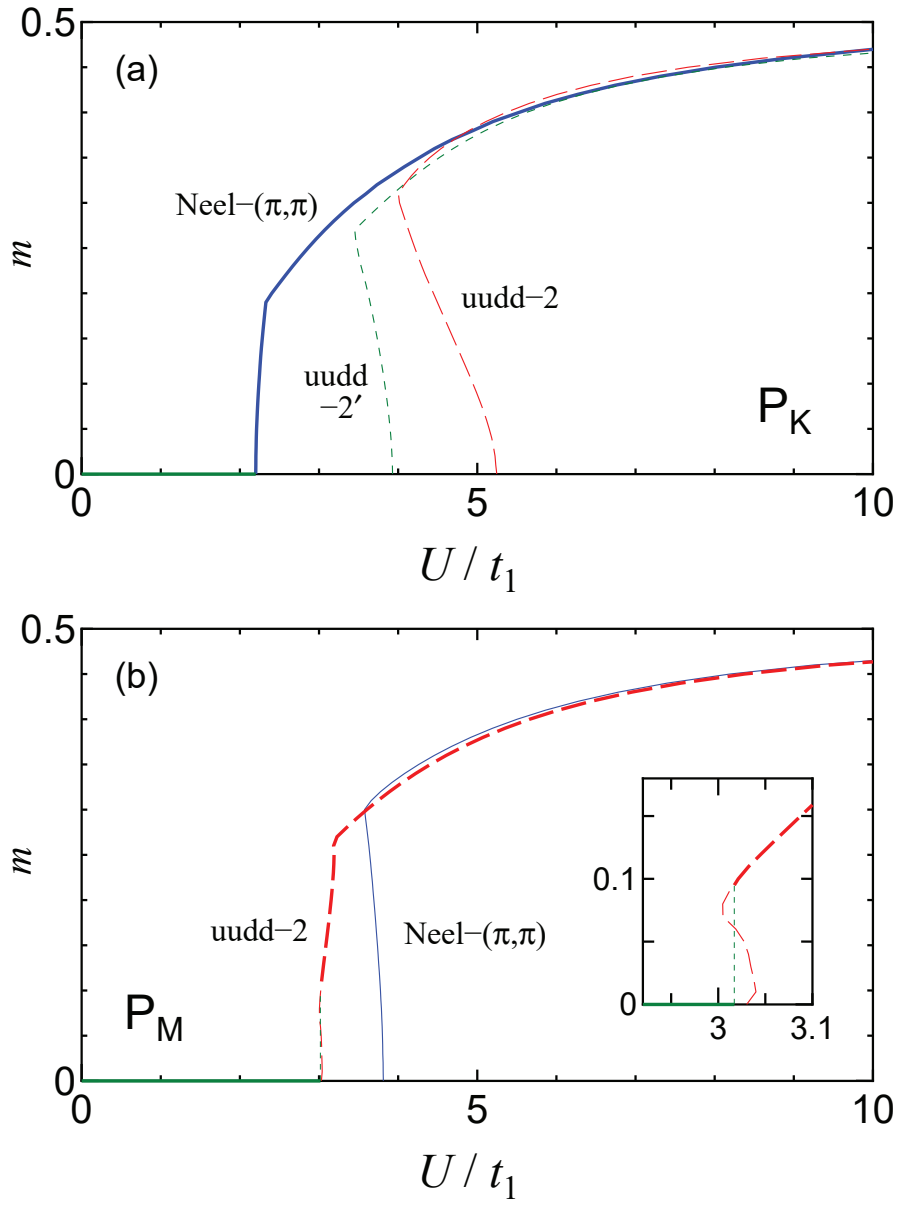

Figure 3.3: The sublattice magnetization m as functions of U at $T = 0$ for the parameter sets (a) P_K and (b) P_M. The blue solid, red dashed, and green short dashed curves are sublattice magnetization m for the Néel-(π, π), uudd-2, and uudd-2′ states, representivity.

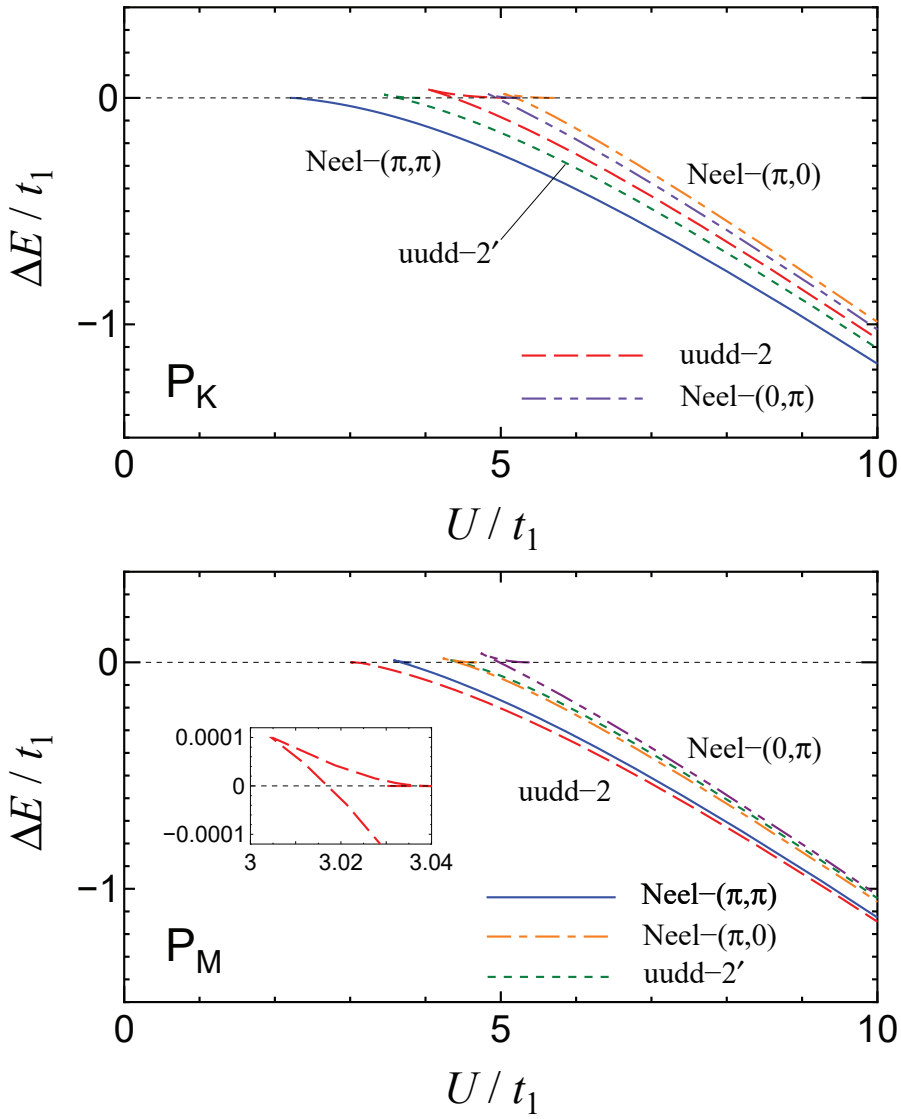

Figure 3.4: Total energy ΔE as functions of U at $T = 0$ for the parameter sets $\mathrm{P_K}$ and $\mathrm{P_M}$. The blue solid, red dashed, green short dashed curves, orange dot-dashed, and perple 2-dot-dashed are total energies ΔE for the Néel-(π, π), Néel-$(\pi, 0)$, Néel-$(0, \pi)$, uudd-2, and uudd-2′ states, representivity.

3.5 Phase Diagram and Effect of Imbalance of Spatial Anisotropy

In this section, we present the results with N=1024 $\times$ 1024.

We expand the parameter range to reveal the effect of the imbalance of spatial anisotropies of two types of triangles. We examine the U dependence of ΔE. Figure 3.5 shows the energies ΔE as functions of U for parameter set P'_{K} and $r_{\mathrm{imb}} = 0.963$. In contrast with P_{K}, , the uudd-2 has the lowest energy, and the phase transition is of the first-order. Figure 3.6 shows the energies ΔE as functions of U for parameter set P'_{M} and $r_{\mathrm{imb}} = 0.671$. In contrast with P_{M}, the Néel-(π, π) state has the lowest energy, and phase transition is of the first-order. For both parameter sets P'_{K} and P'_{M}, as r_{imb} increases, the energy of the Néel-(π, π) state increases, whereas that of the uudd-2 state decreases.

We examine the magnetic structure around U_{c}, which is determined by $\Delta E(U_{\mathrm{c}}) = 0$. Figure 3.7 and 3.9 show the r_{imb} dependence of U_{c} for the Néel-(π, π), Néel-$(0, \pi)$, Néel-$(\pi, 0)$, uudd-2, and uudd-2$'$ states. For both P'_{K} and P'_{M}, as r_{imb} increases, the Neel-(π, π) state is suppressed, whereas the uudd-2 state is enhanced. The energies of the Néel-$(\pi, 0)$, Néel-$(0, \pi)$, and uudd-2$'$ states are higher than lowest one of the Néel-(π, π) and uudd-2 states.

Figure 3.8 and 3.10 show the phase diagrams in the r_{imb}-U plane for parameter sets P_{K} and P_{M}. For parameter set P_{K}, the ground state is the Néel-(π, π) state for $r_{\mathrm{imb}} < 0.951$, whereas it is the uudd-2 state for $r_{\mathrm{imb}} > 0.951$. For parameter set P_{M}, the ground state is the Néel-(π, π) state for $r_{\mathrm{imb}} < 0.826$, whereas it is the uudd-2 state for $r_{\mathrm{imb}} > 0.826$. The phase diagram has a triple point, at which Néel-(π, π), uudd-2, and paramagnetic states coexist. Near the triple point, the phase transition from antiferromagnetic phases to the paramagnetic phase are of the first-order. When the system is far from the triple point, the phase transitions are of the second-order.

The vertical dotted line represents the value of r_{imb} for the λ-Fe system. Increasing U does not change the magnetic structure within the parameter range. In contrast, a slight change in r_{imb} can change the magnetic structure.

3.6 Summary and Discussion

We examined the magnetic structures of the itinerant electron system on the ESCATL in the ground state. We applied the mean-field approximation to the Hubbard model. For the parameter range examined in this thesis, the ground state is likely the Néel-(π,π) or uudd-2 state. In particular,

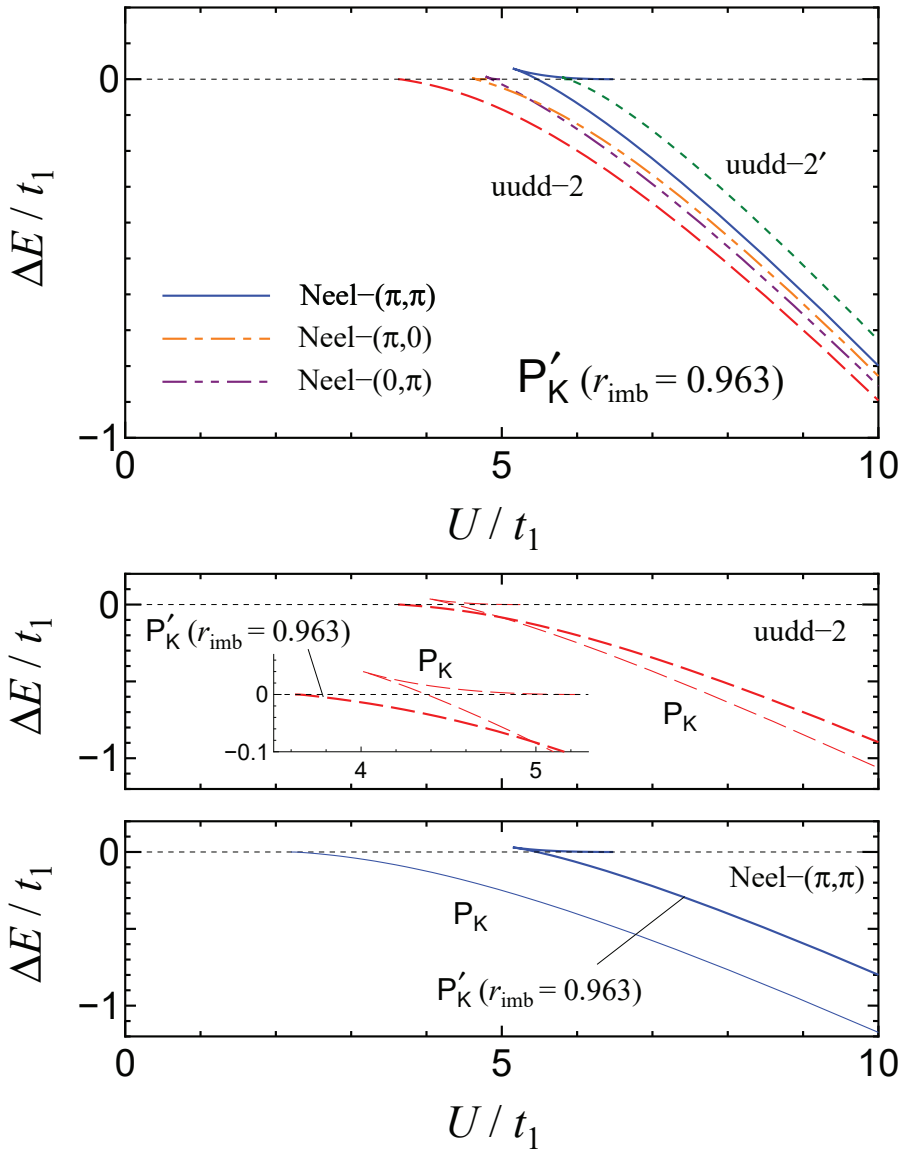

Figure 3.5: Total energy ΔE as functions of U at $T = 0$ for the parameter sets P'_{K}. The blue solid, red dashed, green short dashed curves are sublattice magnetization m for the Néel-(π, π), uudd-2, uudd-2′ states, respectively.

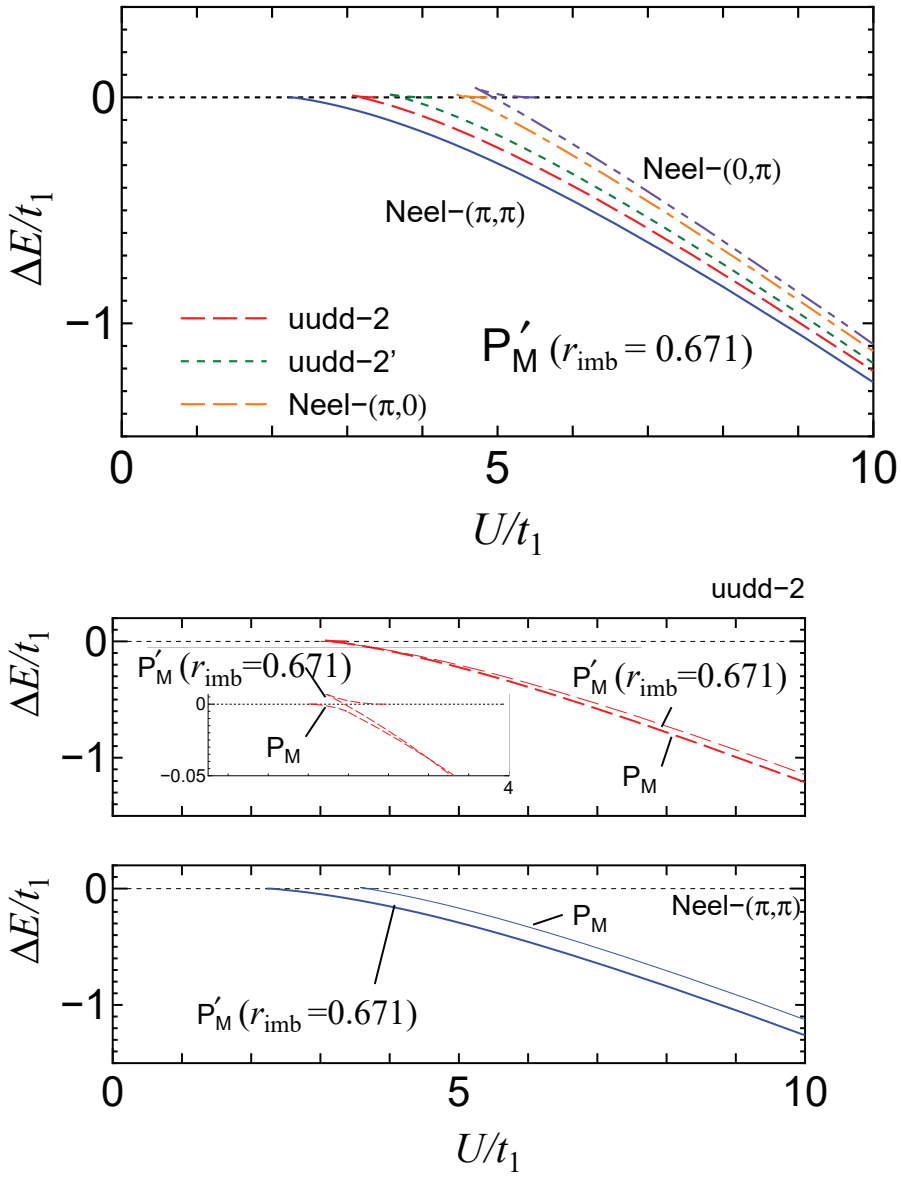

Figure 3.6: Total energy ΔE as a function of U at $T = 0$ for the parameter sets P'_{M}. The blue solid, red dashed, green short dashed curves, orange dot-dashed, and perple 2-dot-dashed are total energies for the Néel-(π, π), Néel-$(\pi, 0)$, Néel-$(0, \pi)$, uudd-2, and uudd-2$'$ states, respectively.

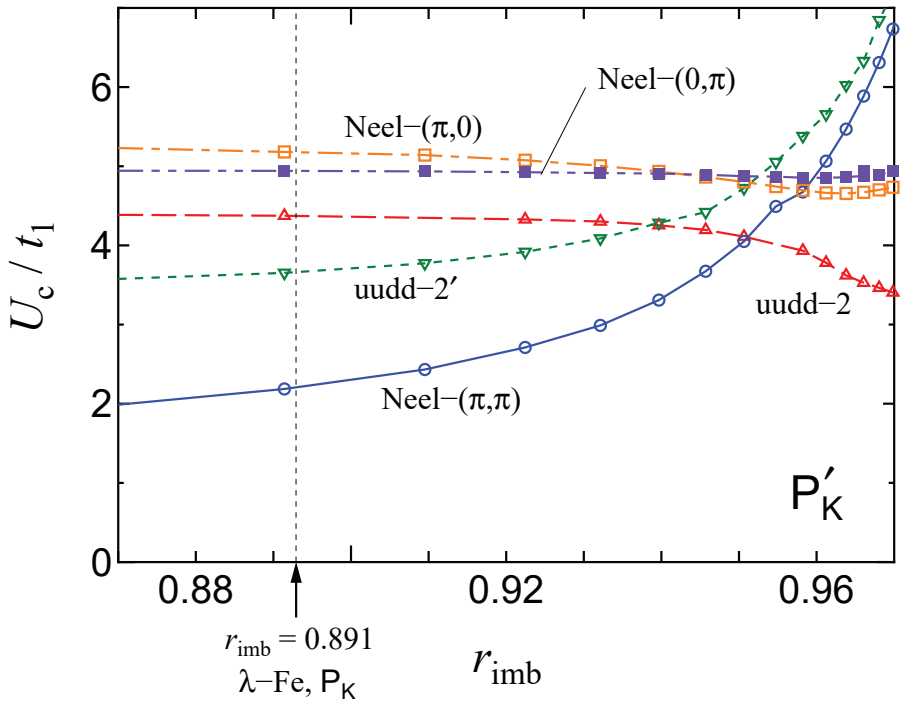

Figure 3.7: The $r_{\rm imb}$ dependence of $U_{\rm c}$ for the parameter set P'_{K}. The open circles, open squares, closed squares, open triangles, and open inverted triangles are $U_{\rm c}$ for the Néel-(π,π), Néel-$(\pi,0)$, Néel-$(0,\pi)$, uudd-2, and uudd-2′ states, respectively. $r_{\rm imb}$ for λ-Fe is $r = 0.891 > r^*_{\rm imb}$ for P'_{K}. The curves are guides to the eye.

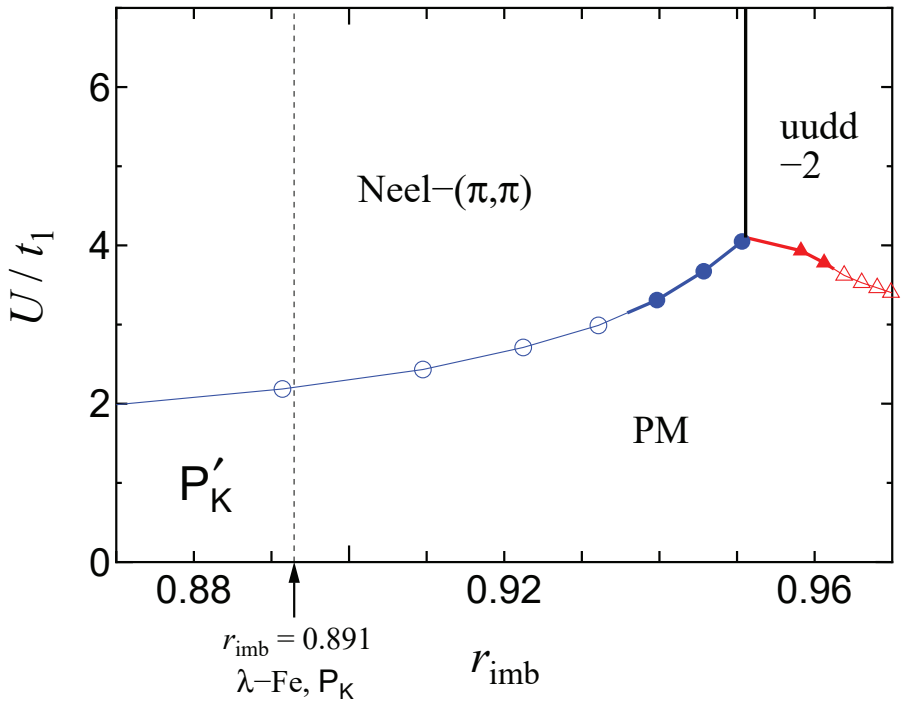

Figure 3.8: Phase diagram in the $r_{\rm imb}$-U plane for the parameter set P'_{K}. The open circles and open triangles are U for the Néel-(π,π) and uudd-2, respectively. $r^*_{\rm imb}$ is phase boundary between the Néel-(π,π) state and uudd-2 states. $r^*_{\rm imb} = 0.951$ for P'_{K}. $r_{\rm imb}$ for λ-Fe is $r = 0.891 > r^*_{\rm imb}$ for P'_{K}. The curves are guides to the eye.

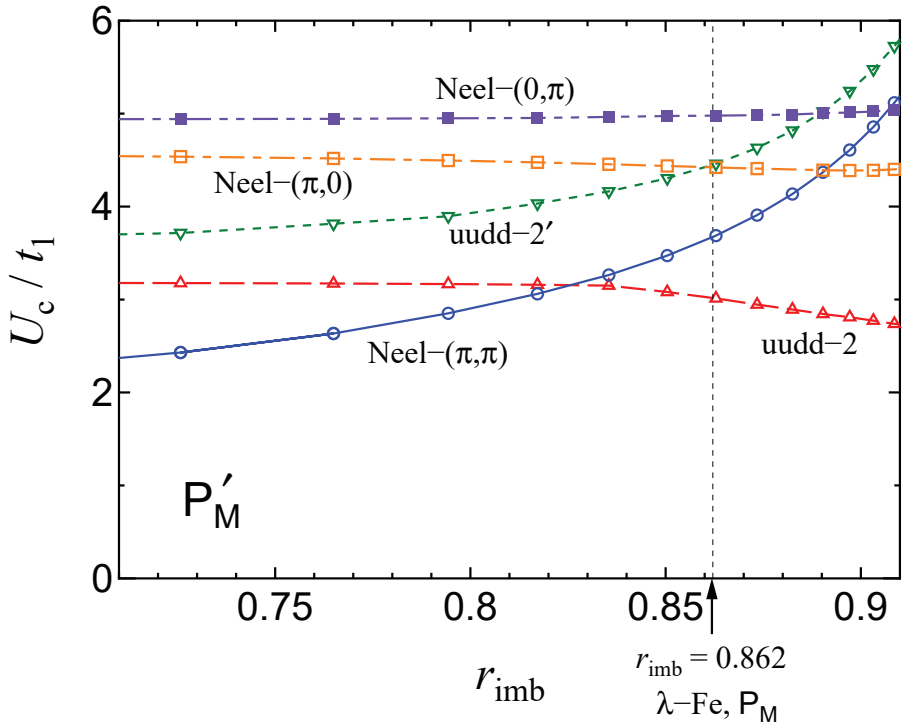

Figure 3.9: The $r_{\rm imb}$ dependence of $U_{\rm c}$ for the parameter set P'_{M}. The open circles, open squares, closed squares, open triangles, and open inverted triangles are $U_{\rm c}$ for the Néel-(π,π), Néel-$(\pi,0)$, Néel-$(0,\pi)$, uudd-2, and uudd-2′ states, respectively. $r_{\rm imb}$ for the λ-Fe system is $r = 0.862 > r^*_{\rm imb}$ for P_{M}. The curves are guides to the eye.

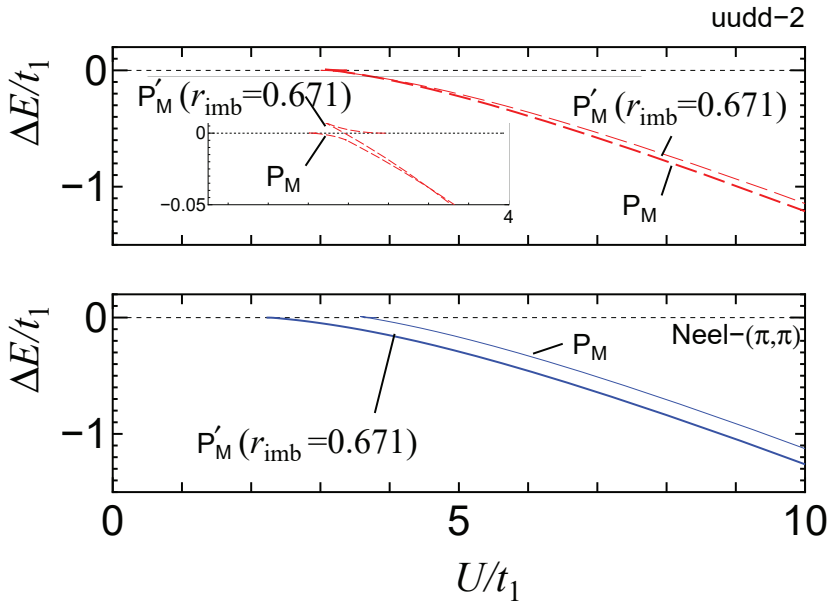

Figure 3.10: Phase diagram in the $r_{\rm imb}$-U plane for the parameter set P'_{M}. The open circles and open triangles are U for the Néel-(π,π) and uudd-2, respectively. $r^*_{\rm imb}$ is phase boundary between the Néel-(π,π) state and uudd-2 states. $r^*_{\rm imb} = 0.826$ for P'_{M}. $r_{\rm imb}$ for the λ-Fe system is $r = 0.862 > r^*_{\rm imb}$ for P_{M}. The curves are guides to the eye.

the uudd-2 state occurs when the imbalance of the spatial anisotropies of the two types of bond triangles, which is a unique feature of the ESCATL, is large. This result is consistent with the previous result on the classical Heisenberg model [28]. The phase transition is of the first order or second order, depending on the parameter set.

In the application to the λ-Fe system, we used parameter sets $\mathrm{P_K}$ and $\mathrm{P_M}$ obtained by Kobayashi and Mori, respectively [53]. For parameter set $\mathrm{P_K}$, the Néel-(π,π) state has the lowest energy near U_c, and the phase transition is of the second-order, whereas for parameter $\mathrm{P_M}$, uudd-2 state has lowest energy near U_c, and the phase transition is of the first-order. For $\mathrm{P_M}$, the energy of the Néel-(π,π) state is slightly higher than that of the uudd-2 state. Hence, the ground state of the λ-Fe system is likely the Néel-(π,π) or uudd-2 state.

The phase diagrams in the r_imb-U plane for parameter sets $\mathrm{P'_K}$ and $\mathrm{P'_M}$ have a triple point, at which the Néel-(π,π), uudd-2, and paramagnetic states coexist. Near the triple points, the phase transitions from antiferromagnetic phases to the paramagnetic phase are of the first-order. When the system is far from the triple points, the phase transitions are of the second-order. It should be examined in future whether the existence of the triple point and the change in the order of the phase transition are universal features in electron systems on the ESCATL.

The nesting vector $\boldsymbol{Q}$ for the Fermi surface in the λ-Fe system is approximately equal to $(\pi/c,0)$. This means that the stable magnetic structure is the Néel-$(\pi/c,0)$ or Néel-$(\pi/c,\pi/a)$ state as explained in the Sect. 1.2. The present result supports the latter state with $(\pi/c,\ \pi/a)$.

In a previus study, the magnetic structure of the λ-Fe system in the ground state was examined within a similar mean-field approximation [53]. However, their model differs from the present model in many ways, resulting in discrepancies in the results. One of the significant differences between the two models lies in the lattice structures. In the previous study, each BETS molecule is the lattice site, whereas in the present study, each dimer of BETS molecules is the lattice site. Hence, the physical meaning of the on-site U is different. In the previous study, U only works between two electrons on the same BETS molecule, whereas in the present study, U works between the two electrons on a dimerized BETS molecule, and such interaction is not included in the previous studies. Therefore, the effect of U differs between the two models. For example, in the previous model, when U increases, the system undergoes successive transitions, which were not found in the present study. The difference in the lattice structure results in the difference in the band filling. In the present model, the relevant band is half-filled, which favors the insulating phase as observed in the λ-Fe system at low temperatures, whereas

it is quarter-filled in the previous model. The number of sublattices differs between the two theories. Another difference is the contribution of the 3d spins. In this thesis, we consider a pure π-electron system on the basis of the current knowledge that the π-electron system is the principal component and the d-spins are passive in the exchange field created by the π-electrons, whereas in previous study, the effect of the 3d-spins has been candidated.

In the parameter region examined in this thesis, the Néel-$(0,\pi)$ and Néel-$(\pi,0)$ states do not occur in the phase diagram. These states should occur in the presnt systems when the parameter range is expanded because they occurs in localized spin systems studies previously [28] when the parameter range is expanded.

In the λ-Fe system, the AF LRO is considered to be stabilized by the factors that originate from the 3d spins of the $FeCl_4$ anions, such as the anisotropy in the spin space and/or the enhanced three dimensionality. As mentioned in Sect. 1.2, the present mean-field approximation implicitly assumes such factors. In future studies, improved theories beyond the mean-field approximation must explicitly incorporate them so that the stable AF LRO in the λ-Fe system is reproduced.

It can be expected that the above results concerning the energies of the antiferromagnetic states are hardly affected by the 3d spins, which are not incorporated in the present model, because the interactions in the π-electron system are much stronger than the other interactions (those in the 3d spin system and those between the π-electrons and 3d spins).

Chapter 4

Summary of Thesis and Conclusion

In Chapter 2, we reviewed the paper on the scaling relations of the mixed crystal λ-Fe_xGa_{1-x} [51]. We introduced the 'reverse' RKKY interaction between the π electrons via the localized 3d spins on the $FeCl_4$ anions and explained the fact that the Coulomb energy U of the λ-Fe system is near the quantum critical point ($U \simeq U_c$). The scaling law for the sublattice magnetization m below T_N but excluding temperatures in the vicinity of T_N suggests that the nesting of the Fermi surface is far from perfect, at least as regards parts of the Fermi surface. This result is consistent with the argument for T_N.

In Chapter 3, we examined the itinerant electron systems on the ESCATL within the mean-field approximation. The ESCATL has a unique feature of the imbalance of the spatial anisotropies. We examined the ground state and revealed the effect of the imbalance. We examined the Néel and uudd phases defined in Fig. 1.3 as collinear spin structures. When the imbalance of the spatial anisotropy is large, the uudd-2 states occur. The phase diagram in the r_{imb}-U plane has a triple point, at which the Néel-(π, π), uudd-2, and paramagnetic states coexist. Near the triple point, the phase transitions from antiferromagnetic phases to the paramagnetic phase are of the first-order. Far from the triple point, these transitions are of the second-order. The study of magnetic structures at finite temperatures and these in magnetic field remains as a future work. Next, we applied the theory to the λ-Fe system. The magnetic structure of the λ-Fe system has been examined by the localized spin model on the ESCATL in the previous study [28]. However, the situation that the Coulomb energy U in the λ-Fe system is near the quantum critical point ($U \simeq U_c$) cannot be reproduced in the localized spin model. Hence, we adopted the itinerant model. We revealed that the ground

state of the λ-$(BETS)_2FeCl_4$ system is likely the Néel-(π, π) or uudd-2 state.

Appendix A

Trapezoidal Formula

We use the trapezoidal formula to calculate Eqs. (3.47) and (3.49). In this appendix, we evaluate the integral error in the trapezoidal formula. Here, we consider a one-dimensional integral. The function $g(k_x)$ is defined

$$S_1 = \int_0^{\pi} g(k_x) dk_x. \tag{A.1}$$

We divide the integral interval into n equal parts and define the points k_{x0}, k_{x1}, k_{x2}, $\cdots$, and k_{xn}. We define S_2 as

$$\begin{aligned} S_2 &= \frac{2}{N} \sum_{k_x} g(k_x) \\ &= \{\frac{1}{2} \delta k_x \sum_{l=0}^{n-1} [g(k_{xl}) + g(k_{xl+1})]\} \end{aligned} \tag{A.2}$$

where $\delta k_x = \frac{\pi}{n}$ and $k_{xl} = \frac{l\pi}{n}$. We define s_1 and s_2 as

$$s_1 = \int_{k_{x0}}^{k_{x1}} dk_x g(k_x) = \int_{k_{x0}}^{k_{x0}+\delta k_x} dk_x g(k_x) \tag{A.3}$$

and

$$s_2 = \frac{1}{2} \delta k_x (g(k_{x0}) + g(k_{x1})). \tag{A.4}$$

The integral error is written as $n|s_1 - s_2|$. The Taylor expansion of

Eq. (A.3) is

$$
\begin{aligned}
s_1 &= \int_{k_{x0}}^{k_{x0}+\delta k_x} dk_x g(k_x) = \int_0^{\delta k_x} d\xi g(k_{x0}+\xi) \\
&= \int_0^{\delta k_x} d\xi [g(k_{x0}) + g'(k_{x0})\xi + \frac{g''(k_{x0})}{2!}(\xi)^2 + \frac{g'''(k_{x0})}{3!}(\xi)^3 \cdots] \\
&= [g(k_{x0})\xi + \frac{g'(k_{x0})}{2}(\xi)^2 + \frac{g''(k_{x0})}{3!}(\xi)^3 + \frac{g'''(k_{x0})}{4!}(\xi)^4 \cdots]_0^{\delta k_x} \\
&= [g(k_{x0})\delta k_x + \frac{g'(k_{x0})}{2}(\delta k_x)^2 + \frac{g''(k_{x0})}{3!}(\delta k_x)^3 + \frac{g'''(k_{x0})}{4!}(\delta k_x)^4 \cdots]. \quad \text{(A.5)}
\end{aligned}
$$

We expand Eqs. (A.4) and (A.3) around k_{x0}. The Taylor expansion of Eq. (A.4) is

$$
\begin{aligned}
s_2 &= \frac{1}{2}\delta k_x (g(k_{x0}) + g(k_{x1})) \\
&= \frac{1}{2}\delta k_x [g(k_{x0}) + g(k_{x0}+\delta k_x)] \\
&= \frac{1}{2}\delta k_x [g(k_{x0}) + g(k_{x0}) + g'(k_{x0})\delta k_x + \frac{g''(k_{x0})}{2!}(\delta k_x)^2 + \frac{g'''(k_{x0})}{3!}(\delta k_x)^3]
\end{aligned} \quad \text{(A.6)}
$$

The integral error $n|s_1 - s_2|$ is

$$
\begin{aligned}
n|s_1 - s_2| &= n\frac{g''(k_{x0})}{3}(\delta k_{x0})^3 - n\frac{g''(k_{x0})}{4}(\delta k_{x0})^3 + \mathrm{O}((\delta k_{x0})^4) \\
&\simeq n\frac{g''(k_{x0})}{12}(\delta k_{x0})^3 = n\frac{g''(k_{x0})}{12}(\frac{\pi}{n})^3 \\
&= \frac{g''(k_{x0})}{12}\frac{\pi^3}{n^2}. \quad \text{(A.7)}
\end{aligned}
$$

Hence, in one-dimensional systems, the integral error is proportional to the number of divisions n^{-2}.

Next, we consider two-dimensional systems. We consider the integral

$$
S_1 = \int_0^{\pi}\int_0^{\pi} g(k_x, k_y) dk_x dk_y \quad \text{(A.8)}
$$

for an arbitrary function $g(k_x, k_y)$. We define S_2 as

$$
S_2 = \left(\frac{2}{N}\right)^2 \sum_{k_x, k_y} g(k_x, k_y)
$$

$$
\begin{aligned}
=&\frac{1}{4}\delta k_x \delta k_y \sum_{l=0}^{n-1}\sum_{l'=0}^{m-1}(g(k_{xl},k_{yl'})+g(k_{xl+1},k_{yl'}) \\
&+g(k_{xl},k_{yl'+1})+g(k_{xl+1},k_{yl'+1})),
\end{aligned} \tag{A.9}
$$

where $\delta k_y = \frac{\pi}{n}$. We define s_1 and s_2 as

$$
s_1 = \int_{k_{x0}}^{k_{x1}}\int_{k_{y0}}^{k_{y1}} dk_x dk_y g(k_x,k_y) \tag{A.10}
$$

and

$$
\begin{aligned}
s_2 =&\frac{1}{4}\delta k_x \delta k_y [g(k_{x0},k_{y0})+g(k_{x0}+\delta k_x,k_{y0}) \\
&+g(k_{x0},k_{y0}+\delta k_y)+g(k_{x0}+\delta k_x,k_y+\delta k_y)],
\end{aligned} \tag{A.11}
$$

respectively. s_1 is

$$
\begin{aligned}
s_1 =& \int_{k_{x0}}^{k_{x0}+\delta k_x}\int_{k_{y0}}^{k_{y0}+\delta k_y} dk_x dk_y g(k_x,k_y) = \int_0^{\delta k_x}\int_0^{\delta k_y} d\xi d\eta g(k_{x0}+\xi,k_{y0}+\eta) \\
=&\int_0^{\delta k_x}\int_0^{\delta k_y} d\xi d\eta (g(k_{x0},k_{y0})+g'(k_{x0},k_{y0})\xi + g'(k_{x0},k_{y0}+\cdots)\eta \\
&+\frac{g''(k_{x0},k_{y0})}{2!}(\eta)^2+\frac{g''(k_{x0},k_{y0})}{2!}(\xi)^2+\frac{g''(k_{x0},k_{y0})}{2!}\xi\eta) \\
=&[[g(k_{x0},k_{y0})\xi\eta + g'(k_{x0},k_{y0})\frac{\xi^2}{2}\eta + g'(k_{x0},k_{y0})\frac{\eta^2}{2}\xi \\
&+\frac{g''(k_{x0},k_{y0})}{2!}\frac{\eta^3}{3}\xi+\frac{g''(k_{x0},k_y)}{2!}\frac{\xi^3}{3}\eta+\frac{g''(k_x,k_y)}{2!}\frac{\xi^2}{2}\frac{\eta^2}{2}+\cdots]_0^{\delta k_x}]_0^{\delta k_y} \\
=&g(k_{x0},k_{y0})\delta k_x\delta k_y + g'(k_{x0},k_{y0})\frac{\delta k_x^2}{2}\delta k_y + g'(k_{x0},k_{y0})\frac{\delta k_x^2}{2}\delta k_y \\
&+\frac{g''(k_{x0},k_{y0})}{2!}\frac{\delta k_x^3}{3}\delta k_y+\frac{g''(k_{x0},k_{y0})}{2!}\frac{\delta k_y^3}{3}\delta k_x+\frac{g''(k_{x0},k_{y0})}{2!}\frac{\delta k_x^2}{2}\frac{\delta k_y^2}{2}+\cdots.
\end{aligned} \tag{A.12}
$$

s_2 is

$$
\begin{aligned}
s_2 =&\frac{1}{4}\delta k_x \delta k_y (g(k_{x0},k_{y0})+g(k_{x0}+\delta k_x,k_{y0}) \\
&+g(k_{x0},k_{y0}+\delta k_y)+g(k_{x0}+\delta k_x,k_y+\delta k_y)) \\
=&\frac{1}{4}\delta k_x \delta k_y [g(k_{x0},k_{y0})+g(k_{x0},k_{y0})
\end{aligned}
$$

$$
\begin{aligned}
&+ g'(k_{x0}, k_{y0})\delta k_x + (\delta k_x)^2 \frac{g''(k_{x0}, k_{y0})}{2!} + \cdots \\
&+ g(k_{x0}, k_{y0}) + g'(k_{x0}, k_{y0})\delta k_y \\
&+ (\delta k_y)^2 \frac{g''(k_{x0}, k_{y0})}{2!} + \cdots \\
&+ g(k_{x0}, k_{y0}) + g'(k_{x0}, k_{y0})\delta k_x \\
&+ g'(k_{x0}, k_{y0})\delta k_y + \frac{g''(k_{x0}, k_{y0})}{2!}\delta k_x \delta k_y + \cdots].
\end{aligned} \tag{A.13}
$$

The integral error $n^2|s_1 - s_2|$ is

$$
\begin{aligned}
n^2|s_1 - s_2| &\propto n^2 g''(k_{x0}, k_{y0})(\frac{\pi^3}{n^3}) \\
&= g''(k_{x0}, k_{y0})(\frac{\pi^3}{n}).
\end{aligned} \tag{A.14}
$$

Hence, in two-dimensional systems, the integral error is proportional to the number of divisions n^{-1}.

Figure A.1 shows the total energy ΔE as a function of U for Néel-(π,π) state. The values of ΔE for number of divisions 1024×1024 are nearly equal to those for divisions 2048×2048.

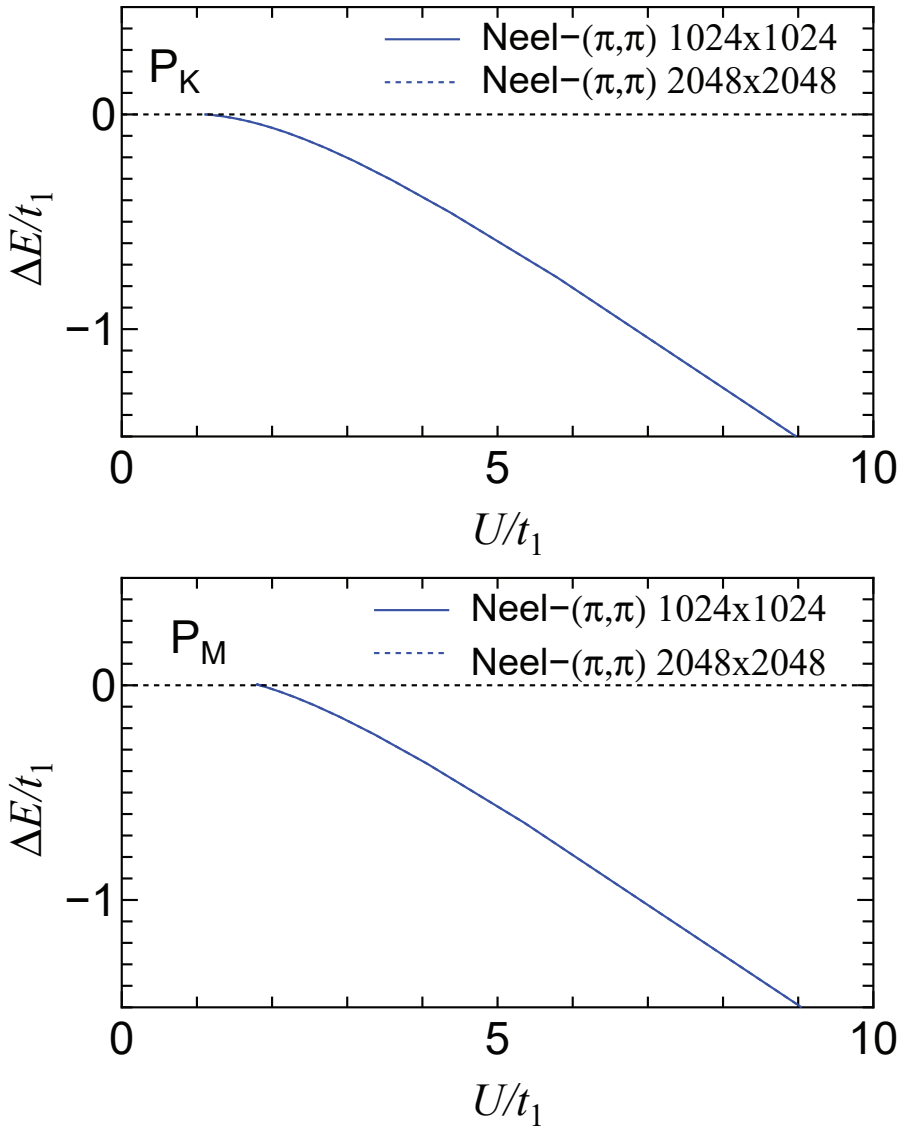

Figure A.1: ΔE as a function of U at $T = 0$ for the parameter sets $\mathrm{P_K}$ and $\mathrm{P_M}$. The blue solid and dotted curves are total energies of the Néel-(π, π) state for 1024×1024 and 2048×2048, respectively.

Appendix B

Linear Response Theory

In this appendix, we derive the susceptibility of free electrons by the linear response theory [63]. We assume the case where a time-independent external field is applied in the z-direction. The Hamiltonian for zeeman energy is written as

$$H_{\rm ext} = -\boldsymbol{M} \cdot \boldsymbol{h} = -Mh. \tag{B.1}$$

The statistical average of M is written as

$$\langle M \rangle = \sum_n \exp(-\beta E_n) M_{nn} / \sum_n \exp(-\beta E_n) = {\rm Tr}(\rho M), \tag{B.2}$$

and E_n is an energy eigenvalue of the Hamiltonian H, Here, ρ is

$$\rho = \exp(-\beta H)/{\rm Tr}\exp(-\beta H) = \exp(-\beta H)/Z, \tag{B.3}$$

where Z is the partition function.

We calculate the statistical average $\langle M \rangle_{\rm ext}$ in the system in the external field h. When $H_{\rm tot} = H + H_{\rm ext}$,

$$\exp(-\beta H_{\rm tot}) = \exp(-\beta H) u(\beta). \tag{B.4}$$

Differentiating both sides of Eq.(B.4) with regard to β, we obtain

$$-H_{\rm tot}\exp(-\beta H_{\rm tot}) = -H\exp(-\beta H)u(\beta) + \exp(-\beta H)\frac{d}{d\beta}u(\beta). \tag{B.5}$$

Hence, we obtain

$$\frac{d}{d\beta}u(\beta) = -\exp(\beta H)H_{\rm ext}\exp(-\beta H)u(\beta) \equiv -H^{\rm M}_{\rm ext}u(\beta), \tag{B.6}$$

where $H^{\rm M}_{\rm ext}$ is in the Heisenberg representation for imaginary time. We integrate both sides of Eq. (B.6) with reagard to β. We obtain

$$\begin{aligned} u(\beta) &= C - \int_0^\beta d\tau H^{\rm M}_{\rm ext}u(\beta) \\ &= C - \int_0^\beta d\tau H^{\rm M}_{\rm ext} - \int_0^\beta d\tau_1 \int_0^\beta d\tau H^{\rm M}_{\rm ext}H^{\rm M}_{\rm ext}u(\beta) \\ &= C - \int_0^\beta d\tau H^{\rm M}_{\rm ext} + {\rm O}(H^2_{\rm ext}). \end{aligned} \tag{B.7}$$

Because $u(\beta) = 1$ when $H_{\rm ext} = 0$, we obtain

$$u(\beta) = 1 - \int_0^\beta d\tau H^{\rm M}_{\rm ext}(\tau) + {\rm O}(H^2_{\rm ext}). \tag{B.8}$$

From Eq. (B.8), we obtain

$$\begin{aligned} \langle M\rangle_{\rm ext} =& {\rm Tr}[\exp(-\beta H)u(\beta)M]/{\rm Tr}[\exp(-\beta H)u(\beta)] \\ =& {\rm Tr}[\exp(-\beta H)\{1 - \int_0^\beta d\tau H^{\rm M}_{\rm ext}(\tau) + {\rm O}(H^2_{\rm ext})\}M]/ \\ & {\rm Tr}[\exp(-\beta H)\{1 - \int_0^\beta d\tau H^{\rm M}_{\rm ext}(\tau) + {\rm O}(H^2_{\rm ext})\}] \\ =& -\int_0^\beta d\tau \langle H^{\rm M}_{\rm ext}(\tau)M\rangle + {\rm O}(H^2_{\rm ext}) \\ =& \chi B + {\rm O}(H^2_{\rm ext}) \end{aligned} \tag{B.9}$$

χ is written as

$$\chi = \int_0^\beta d\tau \langle M^{\rm M}(\tau)M\rangle = \int_0^\beta d\tau \langle e^{\tau H}Me^{-\tau H}M\rangle. \tag{B.10}$$

We derive the Kubo formula. We assume an external field that depends on time. We write the wave function $|\psi(t)\rangle$ in the ground state as

$$|\psi(t)\rangle = \exp(-\frac{iHt}{\hbar})U(t)|\psi(\infty)\rangle, \tag{B.11}$$

where $U(t)$ is a unitary matrix and $\psi(\infty)\rangle$ is the wave function in the ground state for $H_{\rm h} = 0$. Hence, from the Schrödinger equation

$$i\hbar\frac{d}{dt}|\psi(t)\rangle = H|\psi(t)\rangle, \tag{B.12}$$

we obtain

$$i\hbar\frac{d}{dt}U(t) = \exp(\frac{iHt}{\hbar})H_{\rm ext}(t)\exp(-\frac{iHt}{\hbar})U(t) \equiv H^{\rm H}_{\rm ext}(t)U(t). \tag{B.13}$$

By the itiberant approximation, $U(t)$ becomes

$$U(t) = 1 - \frac{i}{\hbar}\int_{\infty}^{t} dt' H^{\rm H}_{\rm ext}(t') + O(H^2_{\rm ext}). \tag{B.14}$$

The statistical average of any operator A is written as

$$\begin{aligned}\langle\psi(t)|A|\psi(t)\rangle &= \langle\psi(t)|u^{\dagger}(t)A^{\rm H}(t)u(t)|\psi(t)\rangle \qquad\qquad (B.15)\\ &= \langle\psi(t)|A^{\rm H}(t)|\psi(t)\rangle - \frac{i}{\hbar}\langle\psi(t)|[A^{\rm H}(t), H^{\rm H}_{\rm ext}(t')]|\psi(t)\rangle + O(H^2_{\rm ext}).\end{aligned}$$

The statistical average of A at time t is written as

$$\mathrm{Tr}[A\rho_{\rm tot}(t)] = \sum_n \rho_n\langle n(t)|A|n(t)\rangle. \tag{B.16}$$

The deviation $\delta\langle A^{\rm H}(t)\rangle$ from the average $\langle A^{\rm H}(t)\rangle$ in the thermal equilibrium is

$$\delta\langle A^{\rm H}(t)\rangle = -\frac{i}{\hbar}\int_{-\infty}^{t} dt'\langle[A^{\rm H}(t), H^{\rm H}_{\rm ext}(t')]\rangle + O(H^2_{\rm ext}) \tag{B.17}$$

We assume the alternating magnetic field $h\exp(-i\omega t')$. An external field $H^{\rm H}_{\rm ext}$ is written as

$$H^{\rm H}_{\rm ext} = -M^{\rm H}(t')h\exp(i\omega(t-t')) \tag{B.18}$$

Substituting M for A in Eq. (B.17), Eq. (B.17) becomes

$$\delta\langle M^{\rm H}(t)\rangle = \chi(\omega)\exp(-i\omega t)h, \tag{B.19}$$

where $\chi(\omega)$ is the dynamical magnetic susceptibility, which written as

$$\chi(\omega) = i \int_{-\infty}^{t} d't \langle [M^{\mathrm{H}}(t), M^{\mathrm{H}}(t')] \rangle \exp(i\omega(t-t')). \tag{B.20}$$

We derive the free electron susceptibility. We substitute

$$M_{\boldsymbol{q}} = \sum_{\boldsymbol{k}\sigma} \sigma c^{\dagger}_{\boldsymbol{k}\sigma} c_{\boldsymbol{k}+\boldsymbol{q}\sigma} \tag{B.21}$$

in the Kubo formula

$$\chi_0(\boldsymbol{q}, \omega) = i \int_0^{\infty} dt \langle [M^{\mathrm{H}}_{\boldsymbol{q}}(t), M^{\mathrm{H}}_{-\boldsymbol{q}}(0)] \exp(i\omega t). \tag{B.22}$$

Because

$$[c^{\dagger}_{\boldsymbol{k}\sigma}(t) c_{\boldsymbol{k}+\boldsymbol{q}\sigma}(t), c^{\dagger}_{\boldsymbol{k}+\boldsymbol{q}\sigma} c_{\boldsymbol{k}\sigma}] = \exp[i \frac{(\epsilon_{\boldsymbol{k}} - \epsilon_{\boldsymbol{k}+\boldsymbol{q}})}{\hbar} t] [c^{\dagger}_{\boldsymbol{k}\sigma} c_{\boldsymbol{k}+\boldsymbol{q}\sigma}, c^{\dagger}_{\boldsymbol{k}+\boldsymbol{q}\sigma} c_{\boldsymbol{k}\sigma}],$$

$c^{\dagger}_{\boldsymbol{k}\sigma}(t) = c^{\dagger}_{\boldsymbol{k}\sigma} e^{i\frac{\epsilon_1}{\hbar}t}$, and

$$[c^{\dagger}_{\boldsymbol{k}\sigma} c_{\boldsymbol{k}+\boldsymbol{q}\sigma}, c^{\dagger}_{\boldsymbol{k}+\boldsymbol{q}} c_{\boldsymbol{k}\sigma}] = c^{\dagger}_{\boldsymbol{k}\sigma} c_{\boldsymbol{k}\sigma} - c^{\dagger}_{\boldsymbol{k}+\boldsymbol{q}\sigma} c_{\boldsymbol{k}+\boldsymbol{q}\sigma},$$

we obtain

$$\begin{aligned} \chi_0(\boldsymbol{q}, \omega) &= i \int_0^{\infty} dt \exp[i(\epsilon_{\boldsymbol{k}+\boldsymbol{q}} - \epsilon_{\boldsymbol{k}} + \hbar\omega)t](f(\epsilon_{\boldsymbol{k}}) - f(\epsilon_{\boldsymbol{k}+\boldsymbol{q}})) \\ &= \frac{f(\boldsymbol{k}) - f(\boldsymbol{k}+\boldsymbol{q})}{\hbar\omega - \epsilon_{\boldsymbol{k}+\boldsymbol{q}} + \epsilon_{\boldsymbol{k}}}, \end{aligned} \tag{B.23}$$

where $\langle c^{\dagger}_{\boldsymbol{k}\sigma} c_{\boldsymbol{k}\sigma} \rangle \equiv f(\epsilon_{\boldsymbol{k}})$ and $\langle c^{\dagger}_{\boldsymbol{k}+\boldsymbol{q}\sigma} c_{\boldsymbol{k}+\boldsymbol{q}\sigma} \rangle \equiv f(\epsilon_{\boldsymbol{k}+\boldsymbol{q}})$.

Appendix C

Derivation of Eq. (3.50)

In this appendix, we derive Eq. (3.50) for the magnetic susceptibility. We consider a π-electron system in a weak magnetic field h^z in the z-axis direction.

The Hubbard Hamiltonian is written as

$$H = H_t + H_U + H_h \tag{C.1}$$

with

$$H_t = \sum_{i,j}\sum_{\sigma} t_{ij} c^{\dagger}_{i\sigma} c_{j\sigma} - \mu \sum_{i}\sum_{\sigma} c^{\dagger}_{i\sigma} c_{i\sigma}, \tag{C.2}$$

$$H_U = U \sum_{i} n_{i\uparrow} n_{i\downarrow}, \tag{C.3}$$

$$H_h = h^z \sum_{i,\boldsymbol{q}} e^{i\boldsymbol{q}\cdot\boldsymbol{r}_i} s^z_{i\sigma}. \tag{C.4}$$

We define $s^z_{i\sigma}$ as

$$s^z_{i\sigma} = \frac{1}{2} \sum_{\sigma_1,\sigma_2} c^{\dagger}_{i\sigma} \sigma^z_{\sigma_1\sigma_2} c_{i\sigma}. \tag{C.5}$$

We assume a unit cell shown in Fig. 2.1 because $(t_2, t_3) \neq (t'_2, t'_3)$. The the lattice constant in c-direction is same as the original lattice. That in a-direction is twice as large as the original lattice. The label $p = 1, 2$ denote two sites in the unit cell.

We define

$$c_{\boldsymbol{k}p\sigma} = \sqrt{\frac{2}{N}} \sum_i e^{-i\boldsymbol{k}\cdot\boldsymbol{r}_{ip}} c_{ip\sigma}, \tag{C.6}$$

where N is the number of the dimerized pairs of BETS molecules, which denotes

$$c^\dagger_{ip\sigma} = \sqrt{\frac{2}{N}} \sum_{\boldsymbol{k}} e^{i\boldsymbol{k}\cdot\boldsymbol{r}_{ip}} c^\dagger_{\boldsymbol{k}p\sigma}, \tag{C.7}$$

where the summation $\sum_{\boldsymbol{k}}$ is taken over a first Brillouin zone. The Hamiltonian Eq. (C.1) is rewritten as

$$\begin{aligned}
H_t + H_U &= \sum_{\boldsymbol{k},\sigma,pp'} \epsilon_{\boldsymbol{k}pp'} c^\dagger_{\boldsymbol{k}p\sigma} c_{\boldsymbol{k}p\sigma} + \frac{1}{2} h^z \sum_{\boldsymbol{k},\boldsymbol{q},p} \sum_{\sigma_1\sigma_2} c^\dagger_{\boldsymbol{k}p\sigma_1} \sigma^z_{\sigma_1\sigma_2} c_{\boldsymbol{k}+\boldsymbol{q}p\sigma_2} \\
&= {\sum_{\boldsymbol{k},\sigma,p,p'}}' \epsilon_{\boldsymbol{k}pp'} c^\dagger_{\boldsymbol{k}p\sigma} c_{\boldsymbol{k}p'\sigma} + \frac{1}{2} h^z {\sum_{\boldsymbol{k},\boldsymbol{q},p}}' \sum_{\sigma_1\sigma_2} c^\dagger_{\boldsymbol{k}p\sigma_1} \sigma^z_{\sigma_1\sigma_2} c_{\boldsymbol{k}+\boldsymbol{q}p\sigma_2} \\
&+ {\sum_{\boldsymbol{k},\sigma,p,p'}}' \epsilon_{\boldsymbol{k}+\boldsymbol{q}pp'} c^\dagger_{\boldsymbol{k}+\boldsymbol{q}p\sigma} c_{\boldsymbol{k}+\boldsymbol{q}p'\sigma} + \frac{1}{2} h^z {\sum_{\boldsymbol{k},\boldsymbol{q},p}}' \sum_{\sigma_1\sigma_2} c^\dagger_{\boldsymbol{k}+\boldsymbol{q}p\sigma_1} \sigma^z_{\sigma_1\sigma_2} c_{\boldsymbol{k}p\sigma_2} \\
&= {\sum_{\boldsymbol{k},\sigma}}' (c^\dagger_{\boldsymbol{k}1\sigma}\ c^\dagger_{\boldsymbol{k}2\sigma}\ c^\dagger_{\boldsymbol{k}+\boldsymbol{q}1\sigma}\ c^\dagger_{\boldsymbol{k}+\boldsymbol{q}2\sigma}) \hat{\mathcal{E}}_{\boldsymbol{k}\sigma} \begin{pmatrix} c_{\boldsymbol{k}1\sigma} \\ c_{\boldsymbol{k}2\sigma} \\ c_{\boldsymbol{k}+\boldsymbol{q}1\sigma} \\ c_{\boldsymbol{k}+\boldsymbol{q}2\sigma} \end{pmatrix},
\end{aligned} \tag{C.8}$$

where

$$\hat{\mathcal{E}}_{\boldsymbol{k}\sigma} = \begin{pmatrix} \epsilon_{\boldsymbol{k}1} & \epsilon^+_{\boldsymbol{k}23} - i\epsilon^-_{\boldsymbol{k}23} & h^z\sigma/2 & 0 \\ \epsilon^+_{\boldsymbol{k}23} + i\epsilon^-_{\boldsymbol{k}23} & \epsilon_{\boldsymbol{k}1} & 0 & h^z\sigma/2 \\ h^z\sigma/2 & 0 & \epsilon_{\boldsymbol{k}+\boldsymbol{q}1} & \epsilon^+_{\boldsymbol{k}+\boldsymbol{q}23} - i\epsilon^-_{\boldsymbol{k}+\boldsymbol{q}23} \\ 0 & h^z\sigma/2 & \epsilon^+_{\boldsymbol{k}+\boldsymbol{q}23} + i\epsilon^-_{\boldsymbol{k}+\boldsymbol{q}23} & \epsilon_{\boldsymbol{k}+\boldsymbol{q}23} \end{pmatrix} \tag{C.9}$$

and the summation ${\sum_{\boldsymbol{k}}}'$ is taken over a Brillouin zone in an antiferromagnetic phase. Here, $\epsilon_{\boldsymbol{k}1} = 2t_1 \cos k_x$, $\epsilon^+_{\boldsymbol{k}23} = (t_2 + t'_2)\cos(k_y) + (t_3 + t'_3)\cos(k_x + k_y)$, $\epsilon^-_{\boldsymbol{k}23} = (t_2 - t'_2)\sin(k_y) + (t_3 - t'_3)\sin(k_x + k_y)$.

The Hamiltonian (C.8) is diagonalized by the unitary transformation

$$\begin{pmatrix} c_{\boldsymbol{k}1\sigma} \\ c_{\boldsymbol{k}2\sigma} \\ c_{\boldsymbol{k}+\boldsymbol{q}1\sigma} \\ c_{\boldsymbol{k}+\boldsymbol{q}2\sigma} \end{pmatrix} = U_{\boldsymbol{k}\sigma} \begin{pmatrix} \alpha_{\boldsymbol{k}\sigma} \\ \beta_{\boldsymbol{k}\sigma} \\ \gamma_{\boldsymbol{k}\sigma} \\ \delta_{\boldsymbol{k}\sigma} \end{pmatrix}, \tag{C.10}$$

where $U_{\boldsymbol{k}\sigma}$ is a unitary matrix.

We derive the eigenvalues and eigenvectors for the matrix $\hat{\mathcal{E}}_{\boldsymbol{k}\sigma}$ by the perturbation theory. The eigenvalues for the zeroth and first order terms of the magnetic field h^z are defined as $E^{(0)}_{\boldsymbol{k}i}$ and $E^{(1)}_{\boldsymbol{k}i}$ (i=1, 2, 3, and 4), respectively. We refer to the eigenvectors for the zeroth and first order terms of the magnetic field h^z are defined as $x_{\boldsymbol{k}i}$ and $\delta\boldsymbol{x}_{\boldsymbol{k}i}$, respectively.

We divide the matrix $\hat{\mathcal{E}}_{\boldsymbol{k}\sigma}$ into

$$\hat{\mathcal{E}}_{\boldsymbol{k}0\sigma} = \begin{pmatrix} \epsilon_{\boldsymbol{k}1} & \epsilon^{+}_{\boldsymbol{k}23} - i\epsilon^{-}_{\boldsymbol{k}23} & 0 & 0 \\ \epsilon^{+}_{\boldsymbol{k}23} + i\epsilon^{-}_{\boldsymbol{k}23} & \epsilon_{\boldsymbol{k}1} & 0 & 0 \\ 0 & 0 & \epsilon_{\boldsymbol{k}+\boldsymbol{q}1} & \epsilon^{+}_{\boldsymbol{k}+\boldsymbol{q}23} - i\epsilon^{-}_{\boldsymbol{k}+\boldsymbol{q}23} \\ 0 & 0 & \epsilon^{+}_{\boldsymbol{k}+\boldsymbol{q}23} + i\epsilon^{-}_{\boldsymbol{k}+\boldsymbol{q}23} & \epsilon_{\boldsymbol{k}+\boldsymbol{q}1} \end{pmatrix} \tag{C.11}$$

and

$$\mathcal{E}_{\boldsymbol{k}1\sigma} = \begin{pmatrix} 0 & 0 & h^z\sigma/2 & 0 \\ 0 & 0 & 0 & h^z\sigma/2 \\ h^z\sigma/2 & 0 & 0 & 0 \\ 0 & h^z\sigma/2 & 0 & 0 \end{pmatrix}. \tag{C.12}$$

We solve the equations

$$(\hat{\mathcal{E}}_{\boldsymbol{k}0\sigma} + \hat{\mathcal{E}}_{\boldsymbol{k}1\sigma})(\boldsymbol{x}_{\boldsymbol{k}i} + \delta\boldsymbol{x}_{\boldsymbol{k}i}) = (E^{(0)}_{\boldsymbol{k}i} + E^{(1)}_{\boldsymbol{k}i})(\boldsymbol{x}_{\boldsymbol{k}i} + \delta\boldsymbol{x}_{\boldsymbol{k}i}) \tag{C.13}$$

and

$$\hat{\mathcal{E}}_{\boldsymbol{k}0\sigma}\boldsymbol{x}_{\boldsymbol{k}i} = E^{(0)}_{\boldsymbol{k}i}\boldsymbol{x}_{\boldsymbol{k}i}. \tag{C.14}$$

From Eq. (C.14), we obtain

$$E^{(0)}_{\boldsymbol{k}1} = \epsilon_{\boldsymbol{k}1} + \sqrt{(\epsilon^{+}_{\boldsymbol{k}23})^2 + (\epsilon^{-}_{\boldsymbol{k}23})^2}, \tag{C.15}$$

$$E^{(0)}_{\boldsymbol{k}2} = \epsilon_{\boldsymbol{k}1} - \sqrt{(\epsilon^{+}_{\boldsymbol{k}23})^2 + (\epsilon^{-}_{\boldsymbol{k}23})^2}, \tag{C.16}$$

$$E^{(0)}_{\boldsymbol{k}3} = E^{(0)}_{\boldsymbol{k}+\boldsymbol{q}1}, \tag{C.17}$$

$$E^{(0)}_{\boldsymbol{k}4} = E^{(0)}_{\boldsymbol{k}+\boldsymbol{q}2}. \tag{C.18}$$

From Eq. (C.14), we obtain eigenvectors

$$\boldsymbol{x}_{\boldsymbol{k}1} = \frac{1}{\sqrt{2}} \begin{pmatrix} -\frac{\sqrt{(\epsilon^+_{\boldsymbol{k}23})^2+(\epsilon^-_{\boldsymbol{k}23})^2}}{\epsilon^+_{\boldsymbol{k}23}+i\epsilon^-_{\boldsymbol{k}23}} \\ 1 \\ 0 \\ 0 \end{pmatrix}, \tag{C.19}$$

$$\boldsymbol{x}_{\boldsymbol{k}2} = \frac{1}{\sqrt{2}} \begin{pmatrix} \frac{\sqrt{(\epsilon^+_{\boldsymbol{k}23})^2+(\epsilon^-_{\boldsymbol{k}23})^2}}{\epsilon^+_{\boldsymbol{k}23}+i\epsilon^-_{\boldsymbol{k}23}} \\ 1 \\ 0 \\ 0 \end{pmatrix}, \tag{C.20}$$

$$\boldsymbol{x}_{\boldsymbol{k}3} = \frac{1}{\sqrt{2}} \begin{pmatrix} 0 \\ 0 \\ -\frac{\sqrt{(\epsilon^+_{\boldsymbol{k}+\boldsymbol{q}23})^2+(\epsilon^-_{\boldsymbol{k}+\boldsymbol{q}23})^2}}{\epsilon^+_{\boldsymbol{k}+\boldsymbol{q}23}+i\epsilon^-_{\boldsymbol{k}+\boldsymbol{q}23}} \\ 1 \end{pmatrix}, \tag{C.21}$$

$$\boldsymbol{x}_{\boldsymbol{k}4} = \frac{1}{\sqrt{2}} \begin{pmatrix} 0 \\ 0 \\ \frac{\sqrt{(\epsilon^+_{\boldsymbol{k}+\boldsymbol{q}23})^2+(\epsilon^-_{\boldsymbol{k}+\boldsymbol{q}23})^2}}{\epsilon^+_{\boldsymbol{k}+\boldsymbol{q}23}+i\epsilon^-_{\boldsymbol{k}+\boldsymbol{q}23}} \\ 1 \end{pmatrix}. \tag{C.22}$$

We express the eigenvector $\delta\boldsymbol{x}_{\boldsymbol{k}i}$ for the first order terms of the magnetic field h^z as a linear combination of the eigenvectors for the zeroth order terms of the magnetic field h^z. $\delta\boldsymbol{x}_{\boldsymbol{k}i}$ is written as

$$\delta\boldsymbol{x}_{\boldsymbol{k}i} = \sum_{j=1}^{N} c_j \boldsymbol{x}_{\boldsymbol{k}j} = c_i \boldsymbol{x}_{\boldsymbol{k}i} + \sum_{j=1, i\neq j}^{N} c_j \boldsymbol{x}_{\boldsymbol{k}j}. \tag{C.23}$$

Using Eq. (C.23) in Eq. (C.13), we obtain

$$\begin{aligned}(\hat{\mathcal{E}}_{\boldsymbol{k}0\sigma}+\hat{\mathcal{E}}_{\boldsymbol{k}1\sigma})(\boldsymbol{x}_{\boldsymbol{k}i}+\delta\boldsymbol{x}_{\boldsymbol{k}i}) =&(\hat{\mathcal{E}}_{\boldsymbol{k}0\sigma}+\hat{\mathcal{E}}_{\boldsymbol{k}1\sigma})((1+c_i)\boldsymbol{x}_{\boldsymbol{k}i}+\sum_{j=1,j\neq i}^{N}c_j\boldsymbol{x}_{\boldsymbol{k}j})\\ =&(E^{(0)}_{\boldsymbol{k}i}+E^{(1)}_{\boldsymbol{k}i})((1+c_i)\boldsymbol{x}_{\boldsymbol{k}i}+\sum_{j=1,j\neq i}^{N}c_j\boldsymbol{x}_{\boldsymbol{k}j}).\end{aligned} \tag{C.24}$$

Therefore, we obtain

$$(\hat{\mathcal{E}}_{\boldsymbol{k}0\sigma}+\hat{\mathcal{E}}_{\boldsymbol{k}1\sigma})(\boldsymbol{x}_{\boldsymbol{k}i}+\sum_{j=1,j\neq i}^{N}\frac{c_j}{1+c_i}\boldsymbol{x}_{\boldsymbol{k}j}) = (E^{(0)}_{\boldsymbol{k}i}+E^{(1)}_{\boldsymbol{k}i})(\boldsymbol{x}_{\boldsymbol{k}i}+\sum_{j=1,j\neq i}^{N}\frac{c_j}{1+c_i}\boldsymbol{x}_{\boldsymbol{k}j}). \tag{C.25}$$

Expanding both sides of Eq. (C.25), we obtain

$$\begin{aligned}&\hat{\mathcal{E}}_{\boldsymbol{k}0\sigma}\boldsymbol{x}_{\boldsymbol{k}i}+\sum_{j=1,j\neq i}^{N}\frac{c_j}{1+c_i}\hat{\mathcal{E}}_{\boldsymbol{k}0\sigma}\boldsymbol{x}_{\boldsymbol{k}j}+\hat{\mathcal{E}}_{\boldsymbol{k}1\sigma}\boldsymbol{x}_{\boldsymbol{k}i}+\sum_{j=1,j\neq i}^{N}\frac{c_j}{1+c_i}\hat{\mathcal{E}}_{\boldsymbol{k}1\sigma}\boldsymbol{x}_{\boldsymbol{k}j}\\ &=E^{(0)}_{\boldsymbol{k}i}\boldsymbol{x}_{\boldsymbol{k}i}+E^{(1)}_{\boldsymbol{k}i}\boldsymbol{x}_{\boldsymbol{k}i}+\sum_{j=1,j\neq i}^{N}\frac{c_j}{1+c_i}E^{(0)}_{\boldsymbol{k}i}\boldsymbol{x}_{\boldsymbol{k}j}+\sum_{j=1,j\neq i}^{N}\frac{c_j}{1+c_i}\hat{\mathcal{E}}_{\boldsymbol{k}1\sigma}\boldsymbol{x}_{\boldsymbol{k}j}.\end{aligned} \tag{C.26}$$

When we can ignore the second-order term of h^z, we obtain

$$\begin{aligned}&\hat{\mathcal{E}}_{\boldsymbol{k}0\sigma}\boldsymbol{x}_{\boldsymbol{k}i}+\sum_{j=1,j\neq i}^{N}\frac{c_j}{1+c_i}\hat{\mathcal{E}}_{\boldsymbol{k}0\sigma}\boldsymbol{x}_{\boldsymbol{k}j}+\hat{\mathcal{E}}_{\boldsymbol{k}1\sigma}\boldsymbol{x}_{\boldsymbol{k}i}\\ &=E^{(0)}_{\boldsymbol{k}i}\boldsymbol{x}_{\boldsymbol{k}i}+E^{(1)}_{\boldsymbol{k}i}\boldsymbol{x}_{\boldsymbol{k}i}+\sum_{j=1,j\neq i}^{N}\frac{c_j}{1+c_i}E^{(0)}_{\boldsymbol{k}i}\boldsymbol{x}_{\boldsymbol{k}j}.\end{aligned} \tag{C.27}$$

Using Eq. (C.14) in Eq. (C.27), we obtain

$$\hat{\mathcal{E}}_{\boldsymbol{k}1\sigma}\boldsymbol{x}_i=E^{(1)}_i\boldsymbol{x}_i+\sum_{j=1,j\neq i}^{N}\frac{c_j}{1+c_i}E^{(0)}_{\boldsymbol{k}i}\boldsymbol{x}_j-\sum_{j=1,j\neq i}^{N}\frac{c_j}{1+c_i}E^{(0)}_{\boldsymbol{k}j}\boldsymbol{x}_j. \tag{C.28}$$

In the case of $i=l$,

$$(\boldsymbol{x}_{\boldsymbol{k}i},\hat{\mathcal{E}}_{\boldsymbol{k}1\sigma}\boldsymbol{x}_{\boldsymbol{k}i})=E^{(1)}_{\boldsymbol{k}i}. \tag{C.29}$$

In the case of $i \neq l$,

$$\begin{aligned}(\boldsymbol{x}_{\boldsymbol{k}l}, \hat{\mathcal{E}}_{\boldsymbol{k}1\sigma}\boldsymbol{x}_{\boldsymbol{k}i}) =&(\boldsymbol{x}_{\boldsymbol{k}l}, E^{(1)}_{\boldsymbol{k}i}\boldsymbol{x}_{\boldsymbol{k}i} + \sum_{j=1,j\neq i}^{N} \frac{c_j}{1+c_i} E^{(0)}_{\boldsymbol{k}i}\boldsymbol{x}_{\boldsymbol{k}j} - \sum_{j=1,j\neq i}^{N} \frac{c_j}{1+c_i} E^{(0)}_{\boldsymbol{k}j}\boldsymbol{x}_{\boldsymbol{k}j}) \\ =&\frac{c_k}{1+c_i} E^{(0)}_{\boldsymbol{k}i} - \frac{c_k}{1+c_i} E^{(0)}_{\boldsymbol{k}l} \\ =&\frac{c_k}{1+c_i}(E^{(0)}_{\boldsymbol{k}i} - E^{(0)}_{\boldsymbol{k}l}). \end{aligned} \tag{C.30}$$

It follows from Eq. (C.30) that

$$\frac{c_k}{1+c_i} = \frac{(\boldsymbol{x}_{\boldsymbol{k}l}, \hat{\mathcal{E}}_{\boldsymbol{k}1\sigma}\boldsymbol{x}_{\boldsymbol{k}i})}{E^{(0)}_{\boldsymbol{k}i} - E^{(0)}_{\boldsymbol{k}l}}. \tag{C.31}$$

From Eqs. (C.23) and (C.31), the eigenvector for the first order term of the magnetic field h^z is

$$\delta\boldsymbol{x}_{\boldsymbol{k}i} = \sum_{j=1,j\neq i}^{N} \frac{c_k}{1+c_i}\boldsymbol{x}_{\boldsymbol{k}j} = \sum_{j=1,j\neq i}^{N} \frac{(\boldsymbol{x}_{\boldsymbol{k}l}, \hat{\mathcal{E}}_{\boldsymbol{k}1\sigma}\boldsymbol{x}_{\boldsymbol{k}i})}{E^{(0)}_{\boldsymbol{k}i} - E^{(0)}_{\boldsymbol{k}l}}\boldsymbol{x}_{\boldsymbol{k}j}. \tag{C.32}$$

Using Eqs. (C.9), (C.15)−(C.22) in Eq. (C.32), we obtain

$$\begin{aligned}\delta\boldsymbol{x}_{\boldsymbol{k}1} =& -\frac{1}{2}\frac{h^z\sigma}{E^{(0)}_1 - E^{(0)}_3}\left\{\frac{\sqrt{[(\epsilon^+_{\boldsymbol{k}+\boldsymbol{q}23})^2 + (\epsilon^-_{\boldsymbol{k}+\boldsymbol{q}23})^2][(\epsilon^+_{\boldsymbol{k}23})^2 + (\epsilon^-_{\boldsymbol{k}23})^2]}}{(\epsilon^+_{\boldsymbol{k}+\boldsymbol{q}23} - i\epsilon^-_{\boldsymbol{k}+\boldsymbol{q}23})(\epsilon^+_{\boldsymbol{k}23} + i\epsilon^-_{\boldsymbol{k}23})} + 1\right\}\boldsymbol{x}_3 \\ &-\frac{1}{2}\frac{h^z\sigma}{E^{(0)}_1 - E^{(0)}_4}\left\{-\frac{\sqrt{[(\epsilon^+_{\boldsymbol{k}+\boldsymbol{q}23})^2 + (\epsilon^-_{\boldsymbol{k}+\boldsymbol{q}23})^2][(\epsilon^+_{\boldsymbol{k}23})^2 + (\epsilon^-_{\boldsymbol{k}23})^2]}}{(\epsilon^+_{\boldsymbol{k}+\boldsymbol{q}23} - i\epsilon^-_{\boldsymbol{k}+\boldsymbol{q}23})(\epsilon^+_{\boldsymbol{k}23} + i\epsilon^-_{\boldsymbol{k}23})} + 1\right\}\boldsymbol{x}_4, \end{aligned} \tag{C.33}$$

$$\begin{aligned}\delta\boldsymbol{x}_{\boldsymbol{k}2} =& -\frac{1}{2}\frac{h^z\sigma}{E^{(0)}_2 - E^{(0)}_3}\left\{\frac{\sqrt{[(\epsilon^+_{\boldsymbol{k}+\boldsymbol{q}23})^2 + (\epsilon^-_{\boldsymbol{k}+\boldsymbol{q}23})^2][(\epsilon^+_{\boldsymbol{k}23})^2 + (\epsilon^-_{\boldsymbol{k}23})^2]}}{(\epsilon^+_{\boldsymbol{k}+\boldsymbol{q}23} - i\epsilon^-_{\boldsymbol{k}+\boldsymbol{q}23})(\epsilon^+_{\boldsymbol{k}23} + i\epsilon^-_{\boldsymbol{k}23})} + 1\right\}\boldsymbol{x}_3 \\ &-\frac{1}{2}\frac{h^z\sigma}{E^{(0)}_2 - E^{(0)}_4}\left\{-\frac{\sqrt{[(\epsilon^+_{\boldsymbol{k}+\boldsymbol{q}23})^2 + (\epsilon^-_{\boldsymbol{k}+\boldsymbol{q}23})^2][(\epsilon^+_{\boldsymbol{k}23})^2 + (\epsilon^-_{\boldsymbol{k}23})^2]}}{(\epsilon^+_{\boldsymbol{k}+\boldsymbol{q}23} - i\epsilon^-_{\boldsymbol{k}+\boldsymbol{q}23})(\epsilon^+_{\boldsymbol{k}23} + i\epsilon^-_{\boldsymbol{k}23})} + 1\right\}\boldsymbol{x}_4, \end{aligned} \tag{C.34}$$

$$\delta \boldsymbol{x}_{\boldsymbol{k}3} = -\frac{1}{2}\frac{h^z\sigma}{E_3^{(0)}-E_1^{(0)}}\left\{\frac{\sqrt{[(\epsilon^+_{\boldsymbol{k}+\boldsymbol{q}23})^2+(\epsilon^-_{\boldsymbol{k}+\boldsymbol{q}23})^2][(\epsilon^+_{\boldsymbol{k}23})^2+(\epsilon^-_{\boldsymbol{k}23})^2]}}{(\epsilon^+_{\boldsymbol{k}+\boldsymbol{q}23}+i\epsilon^-_{\boldsymbol{k}+\boldsymbol{q}23})(\epsilon^+_{\boldsymbol{k}23}-i\epsilon^-_{\boldsymbol{k}23})}+1\right\}\boldsymbol{x}_1$$
$$-\frac{1}{2}\frac{h^z\sigma}{E_3^{(0)}-E_2^{(0)}}\left\{-\frac{\sqrt{[(\epsilon^+_{\boldsymbol{k}+\boldsymbol{q}23})^2+(\epsilon^-_{\boldsymbol{k}+\boldsymbol{q}23})^2][(\epsilon^+_{\boldsymbol{k}23})^2+(\epsilon^-_{\boldsymbol{k}23})^2]}}{(\epsilon^+_{\boldsymbol{k}+\boldsymbol{q}23}+i\epsilon^-_{\boldsymbol{k}+\boldsymbol{q}23})(\epsilon^+_{\boldsymbol{k}23}-i\epsilon^-_{\boldsymbol{k}23})}+1\right\}\boldsymbol{x}_2, \tag{C.35}$$

$$\delta \boldsymbol{x}_{\boldsymbol{k}4} = -\frac{1}{2}\frac{h^z\sigma}{E_4^{(0)}-E_1^{(0)}}\left\{\frac{\sqrt{[(\epsilon^+_{\boldsymbol{k}+\boldsymbol{q}23})^2+(\epsilon^-_{\boldsymbol{k}+\boldsymbol{q}23})^2][(\epsilon^+_{\boldsymbol{k}23})^2+(\epsilon^-_{\boldsymbol{k}23})^2]}}{(\epsilon^+_{\boldsymbol{k}+\boldsymbol{q}23}+i\epsilon^-_{\boldsymbol{k}+\boldsymbol{q}23})(\epsilon^+_{\boldsymbol{k}23}-i\epsilon^-_{\boldsymbol{k}23})}+1\right\}\boldsymbol{x}_1$$
$$-\frac{1}{2}\frac{h^z\sigma}{E_4^{(0)}-E_2^{(0)}}\left\{-\frac{\sqrt{[(\epsilon^+_{\boldsymbol{k}+\boldsymbol{q}23})^2+(\epsilon^-_{\boldsymbol{k}+\boldsymbol{q}23})^2][(\epsilon^+_{\boldsymbol{k}23})^2+(\epsilon^-_{\boldsymbol{k}23})^2]}}{(\epsilon^+_{\boldsymbol{k}+\boldsymbol{q}23}+i\epsilon^-_{\boldsymbol{k}+\boldsymbol{q}23})(\epsilon^+_{\boldsymbol{k}23}-i\epsilon^-_{\boldsymbol{k}23})}+1\right\}\boldsymbol{x}_2. \tag{C.36}$$

The unitary matrix $U_{\boldsymbol{k}\sigma}$ is written as

$$U_{\boldsymbol{k}\sigma} = (\boldsymbol{x}_{\boldsymbol{k}1} + \delta\boldsymbol{x}_{\boldsymbol{k}1}\, \boldsymbol{x}_{\boldsymbol{k}2} + \delta\boldsymbol{x}_{\boldsymbol{k}2}\, \boldsymbol{x}_{\boldsymbol{k}3} + \delta\boldsymbol{x}_{\boldsymbol{k}3}\, \boldsymbol{x}_{\boldsymbol{k}4} + \delta\boldsymbol{x}_{\boldsymbol{k}4}). \tag{C.37}$$

Hence, the components of the unitary matrix

$$\hat{\mathcal{E}}_{\boldsymbol{k}1\sigma} = \begin{pmatrix} u_{\boldsymbol{k}11} & u_{\boldsymbol{k}12} & u_{\boldsymbol{k}13} & u_{\boldsymbol{k}14} \\ u_{\boldsymbol{k}21} & u_{\boldsymbol{k}22} & u_{\boldsymbol{k}32} & u_{\boldsymbol{k}42} \\ u_{\boldsymbol{k}13} & u_{\boldsymbol{k}23} & u_{\boldsymbol{k}33} & u_{\boldsymbol{k}43} \\ u_{\boldsymbol{k}14} & u_{\boldsymbol{k}24} & u_{\boldsymbol{k}34} & u_{\boldsymbol{k}44} \end{pmatrix} \tag{C.38}$$

are written as

$$u_{\boldsymbol{k}11} = -\frac{1}{\sqrt{2}}\frac{\sqrt{(\epsilon^+_{\boldsymbol{k}23})^2+(\epsilon^-_{\boldsymbol{k}23})^2}}{\epsilon^+_{\boldsymbol{k}23}+i\epsilon^-_{\boldsymbol{k}23}}, \tag{C.39}$$

$$u_{\boldsymbol{k}31} = \frac{1}{2}\frac{h^z\sigma}{E_1^{(0)}-E_3^{(0)}}(B_{\boldsymbol{k}}+1)\frac{1}{\sqrt{2}}\frac{\sqrt{(\epsilon^+_{\boldsymbol{k}23})^2+(\epsilon^-_{\boldsymbol{k}23})^2}}{\epsilon^+_{\boldsymbol{k}23}+i\epsilon^-_{\boldsymbol{k}23}}$$
$$+\frac{1}{2}\frac{h^z\sigma}{E_1^{(0)}-E_4^{(0)}}(-B_{\boldsymbol{k}}+1)\frac{1}{\sqrt{2}}\frac{\sqrt{(\epsilon^+_{\boldsymbol{k}23})^2+(\epsilon^-_{\boldsymbol{k}23})^2}}{\epsilon^+_{\boldsymbol{k}23}+i\epsilon^-_{\boldsymbol{k}23}}, \tag{C.40}$$

$$u_{\boldsymbol{k}12} = \frac{1}{\sqrt{2}}\frac{\sqrt{(\epsilon^+_{\boldsymbol{k}23})^2+(\epsilon^-_{\boldsymbol{k}23})^2}}{\epsilon^+_{\boldsymbol{k}23}+i\epsilon^-_{\boldsymbol{k}23}}, \tag{C.41}$$

$$u_{\boldsymbol{k}32} = \frac{1}{2}\frac{h^z\sigma}{E_2^{(0)} - E_3^{(0)}}(B_{\boldsymbol{k}}+1)\frac{1}{\sqrt{2}}\frac{\sqrt{(\epsilon^+_{\boldsymbol{k}23})^2 + (\epsilon^-_{\boldsymbol{k}23})^2}}{\epsilon^+_{\boldsymbol{k}23} + i\epsilon^-_{\boldsymbol{k}23}}$$
$$+ \frac{1}{2}\frac{h^z\sigma}{E_2^{(0)} - E_4^{(0)}}(-B_{\boldsymbol{k}}+1)\frac{1}{\sqrt{2}}\frac{\sqrt{(\epsilon^+_{\boldsymbol{k}23})^2 + (\epsilon^-_{\boldsymbol{k}23})^2}}{\epsilon^+_{\boldsymbol{k}23} + i\epsilon^-_{\boldsymbol{k}23}}, \tag{C.42}$$

$$u_{\boldsymbol{k}33} = -\frac{1}{\sqrt{2}}\frac{\sqrt{(\epsilon^+_{\boldsymbol{k}+\boldsymbol{q}23})^2 + (\epsilon^-_{\boldsymbol{k}+\boldsymbol{q}23})^2}}{\epsilon^+_{\boldsymbol{k}+\boldsymbol{q}23} + i\epsilon^-_{\boldsymbol{k}+\boldsymbol{q}23}}, \tag{C.43}$$

,

$$u_{\boldsymbol{k}13} = \frac{1}{2}\frac{h^z\sigma}{E_2^{(0)} - E_3^{(0)}}(A_{\boldsymbol{k}}+1)\frac{1}{\sqrt{2}}\frac{\sqrt{(\epsilon^+_{\boldsymbol{k}+\boldsymbol{q}23})^2 + (\epsilon^-_{\boldsymbol{k}+\boldsymbol{q}23})^2}}{\epsilon^+_{\boldsymbol{k}+\boldsymbol{q}23} + i\epsilon^-_{\boldsymbol{k}+\boldsymbol{q}23}}$$
$$+ \frac{1}{2}\frac{h\sigma}{E_2^{(0)} - E_4^{(0)}}(-A_{\boldsymbol{k}}+1)\frac{1}{\sqrt{2}}\frac{\sqrt{(\epsilon^+_{\boldsymbol{k}+\boldsymbol{q}23})^2 + (\epsilon^-_{\boldsymbol{k}+\boldsymbol{q}23})^2}}{\epsilon^+_{\boldsymbol{k}+\boldsymbol{q}23} + i\epsilon^-_{\boldsymbol{k}+\boldsymbol{q}23}}, \tag{C.44}$$

$$u_{\boldsymbol{k}34} = \frac{1}{\sqrt{2}}\frac{\sqrt{(\epsilon^+_{\boldsymbol{k}+\boldsymbol{q}23})^2 + (\epsilon^-_{\boldsymbol{k}+\boldsymbol{q}23})^2}}{\epsilon^+_{\boldsymbol{k}+\boldsymbol{q}23} + i\epsilon^-_{\boldsymbol{k}+\boldsymbol{q}23}}, \tag{C.45}$$

$$u_{\boldsymbol{k}14} = \frac{1}{2}\frac{h^z\sigma}{E_2^{(0)} - E_3^{(0)}}(A_{\boldsymbol{k}}+1)\frac{1}{\sqrt{2}}\frac{\sqrt{(\epsilon^+_{\boldsymbol{k}+\boldsymbol{q}23})^2 + (\epsilon^-_{\boldsymbol{k}+\boldsymbol{q}23})^2}}{\epsilon^+_{\boldsymbol{k}+\boldsymbol{q}23} + i\epsilon^-_{\boldsymbol{k}+\boldsymbol{q}23}}$$
$$+ \frac{1}{2}\frac{h^z\sigma}{E_2^{(0)} - E_4^{(0)}}(-A_{\boldsymbol{k}}+1)\frac{1}{\sqrt{2}}\frac{\sqrt{(\epsilon^+_{\boldsymbol{k}+\boldsymbol{q}23})^2 + (\epsilon^-_{\boldsymbol{k}+\boldsymbol{q}23})^2}}{\epsilon^+_{\boldsymbol{k}+\boldsymbol{q}23} + i\epsilon^-_{\boldsymbol{k}+\boldsymbol{q}23}}, \tag{C.46}$$

where

$$A_{\boldsymbol{k}} = \frac{\sqrt{[(\epsilon^+_{\boldsymbol{k}+\boldsymbol{q}23})^2 + (\epsilon^-_{\boldsymbol{k}+\boldsymbol{q}23})^2][(\epsilon^+_{\boldsymbol{k}23})^2 + (\epsilon^-_{\boldsymbol{k}23})^2]}}{(\epsilon^+_{\boldsymbol{k}+\boldsymbol{q}23} - i\epsilon^-_{\boldsymbol{k}+\boldsymbol{q}23})(\epsilon^+_{\boldsymbol{k}23} + i\epsilon^-_{\boldsymbol{k}23})}, \tag{C.47}$$

$$B_{\boldsymbol{k}} = \frac{\sqrt{[(\epsilon^+_{\boldsymbol{k}+\boldsymbol{q}23})^2 + (\epsilon^-_{\boldsymbol{k}+\boldsymbol{q}23})^2][(\epsilon^+_{\boldsymbol{k}23})^2 + (\epsilon^-_{\boldsymbol{k}23})^2]}}{(\epsilon^+_{\boldsymbol{k}+\boldsymbol{q}23} + i\epsilon^-_{\boldsymbol{k}+\boldsymbol{q}23})(\epsilon^+_{\boldsymbol{k}23} - i\epsilon^-_{\boldsymbol{k}23})}. \tag{C.48}$$

We define the sublattice magnetization m as

$$\begin{aligned} m(\boldsymbol{q}) \equiv & \langle s_{jp} \rangle e^{i\boldsymbol{q}\cdot\boldsymbol{r}_{jp}} \\ = & \sum_{\sigma_1,\sigma_2} \frac{1}{2} \langle (c^{\dagger}_{ip\sigma} \sigma^{z}_{\sigma_1\sigma_2} c_{ip\sigma_2}) e^{i\boldsymbol{q}\cdot\boldsymbol{r}_{ip}} \rangle. \end{aligned} \tag{C.49}$$

When we substitute Eq. (C.10) into Eq. (C.49), we obtain

$$\begin{aligned} m(\boldsymbol{q}) = & \left(\frac{1}{N}\right) {\sum_{\boldsymbol{k},\sigma}}' \langle (c^{\dagger}_{\boldsymbol{k}1\sigma} c_{\boldsymbol{k}+\boldsymbol{q}1\sigma} + c^{\dagger}_{\boldsymbol{k}+\boldsymbol{q}1\sigma} c_{\boldsymbol{k}1\sigma}) \rangle \sigma \\ = & \left(\frac{1}{N}\right) {\sum_{\boldsymbol{k},\sigma}}' \{ (u^{*}_{11\sigma} u_{31\sigma} + u^{*}_{31\sigma} u_{11\sigma}) \langle \alpha^{\dagger}_{\boldsymbol{k}\sigma} \alpha_{\boldsymbol{k}\sigma} \rangle + (u^{*}_{12\sigma} u_{32\sigma} + u^{*}_{32\sigma} u_{12\sigma}) \langle \beta^{\dagger}_{\boldsymbol{k}\sigma} \beta_{\boldsymbol{k}\sigma} \rangle \\ & + (u^{*}_{13\sigma} u_{33\sigma} + u^{*}_{33\sigma} u_{13\sigma}) \langle \gamma^{\dagger}_{\boldsymbol{k}\sigma} \gamma_{\boldsymbol{k}\sigma} \rangle + (u^{*}_{14\sigma} u_{34\sigma} + u^{*}_{34\sigma} u_{14\sigma}) \langle \delta^{\dagger}_{\boldsymbol{k}\sigma} \delta_{\boldsymbol{k}\sigma} \rangle \} \sigma \\ = & \frac{h}{N} \sum_{\boldsymbol{k}} \left\{ \frac{f(E^{(0)}_{\boldsymbol{k}1}) - f(E^{(0)}_{\boldsymbol{k}3})}{4(E^{(0)}_{\boldsymbol{k}3} - E^{(0)}_{\boldsymbol{k}1})} + \frac{f(E^{(0)}_{\boldsymbol{k}2}) - f(E^{(0)}_{\boldsymbol{k}4})}{4(E^{(0)}_{\boldsymbol{k}2} - E^{(0)}_{\boldsymbol{k}4})} \right\} C_{\boldsymbol{k}} \\ & + \left\{ \frac{f(E^{(0)}_{\boldsymbol{k}1}) - f(E^{(0)}_{\boldsymbol{k}4})}{4(E^{(0)}_{\boldsymbol{k}4} - E^{(0)}_{\boldsymbol{k}1})} + \frac{f(E^{(0)}_{\boldsymbol{k}2}) - f(E^{(0)}_{\boldsymbol{k}3})}{4(E^{(0)}_{\boldsymbol{k}2} - E^{(0)}_{\boldsymbol{k}3})} \right\} D_{\boldsymbol{k}}, \end{aligned} \tag{C.50}$$

where

$$C_{\boldsymbol{k}} = 1 + \frac{\epsilon^{+}_{\boldsymbol{k}23} \epsilon^{+}_{\boldsymbol{k}+\boldsymbol{q}23} + \epsilon^{+}_{\boldsymbol{k}23} \epsilon^{-}_{\boldsymbol{k}+\boldsymbol{q}23}}{\sqrt{[(\epsilon^{+}_{\boldsymbol{k}+\boldsymbol{q}23})^2 + (\epsilon^{-}_{\boldsymbol{k}+\boldsymbol{q}23})^2][(\epsilon^{+}_{\boldsymbol{k}23})^2 + (\epsilon^{-}_{\boldsymbol{k}23})^2]}}, \tag{C.51}$$

$$D_{\boldsymbol{k}} = 1 - \frac{\epsilon^{+}_{\boldsymbol{k}23} \epsilon^{+}_{\boldsymbol{k}+\boldsymbol{q}23} + \epsilon^{-}_{\boldsymbol{k}23} \epsilon^{-}_{\boldsymbol{k}+\boldsymbol{q}23}}{\sqrt{[(\epsilon^{+}_{\boldsymbol{k}+\boldsymbol{q}23})^2 + (\epsilon^{-}_{\boldsymbol{k}+\boldsymbol{q}23})^2][(\epsilon^{-}_{\boldsymbol{k}23})^2 + \epsilon^{+}_{\boldsymbol{k}23})^2]}}. \tag{C.52}$$

From $\chi(\boldsymbol{q}) \equiv \lim_{h^z \to 0} m(\boldsymbol{q})/h^z$, the spin susceptibility $\chi(\boldsymbol{q})$ is

$$\begin{aligned} \chi(\boldsymbol{q}) = & \frac{1}{N} \sum_{\boldsymbol{k}} \left\{ \frac{f(E^{(0)}_{\boldsymbol{k}1}) - f(E^{(0)}_{\boldsymbol{k}3})}{4(E^{(0)}_{\boldsymbol{k}3} - E^{(0)}_{\boldsymbol{k}1})} + \frac{f(E^{(0)}_{\boldsymbol{k}2}) - f(E^{(0)}_{\boldsymbol{k}4})}{4(E^{(0)}_{\boldsymbol{k}2} - E^{(0)}_{\boldsymbol{k}4})} \right\} C_{\boldsymbol{k}} \\ & + \left\{ \frac{f(E^{(0)}_{\boldsymbol{k}1}) - f(E^{(0)}_{\boldsymbol{k}4})}{4(E^{(0)}_{\boldsymbol{k}4} - E^{(0)}_{\boldsymbol{k}1})} + \frac{f(E^{(0)}_{\boldsymbol{k}2}) - f(E^{(0)}_{\boldsymbol{k}3})}{4(E^{(0)}_{\boldsymbol{k}2} - E^{(0)}_{\boldsymbol{k}3})} \right\} D_{\boldsymbol{k}} \end{aligned} \tag{C.53}$$

Appendix D

Derivation of Eq. (2.15)

In this appendix, we derive Eq. (2.15) for the susceptibility of the free 3d spins. We consider the localized 3d spin system under a small magnetic field h. The Hamiltonian has the term $H = \sum_i hS_i$ where S_i the spin operator with length $S = 5/2$ on the anion site i. We define the magnetization M as

$$M \equiv \langle S_i \rangle. \tag{D.1}$$

Before we derive M, we calculate

$$\begin{aligned}\sum_{S_i=-S}^{S} \exp(-h\beta S_i) &= \frac{\exp(-h\beta S)(1-\exp(h\beta(2S+1)))}{1-\exp(-h\beta S)} \\ &= \frac{\sinh(\frac{\beta(S+\frac{1}{2})h}{2})}{\sinh(\frac{\beta h}{2})}\end{aligned} \tag{D.2}$$

and

$$\begin{aligned}\frac{d}{dh}\sum_{S_i=-S}^{S} \exp(-h\beta S_i) =& \frac{d}{dh}\frac{\sinh(h(S+\frac{1}{2})\beta)}{\sinh(\frac{h\beta}{2})} \\ =& \frac{1}{\sinh^2(\frac{h\beta}{2})}\Big[\Big(S+\frac{1}{2}\Big)\cosh\Big(h\Big(S+\frac{1}{2}\Big)\beta\Big)\sinh\Big(\frac{h\beta}{2}\Big) \\ & - \frac{h}{2}\sinh\Big(h\Big(S+\frac{1}{2}\Big)\beta\Big)\cosh\Big(\frac{h\beta}{2}\Big)\Big].\end{aligned} \tag{D.3}$$

The magnetization M is

$M \equiv \langle S_i \rangle$

$$
\begin{aligned}
&= \frac{\sum_{S_i=-S}^{S} S_i \exp(-h\beta S_i)}{\sum_{S_i=-S}^{S} \exp(-h\beta S_i)} \qquad \text{(D.4)}\\
&= \frac{-\frac{d}{dh}\sum_{S_i=-S}^{S} \exp(-h\beta S_i)}{\sum_{S_i=-S}^{S} \exp(-h\beta S_i)}\\
&= \frac{1}{\sinh(\frac{h\beta}{2})\sinh(h(S+\frac{1}{2})\beta)}\Big[\Big(S+\frac{1}{2}\Big)\cosh\Big(h\Big(S+\frac{1}{2}\Big)\beta\Big)\sinh\Big(\frac{h\beta}{2}\Big)\\
&\quad -\frac{1}{2}\sinh\Big(h\Big(S+\frac{1}{2}\Big)\beta\Big)\cosh\Big(\frac{h\beta}{2}\Big)\Big]\\
&= \Big(S+\frac{1}{2}\Big)\coth\Big(h\Big(S+\frac{1}{2}\Big)\beta\Big) - \frac{1}{2}\coth\Big(\frac{h\beta}{2}\Big)\\
&= S\Big(\frac{2S+1}{2S}\Big)\coth\Big(h\Big(S+\frac{1}{2}\Big)\beta\Big) - S\frac{1}{2S}\coth\Big(\frac{h\beta}{2}\Big)\\
&= SB_S(\beta h S), \qquad \text{(D.5)}
\end{aligned}
$$

where

$$
B_S(x) = \Big(\frac{2S+1}{2S}\Big)\coth\Big(\beta\Big(\frac{2S+1}{2S}\Big)x\Big) - \frac{1}{2S}\coth\Big(\beta\frac{x}{2S}\Big) \qquad \text{(D.6)}
$$

is the Brillouin function.

When h is small, x is small. When x is sufficiently small,

$$
\begin{aligned}
\coth(x) &= \frac{\exp(x)+\exp(-x)}{\exp(x)-\exp(-x)} \qquad \text{(D.7)}\\
&= \frac{1+x+\frac{x^2}{2}+\frac{x^3}{6}+\frac{x^4}{24}+1-x+\frac{x^2}{2}+\frac{-x^3}{6}+\frac{x^4}{24}}{1+x+\frac{x^2}{2}+\frac{x^3}{6}+\frac{x^4}{24}-1+x-\frac{x^2}{2}-\frac{-x^3}{6}-\frac{x^4}{24}}\\
&= \frac{2+x^2+\frac{x^4}{12}}{2x+\frac{x^3}{3}} = \frac{1}{x}+\frac{x}{3}-\frac{\frac{x^4}{72}}{x+\frac{x^3}{6}}\\
&= \frac{1}{x}+\frac{x}{3}
\end{aligned}
$$

and

$$
\begin{aligned}
B_S(x) &= \big(\frac{2S+1}{2S}\big)\big(\frac{1}{\beta(\frac{2S+1}{2S})x}\big)+\big(\beta\big(\frac{2S+1}{6S}\big)x\big)-\frac{1}{2S}\big(\frac{1}{\beta\frac{x}{2S}}+\beta\frac{x}{6S}\big)\\
&= \frac{1}{\beta x}+\frac{\beta}{3}\big(\frac{2S+1}{2S}\big)^2 x-\frac{1}{\beta x}-\frac{x}{12S^2} = \frac{(4S^2+4S)x}{12S^2}
\end{aligned}
$$

$$= \frac{(S+1)x}{3S}. \tag{D.8}$$

From Eqs. (D.4) and (D.8), we obtain

$$M = \frac{(S+1)Sh\beta}{3}. \tag{D.9}$$

From $\chi_2(T) = \lim_{h\to 0} \frac{M}{h}$, the susceptibility of the free 3d spin $\chi_2(T)$ is

$$\chi_2(T) = \frac{(S+1)S}{3T}. \tag{D.10}$$

Appendix E

Derivation of Eq. (2.19)

In this appendix, we apply the random phase approximation (RPA) to the Hubbard model and derive the spin susceptibility of pure π-electron system [64, 65].

We derive the unitary matrix to derive the spin susceptibility. We consider the Schrödinger equation

$$i\hbar\frac{d\psi}{d\tau} = H\psi \tag{E.1}$$

for the wave function of the system $\psi(\tau)$. Introducing $\psi(\tau_0)$ for the wave function at time τ_0, we obtain

$$\psi(\tau) = e^{\frac{iH(\tau-\tau_0)}{\hbar}}\psi(\tau_0) \tag{E.2}$$

as the relational equation between $\psi(\tau)$ and $\psi(\tau_0)$. Here, we introduce the variable function

$$U_H(\tau,\tau_0) = e^{-iH(\tau-\tau_0)/\hbar}. \tag{E.3}$$

The variable function $U(\tau,\tau_0)$ is a unitary matrix. Differentiating both sides of Eq. (E.3) by τ, we obtain

$$\begin{aligned}\frac{dU_H(\tau,\tau_0)}{d\tau} &= -\frac{iH}{\hbar}e^{-H(\tau-\tau_0)/\hbar} \\ &= \frac{-iH}{\hbar}U_H(\tau,\tau_0)\end{aligned} \tag{E.4}$$

Integrating both sides of Eq. (E.4) with τ_1, we obtain

$$U_H(\tau,\tau_0) = C + \left(-\frac{i}{\hbar}\right)\int_{\tau_0}^{\tau} d\tau_1 U_H(\tau_1,\tau_0)H, \tag{E.5}$$

where C is an integration constant. From $U(\tau_0,\tau_0) = 1$, we obtain $C = 1$. Hence,

$$U_H(\tau,\tau_0) = 1 + \left(-\frac{i}{\hbar}\right)\int_{\tau_0}^{t} d\tau_1 U_H(\tau_1,\tau_0)H. \tag{E.6}$$

We apply the itinerant approximation to Eq. (E.6), which leads to

$$\begin{aligned} U_H(\tau,\tau_0) =& 1 + \left(-\frac{i}{\hbar}\right)\int_{\tau_0}^{\tau} d\tau_1 H(\tau_1) \\ &+ \left(-\frac{i}{\hbar}\right)^2 \int_{\tau_0}^{\tau} d\tau_1 \int_{\tau_0}^{\tau} d\tau_2 H(\tau_1)H(\tau_2) \\ &+ \cdots + \left(-\frac{i}{\hbar}\right)^n \int_{\tau_0}^{\tau} d\tau_1 \cdots \int_{\tau_0}^{\tau} d\tau_n H(\tau_1)H(\tau_2)\cdots H(\tau_n) + \cdots. \end{aligned} \tag{E.7}$$

We write Eq. (E.7) in a symmetrical form. We define the ordering operator

$$\mathrm{T}[A(\tau)B(\tau')] = A(\tau)B(\tau')\theta(\tau-\tau') \pm B(\tau')B(\tau)\theta(\tau'-\tau), \tag{E.8}$$

where $\theta(x)$ is Heaviside step function. Here, $\pm$ is taken as $+$ and $-$ when A and B are Bose operators and Fermi operators, respectively. Equation (E.7) is written as

$$U_H(\tau,\tau_0) = 1 + \sum_{n=1}^{\infty}\frac{1}{n!}\left(-\frac{i}{\hbar}\right)^n \int_{\tau_0}^{\tau} \cdots d\tau_n \mathrm{T}[H_1(\tau_1)\cdots H_1(\tau_n)]. \tag{E.9}$$

We define the spin susceptibility $\chi_s^{zz}(\boldsymbol{q}, i\omega_m)$ and spin operator $S_{\boldsymbol{q}}^z(\tau)$ as

$$\chi_s^{zz}(\boldsymbol{q}, i\omega_m) = \frac{1}{N}\int_0^{\beta} e^{i\omega_m\tau}\langle S_{\boldsymbol{q}}^z(\tau)S_{-\boldsymbol{q}}^z\rangle d\tau. \tag{E.10}$$

and

$$S_{\boldsymbol{q}}^z = \frac{1}{2}\sum_{\boldsymbol{k}}(c_{\boldsymbol{k}\uparrow}^{\dagger}c_{\boldsymbol{k}+\boldsymbol{q}\uparrow} - c_{\boldsymbol{k}\downarrow}^{\dagger}c_{\boldsymbol{k}+\boldsymbol{q}\downarrow}), \tag{E.11}$$

representivity. Using Eq. (E.11) in Eq. (E.10), we obtain

$$\begin{aligned}\chi_s^{zz}(\boldsymbol{q}, i\omega_m) &= \frac{1}{N}\int_0^\beta e^{i\omega_m\tau}\sum_{\boldsymbol{k},\boldsymbol{k}'}\langle S_{\boldsymbol{q}}^z(\tau)S_{-\boldsymbol{q}}^z\rangle d\tau \\ &= \frac{1}{4N}\int_0^\beta e^{i\omega_m\tau}\langle(c_{\boldsymbol{k}\uparrow}^\dagger(\tau)c_{\boldsymbol{k}+\boldsymbol{q}\uparrow}(\tau) - c_{\boldsymbol{k}\downarrow}^\dagger(\tau)c_{\boldsymbol{k}+\boldsymbol{q}\downarrow}(\tau))(c_{\boldsymbol{k}\uparrow}^\dagger c_{\boldsymbol{k}-\boldsymbol{q}\uparrow} - c_{\boldsymbol{k}\downarrow}^\dagger c_{\boldsymbol{k}-\boldsymbol{q}\downarrow})\rangle d\tau.\end{aligned} \tag{E.12}$$

We define spin susceptibility $\chi^{\sigma\sigma'}(\boldsymbol{q}, i\omega_m)$ as

$$\chi^{\sigma\sigma'}(\boldsymbol{q}, i\omega_m) = \frac{1}{N}\int_0^\beta e^{i\omega_m\tau}\sum_{\boldsymbol{k}_1,\boldsymbol{k}_2}\langle c_{\boldsymbol{k}_1\sigma}^\dagger c_{\boldsymbol{k}_1+\boldsymbol{q}\sigma}c_{\boldsymbol{k}_2\sigma'}^\dagger c_{\boldsymbol{k}_2-\boldsymbol{q}\sigma'}\rangle. \tag{E.13}$$

From Eqs. (E.12) and (E.13), we obtain

$$\chi_s^{zz}(\boldsymbol{q}, i\omega_m) = \frac{1}{4}(\chi^{\uparrow\uparrow}(\boldsymbol{q}, i\omega_m) + \chi^{\downarrow\downarrow}(\boldsymbol{q}, i\omega_m) + \chi^{\downarrow\uparrow}(\boldsymbol{q}, i\omega_m) + \chi^{\uparrow\downarrow}(\boldsymbol{q}, i\omega_m)). \tag{E.14}$$

We derive the spin susceptibility. We consider the grand partition function

$$\Xi = \mathrm{Tr}[e^{-\beta(H-\mu N)}]. \tag{E.15}$$

The expectation value for an arbitrary operator A is written as

$$\begin{aligned}\langle A\rangle &= \frac{\mathrm{Tr}[e^{-\beta H}A]}{\mathrm{Tr}[e^{-\beta H}]} \\ &= \frac{\mathrm{Tr}[e^{-\beta(H_t+H_U)}A]}{\mathrm{Tr}[e^{-\beta(H_t+H_U)}]} \\ &= \frac{\mathrm{Tr}[U_{H_t}(\beta)U_{H_U}(\beta)A]}{\mathrm{Tr}[U_{H_t}(\beta)U_{H_U}(\beta)]}.\end{aligned} \tag{E.16}$$

The grand canonical partition function Ξ is written as

$$\Xi = \mathrm{Tr}[e^{-\beta(H_t+H_U)}] = \mathrm{Tr}[U_{H_t}(\beta)U_{H_U}(\beta)]. \tag{E.17}$$

For a noninteraction system, the expectation value of A is written as

$$\langle A\rangle_0 = \frac{\mathrm{Tr}[e^{-\beta H}A]}{\mathrm{Tr}[e^{-\beta H}]} = \frac{\mathrm{Tr}[e^{-\beta H_t}A]}{\mathrm{Tr}[e^{-\beta H_t}]} = \frac{\mathrm{Tr}[U_{H_t}(\beta)A]}{\mathrm{Tr}[U_{H_t}(\beta)]}. \tag{E.18}$$

The partition function Z is written as

$$Z = \mathrm{Tr}[e^{-\beta H_t}] = \mathrm{Tr}[U_{H_t}(\beta)]. \tag{E.19}$$

Expressing the grand partition function Ξ in terms of the expectation value of $U_{H_U}(\beta)$, we obtain

$$\begin{aligned}
\Xi &= \mathrm{Tr}[U_{H_t}(\beta)U_{H_U}(\beta)] \\
&= \mathrm{Tr}[U_{H_t}(\beta)]\frac{\mathrm{Tr}[U_{H_t}(\beta)U_{H_U}(\beta)]}{\mathrm{Tr}[U_{H_t}(\beta)]} \\
&= \mathrm{Tr}[U_{H_t}(\beta)]\frac{\mathrm{Tr}[U_{H_t}(\beta)U_{H_U}(\beta)]}{\mathrm{Tr}[U_{H_t}(\beta)]} \\
&= \mathrm{Tr}[U_{H_t}(\beta)]\langle U_{H_U}(\beta)\rangle_0.
\end{aligned} \tag{E.20}$$

The Green functions $G(\boldsymbol{k},\tau)$ and $G(\boldsymbol{k},i\omega_n)$ for interacting systems are

$$G(\boldsymbol{k},\tau) = -\langle T_\tau[c_{\boldsymbol{k}\sigma}(\tau)c^\dagger_{\boldsymbol{k}\sigma}]\rangle = T\sum_n e^{-\omega_n\tau}G(\boldsymbol{k},i\omega_n), \tag{E.21}$$

$$G(\boldsymbol{k},i\omega_n) = \int_0^\beta d\tau e^{i\omega_n\tau}G(\boldsymbol{k},\tau). \tag{E.22}$$

The Green functions $G_0(\boldsymbol{k},\tau)$ and $G_0(\boldsymbol{k},i\omega_n)$ for noninteracting systems are

$$G_0(\boldsymbol{k},\tau) = -\langle T_\tau[c_{\boldsymbol{k}\sigma}(\tau)c^\dagger_{\boldsymbol{k}\sigma}]\rangle_0 = T\sum_n e^{-\omega_n\tau}G_0(\boldsymbol{k},i\omega_n), \tag{E.23}$$

$$G_0(\boldsymbol{k},i\omega_n) = \int_0^\beta d\tau e^{i\omega_n\tau}G_0(\boldsymbol{k},\tau). \tag{E.24}$$

The free electron susceptibility $\chi_0(\boldsymbol{q},i\nu_m)$ is defined as

$$\begin{aligned}
\chi_0(\boldsymbol{q},i\nu_m) &\equiv \int_0^\beta d\tau e^{i\nu_m\tau}\sum_{\boldsymbol{k},k'}\langle c^\dagger_{\boldsymbol{k}\sigma}c_{\boldsymbol{k}+\boldsymbol{q}\sigma}c^\dagger_{\boldsymbol{k}'+\boldsymbol{q}\sigma'}c_{\boldsymbol{k}'\sigma'}\rangle_0 \\
&= -\frac{T}{N}\sum_{\boldsymbol{k},\omega_n} G_0(\boldsymbol{k},i\omega_n)G_0(\boldsymbol{k}+\boldsymbol{q},i\omega_n+i\nu_m).
\end{aligned} \tag{E.25}$$

A perturbation expansion of Eq. (E.13) is

$$\begin{aligned}\chi_s^{\sigma\sigma'}(\boldsymbol{q}, i\nu_n) &= \frac{1}{N}\int_0^\beta e^{i\omega_m\tau}\sum_{\boldsymbol{k}_1,\boldsymbol{k}_2}\langle c^\dagger_{\boldsymbol{k}_1\sigma}c_{\boldsymbol{k}_1+\boldsymbol{q}\sigma}c^\dagger_{\boldsymbol{k}_2\sigma'}c_{\boldsymbol{k}_2-\boldsymbol{q}\sigma'}\rangle \\ &= \frac{1}{N}\int_0^\beta e^{i\omega_m\tau}\sum_{\boldsymbol{k}_1,\boldsymbol{k}_2}\frac{\langle U_{H_U}(\beta)c^\dagger_{\boldsymbol{k}_1\sigma}c_{\boldsymbol{k}_1+\boldsymbol{q}\sigma}c^\dagger_{\boldsymbol{k}_2\sigma'}c_{\boldsymbol{k}_2-\boldsymbol{q}\sigma'}\rangle_0}{\langle U_{H_U}(\beta)\rangle_0}. \end{aligned} \tag{E.26}$$

We substitute Eq. (E.7) into Eq. (E.26). We consider Bloch-de Dominics theorem. We define

$$A_i(\tau_i)A_j(\tau_j) \equiv \langle T_\tau[A_j(\tau_i)A_j(\tau_j)]\rangle_0 \tag{E.27}$$

as a contraction. Using Eq. (E.27), we obtain

$$\langle T_\tau[A_1(\tau_1)\cdots A_n(\tau_n)]\rangle_0 = \sum_P(-1)^{\xi_p}A_{i_1}A_{i_2}A_{i_3}A_{i_4}\cdots A_{i_{n-1}}A_{i_n}\cdots. \tag{E.28}$$

Here, $(-1)^{\xi_p}$ is equal to 0 and 1 when the substitution is an even substitution and when it is an odd substitution, respectively. The zeroth-order term is

$$\frac{1}{N}\int_0^\beta e^{i\omega_m\tau}\sum_{\boldsymbol{k},\boldsymbol{k}'}\langle c^\dagger_{\boldsymbol{k}_1\sigma}c^\dagger_{\boldsymbol{k}_2\sigma'}c_{\boldsymbol{k}_1+\boldsymbol{q}\sigma}c_{\boldsymbol{k}_2+\boldsymbol{q}\sigma'}\rangle_0 \equiv \chi_0(\boldsymbol{q}, i\nu_n). \tag{E.29}$$

The first-order term is

$$\begin{aligned}&\frac{1}{N}\int_0^\beta \tau e^{i\omega_m\tau}\sum_{\boldsymbol{k},\boldsymbol{k}'}\left(-\frac{i}{\hbar}\right)\int_0^\beta d\tau_1\langle H_U(\beta)c^\dagger_{\boldsymbol{k}_1\sigma}c_{\boldsymbol{k}_1+\boldsymbol{q}\sigma}c^\dagger_{\boldsymbol{k}_2+\boldsymbol{q}\sigma'}c_{\boldsymbol{k}_2\sigma'}\rangle_0 \\ =&\frac{1}{N}\int_0^\beta d\tau e^{i\omega_m\tau}\sum_{\boldsymbol{k},\boldsymbol{k}'}\left(-\frac{i}{\hbar}\right)\int_0^\beta d\tau_1\langle\sum_{\boldsymbol{k},\boldsymbol{k}'}\sum_{\boldsymbol{k}_1,\boldsymbol{k}_2}Uc^\dagger_{\boldsymbol{k}_1\sigma}c_{\boldsymbol{k}_1+\boldsymbol{q}\sigma}c^\dagger_{\boldsymbol{k}_2+\boldsymbol{q}\sigma'}c_{\boldsymbol{k}_2\sigma'}c^\dagger_{\boldsymbol{k}\sigma}c_{\boldsymbol{k}+\boldsymbol{q}\sigma}c^\dagger_{\boldsymbol{k}'+\boldsymbol{q}\sigma'}c_{\boldsymbol{k}'\sigma'}\rangle_0 \\ =&\frac{1}{N}\int_0^\beta d\tau e^{i\omega_m\tau}\sum_{\boldsymbol{k},\boldsymbol{k}'}\left(-\frac{i}{\hbar}\right)\int_0^\beta d\tau_1\sum_{\boldsymbol{k},\boldsymbol{k}'}\sum_{\boldsymbol{k}_1,\boldsymbol{k}_2}U\langle c_{\boldsymbol{k}_1\sigma}c^\dagger_{\boldsymbol{k}_1\sigma}\rangle_0\langle c_{\boldsymbol{k}_1+\boldsymbol{q}\sigma'}c^\dagger_{\boldsymbol{k}_1+\boldsymbol{q}\sigma'}\rangle_0, \\ &\langle c_{\boldsymbol{k}_2\sigma}c^\dagger_{\boldsymbol{k}_2\sigma}\rangle_0\langle c_{\boldsymbol{k}_2+\boldsymbol{q}\sigma'}c^\dagger_{\boldsymbol{k}_2+\boldsymbol{q}\sigma'}\rangle_0 \\ =&\frac{1}{N}\int_0^\beta d\tau e^{i\omega_m\tau}\sum_{\boldsymbol{k},\boldsymbol{k}'}\left(-\frac{i}{\hbar}\right)\int_0^\beta d\tau_1\sum_{\boldsymbol{k},\boldsymbol{k}'}\sum_{\boldsymbol{k}_1,\boldsymbol{k}_2}UG_0(\boldsymbol{k}_1+\boldsymbol{q},\tau)G_0(\boldsymbol{k}_1,\tau) \\ &G_0(\boldsymbol{k}_2,\tau)G_0(\boldsymbol{k}_2+\boldsymbol{q},\tau) \\ =&U\chi_0(\boldsymbol{q}, i\nu_n)\chi_0(\boldsymbol{q}, i\nu_n). \end{aligned} \tag{E.30}$$

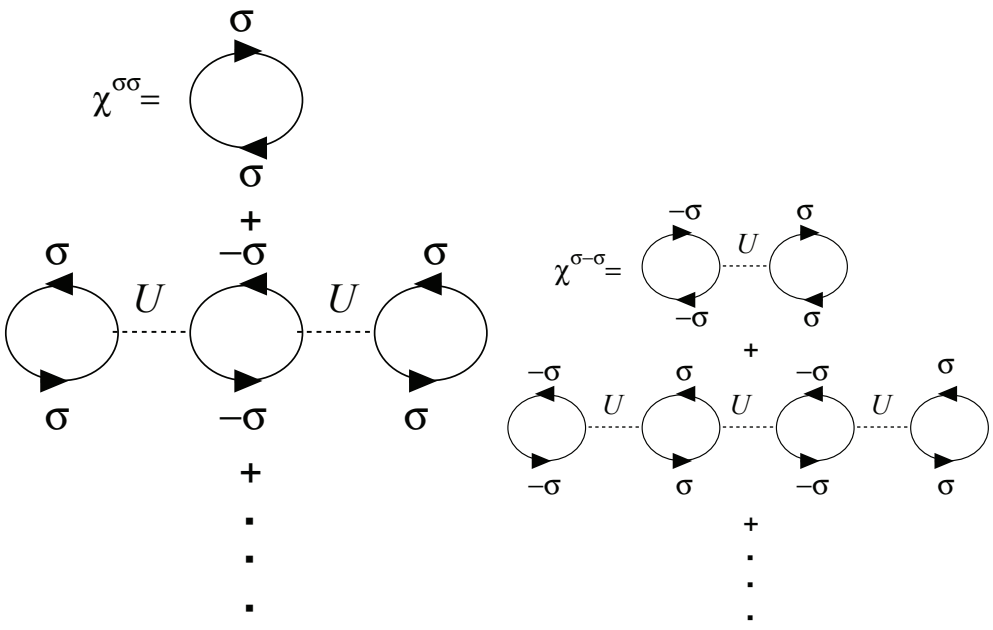

Figure E.1: Diagrams of $\chi^{\sigma\sigma}$ and $\chi^{\sigma-\sigma}$ by RPA.

Therefore, the free spin susceptibility $\chi(\boldsymbol{q}, i\nu_n)$ is

$$\begin{aligned}\chi(\boldsymbol{q}, i\nu_n) &= \chi_0(\boldsymbol{q}, i\nu_n) + U\chi_0(\boldsymbol{q}, i\nu_n)\chi_0(\boldsymbol{q}, i\nu_n) \\ &\quad + U^2\chi_0(\boldsymbol{q}, i\nu_n)\chi_0(\boldsymbol{q}, i\nu_n)\chi_0(\boldsymbol{q}, i\nu_n)\chi_0(\boldsymbol{q}, i\nu_n)\cdots \\ &= \chi_0(\boldsymbol{q}, i\nu_n)(1 + U\chi_0(\boldsymbol{q}, i\nu_n)\cdot\cdot) \\ &= \chi_0(\boldsymbol{q}, i\nu_n)(1 + U\chi(\boldsymbol{q}, i\nu_n)). \end{aligned} \tag{E.31}$$

From Eq. (E.31), we obtain

$$\chi(\boldsymbol{q}, i\nu_n) = \frac{\chi_0(\boldsymbol{q}, i\nu_n)}{1 - U\chi_0(\boldsymbol{q}, i\nu_n)}. \tag{E.32}$$

The critical value U_c of the Coulomb energy satisfies

$$1 = U_\mathrm{c}\chi_0(\boldsymbol{q}, i\nu_n = 0). \tag{E.33}$$

From Eq. (E.15), we obtain

$$U_\mathrm{c} = \frac{1}{\chi_0(\boldsymbol{q}, i\nu_n = 0)}. \tag{E.34}$$

Appendix F

Derivation of Eqs. (2.28) and (2.29)

In this appendix, we derive the sublattice magnetizations of π-electrons and 3d spins in the mean-field approximation.

The model Hamiltonian is written as

$$H = H_t + H_U + H_J \tag{F.1}$$

with

$$H_t = \sum_{i,j}\sum_{\sigma} t_{ij} c^{\dagger}_{i\sigma} c_{i\sigma} - \mu \sum_{i}\sum_{\sigma} c^{\dagger}_{i\sigma} c_{i\sigma}, \tag{F.2}$$

$$H_U = U \sum_{i} n_{i\uparrow} n_{i\downarrow}, \tag{F.3}$$

$$H_J = \sum_{(i,i')}\sum_{\mu=x,y,z} \theta_{i'} J^{\mu}_{12} S^{\mu}_{i'} s^{\mu}_{i}. \tag{F.4}$$

The Hamiltonian in the mean-field approximation is

$$H_U = U \sum_{i} (\langle n_{i\uparrow}\rangle n_{i\downarrow} + n_{i\uparrow}\langle n_{i\downarrow}\rangle - \langle n_{i\uparrow}\rangle\langle n_{i\uparrow}\rangle), \tag{F.5}$$

$$H_J = \sum_{(i,i')}\sum_{\mu=x,y,z} \theta_{i'} J^{\mu}_{12} (\langle S^{\mu}_{i'}\rangle s^{\mu}_{i} + S^{\mu}_{i'}\langle s^{\mu}_{i}\rangle - \langle S^{\mu}_{i'}\rangle\langle s^{\mu}_{i}\rangle). \tag{F.6}$$

We define the sublattice magnetizations M and m of the π electrons and 3d spins as

$$M \equiv \langle S^z_{i'} \rangle, \tag{F.7}$$

and

$$m \equiv \frac{1}{2} \sum_{\sigma_1 \sigma_2} \langle c^\dagger_{i\sigma_1} \sigma^z_{\sigma_1\sigma_2} c_{i\sigma_2} \rangle = \frac{1}{2} \langle (n_{i\uparrow} - n_{i\downarrow}) \rangle, \tag{F.8}$$

respectively. Because

$$M = \frac{\sum_{S^z_{i'}=-S}^{S} S^z_{i'} e^{-J_{12} m S^z_{i'} \beta}}{\sum_{S^z_{i'}=-S}^{S} e^{-J_{12} m S^z_{i'} \beta}} = \frac{\frac{d}{d\beta} \sum_{S^z_{i'}=-S}^{S} \frac{-1}{J_{12}m} e^{-J_{12} m S^z_{i'} \beta}}{\sum_{S^z_{i'}=-S}^{S} e^{-J_{12} m S^z_{i'} \beta}} \tag{F.9}$$

and

$$\begin{aligned} \sum_{S^z_{i'}=-S}^{S} e^{-J_{12} m S^z_{i'} \beta} =& \frac{e^{J_{12} m S \beta} (1 - e^{-J_{12} m (2S+1) \beta})}{1 - e^{-J_{12} m \beta}} \\ =& \frac{(e^{J_{12} m (S+\frac{1}{2}) \beta} - e^{-J_{12} m (S+\frac{1}{2}) \beta})}{e^{\frac{J_{12} m \beta}{2}} - e^{-\frac{J_{12} m \beta}{2}}} = \frac{\sinh(J_{12} m (S+\frac{1}{2}) \beta)}{\sinh(\frac{J_{12} m \beta}{2})}, \end{aligned} \tag{F.10}$$

$$\begin{aligned} &\frac{d}{d\beta} \sum_{S^z_{i'}=-S}^{S} e^{-J_{12} m S^z_{i'} \beta} = \frac{d}{d\beta} \frac{\sinh(J_{12} m (S+\frac{1}{2}) \beta)}{\sinh(\frac{J_{12} m \beta}{2})} \\ =& \frac{1}{\sinh^2(\frac{J_{12} m \beta}{2})} \Big[J_{12} m \Big(S + \frac{1}{2} \Big) \cosh\Big(J_{12} m \Big(S + \frac{1}{2} \Big) \beta \Big) \sinh\Big(\frac{J_{12} m \beta}{2} \Big) \\ &- \frac{J_{12} m}{2} \sinh\Big(J_{12} m \Big(S + \frac{1}{2} \Big) \beta \Big) \cosh\Big(\frac{J_{12} m \beta}{2} \Big) \Big], \end{aligned} \tag{F.11}$$

we obtain

$$\begin{aligned} M =& \frac{1}{\sinh(\frac{J_{12} m \beta}{2}) \sinh(J_{12} m (S+\frac{1}{2}) \beta)} \Big[\Big(S + \frac{1}{2} \Big) \cosh\Big(J_{12} m \Big(S + \frac{1}{2} \Big) \beta \Big) \sinh\Big(\frac{J_{12} m \beta}{2} \Big) \\ &- \frac{1}{2} \sinh\Big(J_{12} m \Big(S + \frac{1}{2} \Big) \beta \Big) \cosh\Big(\frac{J_{12} m \beta}{2} \Big) \Big] \\ =& (S + \frac{1}{2}) \coth\Big[J_{12} m (S + \frac{1}{2}) \beta \Big] - \frac{1}{2} \coth\Big(\frac{J_{12} m \beta}{2} \Big) \end{aligned}$$

$$=SB_S(J_{12}mS). \tag{F.12}$$

We derive the sublattice magnetization m. Because $n = \langle n_{i\uparrow}\rangle + \langle n_{i\downarrow}\rangle$,

$$\langle n_{i\uparrow}\rangle = \frac{n}{2} + m \tag{F.13}$$

and

$$\langle n_{i\downarrow}\rangle = \frac{n}{2} - m. \tag{F.14}$$

Using Eqs. (F.13) and (F.14) in Eqs. (F.5) and (F.6), we obtain

$$\begin{aligned} H_U &= U\sum_i(\langle n_{i\uparrow}\rangle n_{i\downarrow} + n_{i\uparrow}\langle n_{i\downarrow}\rangle - \langle n_{i\uparrow}\rangle\langle n_{i\uparrow}\rangle) \\ &= U\sum_i[\frac{n}{2}(n_{i\downarrow}+n_{i\uparrow}) + m(n_{i\downarrow}-n_{i\uparrow}) + (\frac{n^2}{4}-m^2)] \end{aligned} \tag{F.15}$$

and

$$\begin{aligned} H_J &= \sum_{(i,i')}\sum_{\mu=x,y,z}\theta_{i'}J_{12}^{\mu}(\langle S_{i'}^{\mu}\rangle s_i^{\mu} + S_{i'}^{\mu}\langle s_i^{\mu}\rangle - \langle S_{i'}^{\mu}\rangle\langle s_i^{\mu}\rangle) \\ &= \sum_{(i,i')}\sum_{\mu=x,y,z}\theta_{i'}J_{12}^{\mu}(Ms_i^{\mu} + S_{i'}^{\mu}m - Mm). \end{aligned} \tag{F.16}$$

Equation (F.16) is rewritten as

$$H_t = \sum_{\boldsymbol{k}\sigma}(\xi_{\boldsymbol{k}} + \delta_{\boldsymbol{k}})c_{\boldsymbol{k}\sigma}^{\dagger}c_{\boldsymbol{k}\sigma}, \tag{F.17}$$

$$\begin{aligned} H_U &= U\sum_i\frac{n}{2}(n_{i\downarrow}+n_{i\uparrow}) + m(n_{i\downarrow}-n_{i\uparrow}) + (\frac{n^2}{4}-m^2) \\ &= U\sum_{\boldsymbol{k}}\sum_{\sigma}(\frac{n}{2}-m\sigma)c_{\boldsymbol{k}\sigma}^{\dagger}c_{\boldsymbol{k}+\boldsymbol{q}\sigma} + (\frac{n^2}{4}-m^2), \end{aligned} \tag{F.18}$$

$$\begin{aligned} H_J &= \sum_{(i,i')}\sum_{\mu=x,y,z}\theta_{i'}J_{12}^{\mu}(-Ms_i^{\mu} - S_{i'}^{\mu}m + Mm) \\ &= \sum_{\boldsymbol{k}}(-\frac{1}{2}J_{\boldsymbol{12}}Mc_{\boldsymbol{k}\sigma}^{\dagger}c_{\boldsymbol{k}+\boldsymbol{q}\sigma} - \sum_{i'}J_{12}mS_{i'}^{z} + NJ_{12}Mm). \end{aligned} \tag{F.19}$$

In the antiferromagnetic phase, the Hamiltonian is written as

$$H_t = \sum_{\boldsymbol{k}\sigma}{}' (\xi_{\boldsymbol{k}} c^\dagger_{\boldsymbol{k}\sigma} c_{\boldsymbol{k}\sigma} + \xi_{\boldsymbol{k}+\boldsymbol{q}} c^\dagger_{\boldsymbol{k}+\boldsymbol{q}\sigma} c_{\boldsymbol{k}+\boldsymbol{q}\sigma}), \tag{F.20}$$

$$\begin{aligned} H_U &= U \sum_{\boldsymbol{k}} \sum_{\sigma} \Big(\frac{n}{2} - m\sigma \Big) c^\dagger_{\boldsymbol{k}\sigma} c_{\boldsymbol{k}+\boldsymbol{q}\sigma} + \Big(\frac{n^2}{4} - m^2 \Big) \\ &= U \sum_{\boldsymbol{k}}{}' \sum_{\sigma} (\frac{n}{2} - m\sigma)(c^\dagger_{\boldsymbol{k}\sigma} c_{\boldsymbol{k}+\boldsymbol{q}\sigma} + c^\dagger_{\boldsymbol{k}+\boldsymbol{q}\sigma} c_{\boldsymbol{k}\sigma}) + \Big(\frac{n^2}{4} - m^2 \Big), \end{aligned} \tag{F.21}$$

$$\begin{aligned} H_J &= -\sum_{\boldsymbol{k},\sigma} \frac{1}{2} J_{12} M c^\dagger_{\boldsymbol{k}\sigma} c_{\boldsymbol{k}+\boldsymbol{q}\sigma} - \sum_{i'} J_{12} m S^z_{i'} + J_{12} M m \\ &= \sum_{\boldsymbol{k},\sigma}{}' J_{12} M (c^\dagger_{\boldsymbol{k}\sigma} c_{\boldsymbol{k}+\boldsymbol{q}\sigma} + c^\dagger_{\boldsymbol{k}+\boldsymbol{q}\sigma} c_{\boldsymbol{k}\sigma}) + \sum_{i'} J_{12} m S^z_{i'} + J_{12} M m. \end{aligned} \tag{F.22}$$

From Eqs. (F.20), (F.21) and (F.22), the Hamiltonian is written as

$$H = \sum_{\boldsymbol{k}\sigma}{}' (c^\dagger_{\boldsymbol{k}\sigma} c^\dagger_{\boldsymbol{k}+\boldsymbol{q}\sigma}) \hat{\mathcal{E}}_{\boldsymbol{k}\sigma} \begin{pmatrix} c_{\boldsymbol{k}\sigma} \\ c_{\boldsymbol{k}+\boldsymbol{q}\sigma} \end{pmatrix}, \tag{F.23}$$

where

$$\hat{\mathcal{E}}_{\boldsymbol{k}\sigma} = \begin{pmatrix} \xi_{\boldsymbol{k}} & -\alpha_2\sigma \\ -\alpha_2\sigma & \xi_{\boldsymbol{k}+\boldsymbol{q}} \end{pmatrix}. \tag{F.24}$$

The Hamiltonian Eq. (F.23) is diagonalized by the unitary transformation $\begin{pmatrix} c_{\boldsymbol{k}\sigma} \\ c_{\boldsymbol{k}+\boldsymbol{q}\sigma} \end{pmatrix} = U_{\boldsymbol{k}\sigma} \begin{pmatrix} \alpha_{\boldsymbol{k}\sigma} \\ \beta_{\boldsymbol{k}\sigma}, \end{pmatrix}$ as

$$H = \sum_{\boldsymbol{k}\sigma}{}' (E^+_{\boldsymbol{k}} \alpha^\dagger_{\boldsymbol{k}\sigma} \alpha_{\boldsymbol{k}\sigma} + E^-_{\boldsymbol{k}} \beta^\dagger_{\boldsymbol{k}\sigma} \beta_{\boldsymbol{k}\sigma}), \tag{F.25}$$

where

$$E^\pm_{\boldsymbol{k}} = \frac{\xi_{\boldsymbol{k}} + \xi_{\boldsymbol{k}+\boldsymbol{q}}}{2} \pm \sqrt{\left(\frac{\xi_{\boldsymbol{k}} - \xi_{\boldsymbol{k}+\boldsymbol{q}}}{2} \right)^2 + \alpha_2^2}. \tag{F.26}$$

The unitary matrix is expressed as the rotation matrix

$$U_{\boldsymbol{k}\sigma} = \begin{pmatrix} \cos(\theta_{\boldsymbol{k}}) & -\sigma\sin(\theta_{\boldsymbol{k}}) \\ \sigma\sin(\theta_{\boldsymbol{k}}) & \cos(\theta_{\boldsymbol{k}}) \end{pmatrix}, \tag{F.27}$$

where

$$\cos(2\theta_{\boldsymbol{k}}) = -\frac{\xi_{\boldsymbol{k}\sigma} - \xi_{\boldsymbol{k}+\boldsymbol{q}\sigma}}{\sqrt{(\xi_{\boldsymbol{k}\sigma} - \xi_{\boldsymbol{k}+\boldsymbol{q}\sigma})^2 + \alpha_2^2}}, \tag{F.28}$$

$$\sin(2\theta_{\boldsymbol{k}}) = -\frac{\alpha_2}{\sqrt{(\xi_{\boldsymbol{k}\sigma} - \xi_{\boldsymbol{k}+\boldsymbol{q}\sigma})^2 + \alpha_2^2}}, \tag{F.29}$$

$$\alpha_2 = \frac{1}{2}J_{12}M + Um. \tag{F.30}$$

Hence, we obtain

$$m = \frac{1}{2N}{\sum_{\boldsymbol{k}}}' \sum_{\sigma} \sin(2\theta_{\boldsymbol{k}})(\langle\beta^\dagger_{\boldsymbol{k}\sigma}\beta^\dagger_{\boldsymbol{k}\sigma}\rangle - \langle\alpha^\dagger_{\boldsymbol{k}\sigma}\alpha^\dagger_{\boldsymbol{k}\sigma}\rangle). \tag{F.31}$$

Using Eq. (F.29) in Eq. (F.31), we obtain

$$m = \frac{1}{N}{\sum_{\boldsymbol{k}}}' \frac{\alpha_2}{\sqrt{(\xi_{\boldsymbol{k}\sigma} - \xi_{\boldsymbol{k}+\boldsymbol{q}\sigma})^2 + \alpha_2^2}}(f(E^-_{\boldsymbol{k}}) - f(E^+_{\boldsymbol{k}})), \tag{F.32}$$

where $\langle\alpha^\dagger_{\boldsymbol{k}\sigma}\alpha^\dagger_{\boldsymbol{k}\sigma}\rangle = f(E^+_{\boldsymbol{k}})$ and $\langle\beta^\dagger_{\boldsymbol{k}\sigma}\beta^\dagger_{\boldsymbol{k}\sigma}\rangle = f(E^-_{\boldsymbol{k}})$, $\bar{\xi_{\boldsymbol{k}}} \equiv \frac{\xi_{\boldsymbol{k}}+\xi_{\boldsymbol{k}+\boldsymbol{q}}}{2}$, $\delta_{\boldsymbol{k}} \equiv \frac{\xi_{\boldsymbol{k}}-\xi_{\boldsymbol{k}+\boldsymbol{q}}}{2}$, and $E_{\boldsymbol{k}} \equiv \sqrt{\bar{\xi_{\boldsymbol{k}}}^2 + {\alpha_2}^2}$.

From Eq. (F.32), we obtain

$$\begin{aligned} m =& \frac{1}{N}{\sum_{\boldsymbol{k}}}' \frac{\alpha_2}{E_{\boldsymbol{k}}}(f(E^-_{\boldsymbol{k}}) - f(E^+_{\boldsymbol{k}})) \\ =& \frac{1}{N}{\sum_{\boldsymbol{k}}}' \frac{\alpha_2}{E_{\boldsymbol{k}}}\Big(\frac{e^{(E_{\boldsymbol{k}}-\delta_{\boldsymbol{k}})/2k_BT} - e^{-(E_{\boldsymbol{k}}-\delta_{\boldsymbol{k}})/2k_BT}}{e^{(E_{\boldsymbol{k}}-\delta_{\boldsymbol{k}})/2k_BT} + e^{-(E_{\boldsymbol{k}}-\delta_{\boldsymbol{k}})/2k_BT}} \\ & - \frac{e^{(E_{\boldsymbol{k}}+\delta_{\boldsymbol{k}})/2k_BT} - e^{-(E_{\boldsymbol{k}}-\delta_{\boldsymbol{k}})/2k_BT}}{e^{(E_{\boldsymbol{k}}+\delta_{\boldsymbol{k}})/2k_BT} + e^{-(E_{\boldsymbol{k}}+\delta_{\boldsymbol{k}})/2k_BT}}\Big) \\ =& \frac{1}{N}{\sum_{\boldsymbol{k}}}' \frac{\alpha_2}{E_{\boldsymbol{k}}}\Big(\tanh\Big(\frac{E_{\boldsymbol{k}} - \delta_{\boldsymbol{k}}}{2k_BT}) + \tanh(\frac{E_{\boldsymbol{k}} + \delta_{\boldsymbol{k}}}{2k_BT}\Big)\Big). \end{aligned} \tag{F.33}$$

Reference

[1] L. Balents, Nature **464**, 199 (2010).

[2] K. Kanoda and R. Kato, Annu. Rev. Condens. Matter Phys. **2**, 167 (2011).

[3] T. Isono, H. Kamo, A. Ueda, K. Takahashi, M. Kimata, H. Tajima, S. Tsuchiya, T. Terashima, S. Uji, and H. Mori, Phys. Rev. Lett. **112**, 177201 (2014).

[4] P. Hauke, Phys. Rev. B **87**, 014415 (2013).

[5] E. P. Scriven and B. J. Powell, Phys. Rev. Lett. **109**, 097206 (2012).

[6] A. V. Chubukov, and O. A. Starykh, Phys. Rev. Lett. **110**, 217210 (2013).

[7] O. A. Starykh, and L. Balents, Phys. Rev. Lett. **98**, 077205 (2007).

[8] M. Kohno, O. A. Starykh, and L. Balents, Nat. Phys. **3**, 790 (2007).

[9] Z. Weihong, R. H. McKenzie, and R. R. P. Singh, Phys. Rev. B **59**, 14367 (1999), and references in Ref. 11.

[10] Y. Shimizu, K. Miyagawa, K. Kanoda, M. Maesato, and G. Saito, Phys. Rev. Lett. **91**, 107001 (2003).

[11] T. Ono, H. Tanaka, H. A. Katori, F. Ishikawa, H. Mitamura and T. Goto, Phys. Rev. B **67**, 104431 (2003).

[12] T. Ono, H. Tanaka, O. Kolomiyets, H. Mitamura, T. Goto, K. Nakajima, S. Oosawa, Y. Koike, K. Kakurai, J. Klenke, P. Smeibidle and M. Meiβner, J. Phys. Condens. Matter **16**, S773 (2004).

[13] S. Gopalan, T. M. Rice, and M. Sigrist, Phys. Rev. B **4**9, 8901 (1994).

[14] M. Onoda and N. Nishiguchi, J. Solid State Chem. **127**, 359 (1996).

[15] S. Miyahara, M. Troyer, D. C. Johnston, and K. Ueda, J. Phys. Soc. Jpn. **67**, 3918 (1998).

[16] M. Onoda and J. Hasegawa, J. Phys.: Condens. Matter **18**, 2109 (2006).

[17] A. H. Castro Neto, F. Guinea, N. M. R. Peres, K. S. Novoselov, and A. K. Geim, Rev. Mod. Phys. **81**, 109 (2009).

[18] Y. Miura, R. Hirai, Y. Kobayashi, and M. Sato, J. Phys. Soc. Jpn. **75**,084707 (2006), and references therein.

[19] M. Tokumoto, T. Naito, H. Kobayashi, A. Kobayashi, V. N. Laukhin, L. Brossard, and P. Cassoux: Synth. Met. **86**, 2161 (1997).

[20] L. Brossard, R. Clerac, C. Coulon, M. Tokumoto, T. Ziman, D. K. Petrov, V. N. Laukhin, M. J. Naughton, A. Audouard, F. Goze, A. Kobayashi, H. Kobayashi, and P. Cassoux: Eur. Phys. J. B **1**, 439 (1998).

[21] H. Akiba, S. Nakano, Y. Nishio, K. Kajita, B. Zhou, A. Kobayashi, and H. Kobayashi, J. Phys. Soc. Jpn. **78**, 033601 (2009).

[22] H. Akiba, K. Nobori, K. Shimada, Y. Nishio, K. Kajita, B. Zhou, A. Kobayashi, and H. Kobayashi, J. Phys. Soc. Jpn. **80**, 063601 (2011).

[23] T. Mori and M. Katsuhara, J. Phys. Soc. Jpn. **71**, 826 (2002).

[24] S. Fukuoka, T. Minamidate, N. Matsunaga, Y. Ihara, and A. Kawamoto, J. Phys. Soc. Jpn. **89**, 073704 (2020).

[25] H. B. Cui, S. Otsubo, Y. Okano, and H. Kobayashi, Chem. Lett. **34**, 254 (2005).

[26] T. Minamidate, Y. Oka, H. Shindo, T. Yamazaki, N. Matsunaga, K. Nomura, and A. Kawamoto, J. Phys. Soc. Jpn. **84**, 063704 (2015).

[27] T. Minamidate, H. Shindo, Y. Ihara, A. Kawamoto, N. Matsunaga, and K. Nomura, Phys. Rev. B **97**, 104404 (2018).

[28] K. Sakakida, and H.Shimahara, J. Phys. Soc. Jpn. **86**, 124709 (2017).

[29] D. D. Osheroff, M. C. Cross, and D. S. Fisher, Phys. Rev. Lett. **44**, 792 (1980).

[30] M. Roger, J. M. Delrieu, and J. H. Hetherington, Phys. Rev. Lett. **45**, 137 (1980).

[31] T. Kimura, S. Ishihara, H. Shintani, T. Arima, K. T. Takahashi, K. Ishizaka, and Y. Tokura, Phys. Rev. B **68**, 060403(R) (2003).

[32] A. Munoz, M. T. Casáis, J. A. Alonso, M. J. Martínez-Lope, J. L. Martínez, and M. T. Fernández-Díaz, Inorg. Chem. **40**, 1020 (2001).

[33] T. A. Kaplan, Phys. Rev. B **80**, 012407 (2009).

[34] T. Zou, Y.-Q. Cai, C. R. dela Cruz, V. O. Garlea, S. D. Mahanti, J.-G. Cheng, and X. Ke, Phys. Rev. B **94**, 214406 (2016).

[35] H. Kobayashi, H. Cui, and A. Kobayashi Chem. Rev. **104**, 5265 (2004).

[36] H. Kobayashi, H. Tomita, T. Naito, A. Kobayashi, F. Sakai, T. Watanabe, and P. Cassoux: J. Am. Chem. Soc. **118**, 368 (1996).

[37] A. Kobayashi, T. Udagawa, H. Tomita, T. Naito, and H. Kobayashi, Chem. Lett. **22**, 2179 (1993).

[38] H. Kobayashi, T. Udagawa, H. Tomita, K. Bun, T. Naito, and A. Kobayashi, Chem. Lett. **22**, 1559 (1993).

[39] A. Sato, E. Ojima, H. Akutsu, H. Kobayashi, A. Kobayashi, and P. Cassoux, Chem. Lett. **27**, 673 (1998).

[40] N. D. Mermin and H. Wagner, Phys. Rev. Lett. **17**, 1133 (1966).

[41] H. Shimahara and K. Ito, J. Phys. Soc. Jpn. **83**, 114702 (2014).

[42] T. Sasaki, H. Uozaki, S. Endo, and N. Toyota, Synth. Met. **120**, 759 (2001).

[43] M. Tokumoto, H. Tanaka, T. Otsuka, H. Kobayashi, and A. Kobayashi, Polyhedron **24**, 2793 (2005).

[44] O. Cépas, R. H. McKenzie, and J. Merino, Phys. Rev. B **65**, 100502 (2002).

[45] H. Shimahara, J. Phys. Soc. Jpn. **87**, 043702 (2018).

[46] H. Shimahara, J. Phys. Soc. Jpn. **88**, 043001 (2019).

[47] H. Shimahara, J. Phys. Soc. Jpn. **89**, 043001 (2020).

[48] Y. Oshima, H.-B. Cui, and R. Kato, Magnetochemistry **3**, 10 (2017).

[49] K. Ito and H. Shimahara, J. Phys. Soc. Jpn. **85**, 024704 (2016).

[50] H. Shimahara and K. Ito, J. Phys. Soc. Jpn. **85**, 043708 (2016).

[51] H. Shimahara and Y. Kono, J. Phys. Soc. Jpn. **86**, 043704 (2017).

[52] J. Hubbard, Proc. Roy. Soc. (London) A **276**, 238 (1963).

[53] C. Hotta and H. Fukuyama, J. Phys. Soc. Jpn. **69**, 2577 (2000).

[54] M. Terao and Y. Ohashi, Physica C **412-414**, 324 (2004).

[55] M. A. Ruderman and C. Kittel, Phys. Rev. **96**, 99 (1954).

[56] T. Kasuya, Prog. Theor. Phys. **16**, 45 (1956).

[57] K. Yosida, Phys. Rev. **106**, 893 (1957).

[58] S. Uji, H. Shinagawa, C. Terakura, T. Terashima, T. Yakabe, Y. Terai, M. Tokumoto, A. Kobayashi, H. Tanaka, and H. Kobayashi, Phys. Rev. B **64**, 024531 (2001).

[59] H. Akiba, H. Sugawara, K. Nobori, K. Shimada, N. Tajima, Y. Nishio, K. Kajita, B. Zhou, A. Kobayashi, and H. Kobayashi, J. Phys. Soc. Jpn. **81**, 053601 (2012).

[60] H. Kobayashi, A. Sato, H. Tanaka, A. Kobayashi, and P. Cassoux, Coord. Chem. Rev. **190-192**, 921 (1999).

[61] S. Uji, H. Shinagawa, T. Terashima, Y. Yakabe, Y. Terai, M. Tokumoto, A. Kobayashi, H. Tanaka, and H. Kobayashi, Nature (London) **410**, 908 (2001).

[62] M. Houzet, A. Buzdin, L. Bulaevskii, and M. Maley, Phys. Rev. Lett. **88**, 227001 (2002).

[63] 倉本義夫：「量子多体物理学」，朝倉書店，2010, 1.

[64] 高野文彦：「多体問題」，培風館，1993, 9.

[65] 押山淳，天能精一朗，杉野修，大野かおる，今田正俊：「計算科学 3」，岩波書店，2012, 7.

公表論文

1. On Scaling Relations of Organic Antiferromagnets with Magnetic Anions
   Hiroshi Shimahara and Yuki Kono
   Journal of the Physical Society of Japan, **86**, 043704-1 - 043704-5 (2017).

2. Magnetic Structures of Electron Systems on the Extended Spatially Completely Anisotropic Triangular Lattice near Quantum Critical Points
   Yuki Kono and Hiroshi Shimahara
   Journal of the Physical Society of Japan, **90**, 024708-1 - 124711-8 (2021).